

DISCOVERY AND CHARACTERIZATION OF MOLECULAR SUBTYPES IN HIGH-
GRADE UROTHELIAL CARCINOMA

Jeffrey Stuart Damrauer

A dissertation submitted to the faculty at the University of North Carolina at Chapel Hill
in partial fulfillment of the requirements for the degree of Doctor of Philosophy in the
Curriculum of Genetics and Molecular Biology in the School of Medicine.

Approved by:

William Y. Kim

Ian J. Davis

Carol A. Otey

Joel S. Parker

Norman E. Sharpless

©2014
Jeffrey Stuart Damrauer
ALL RIGHTS RESERVED

ABSTRACT

Jeffrey Stuart Damrauer: Discovery and characterization of molecular subtypes in high-grade urothelial carcinoma
(Under the direction of William Y. Kim)

Bladder Cancer is the 4th most commonly diagnosed cancer in men and the 8th most deadly. While non-muscle invasive bladder cancer has a relatively high 5 year survival rate, muscle invasive bladder cancer ($\geq T_2$) has a 5 year survival rate of ~50% with the number decreasing to 15% for non-organ confined disease. Multiple groups have performed molecular characterization of bladder tumors in an effort to identify bladder cancer subtypes. These groups have been able to effectively differentiate non-muscle invasive disease (low-grade) from muscle invasive (high-grade); since pathologists can reliably identify LG and HG tumors, molecular signatures of these two groups are not clinically useful. We sought to define whether there are intrinsic molecular subtypes of high-grade bladder cancer. Consensus Clustering performed on gene expression data from a meta-dataset of high-grade, muscle invasive bladder tumors identified two intrinsic, molecular subsets of high-grade bladder cancer: “luminal” and “basal-like” that have characteristics of different stages of urothelial differentiation, reflect the luminal and basal-like molecular subtypes of breast cancer, and have clinically meaningful differences in outcome. Prediction analysis of microarrays (PAM) defined a gene set predictor: Bladder cancer Analysis of Subtypes by Expression (BASE47) that accurately classifies the subtypes. Our data demonstrate that there are

at least two molecularly and clinically distinct subtypes of high-grade bladder cancer. As an appreciation of subtype heterogeneity has revolutionized the care of breast cancer, these results also suggest stratification for therapy is indicated in bladder cancer as well.

ACKNOWLEDGMENTS

First, thank you to everyone who has played a role in this project and more generally in my graduate career, this long journey would not have been as rewarding or enjoyable without all of you.

I would like to thank my thesis advisor, Billy Kim. Billy provided me with a wonderful lab environment and surrounded me with all of the tools needed to become a successful scientist. Additionally his mentoring, encouragement and patience with me throughout my graduated studies and numerous projects has allowed me to grow and thrive over the past 6 years and will stay with me as I continue my career in science.

Additionally, I would like to thank my committee, Drs. Ned Sharpless, Ian Davis, Carol Otey, Joel Parker and former member Derek Chiang, for their support and critical analysis over the course of my project.

A special thank you to Dr. Katherine Hoadley for her help and guidance in all things bioinformatics and TCGA. There is no doubt that without Katie's help I would not have been as successful as I was in executing this project. Additionally, she has been a source of reassurance and laughter throughout the ups and downs of graduate school.

I would like to thank my collaborators, including Dr. Charles Perou and his lab for their expertise in subtype discovery and bioinformatics. Also, I would like to thank the Sharpless and Yeh labs for sharing their advice, guidance and reagents.

None of this would have been possible without the support of the members of the Kim Lab, both current and former. Their help both scientifically and otherwise, have made the past 6 years fly by.

Additionally, I would like to acknowledge my past mentors, Drs. Denis Guttridge and Susan Kandarian. Both of whom gave me a strong foundation in which I was able to build on during my time at UNC.

Finally, I would like to thank my entire family. You have been there through everything, and I can't even begin to explain how each one of you has impacted me and helped me along his journey. To my parents, I can't say enough to thank you for all you have done to support me; your belief in me during whatever challenge or obstacle I faced as helped be to be the person I am today. Last but not least, I would like to thank my beautiful wife, Jodie. You have been a constant source of joy, enthusiasm and laughter, I don't know if I could have done this without you by my side. I love you.

TABLE OF CONTENTS

LIST OF FIGURES	ix
LIST OF TABLES	xi
LIST OF ABBREVIATIONS.....	xii
Chapter 1: Bladder Cancer Pathology and Histologic Subtypes	1
1.1 Epidemiology	1
3.2 Risk Factors.....	3
1.3 Bladder Histology, Staging and Pathologic Subtypes	6
1.4 Bladder Cancer Treatment	10
1.5 Summary	12
Chapter 2: Bladder Cancer Genetics and Molecular Subtyping.....	13
2.1 Bladder Cancer Genetics	13
2.2 Molecular Signatures of Bladder Cancer.....	19
Summary	24
Chapter 3: Intrinsic subtypes of high-grade bladder cancer reflect the hallmarks of breast cancer biology	25
3.1 Overview.....	25
3.2 Introduction.....	26

3.3 Results.....	28
3.4 Discussion	36
3.5 Materials and Methods	39
3.6 Figures.....	42
3.7 Supplemental Figures.....	55
Chapter 4: Future Directions.....	64
4.1 BASE47 as a prognostic tool.....	64
4.2 BASE47 as a predictive tool.....	66
APPENDIX A: SAM GENE LIST	70
APPENDIX B: PAM GENE LIST	105
APPENDIX C: GENE SET ENRICHMENT ANALYSIS	108
REFERENCES.....	129

LIST OF FIGURES

FIGURE 1: BLADDER HISTOLOGY.....	7
FIGURE 2: BLADDER CANCER STAGING	9
FIGURE 3: GENOMIC ALTERATION IN BLADDER CANCER.....	17
FIGURE 5: DISCOVERY OF TWO DISTINCT SUBTYPES OF BLADDER CANCER.....	44
FIGURE 6: GENERATION OF THE BASE47 SUBTYPE PREDICTOR.....	45
FIGURE 7: COMPARISON OF BASE47 CALLS TO PREVIOUSLY PUBLISHED SUBTYPES CALLS ON THE TCGA DATASET	47
FIGURE 8: LUMINAL AND BASAL BLADDER CANCER HAVE DIFFERENTIAL SURVIVAL AND ARE ASSOCIATED WITH DISTINCT GENOMIC ALTERATIONS.....	48
FIGURE 9: BASAL AND LUMINAL BLADDER CANCER HAVE DISTINCT CLINICAL FEATURES.	49
FIGURE 10: BASAL-LIKE AND LUMINAL BLADDER CANCER CORRELATE TO THE INTRINSIC MOLECULAR SUBTYPES OF BREAST CANCER.....	50
FIGURE 11: A SUBSET OF BASAL-LIKE BLADDER TUMORS ARE CLAUDIN-LOW.....	52
FIGURE 12: PROPOSED MODEL OF UROTHELIAL TUMORGENESIS AND RELATIONSHIPS TO INTRINSIC SUBTYPES OF BREAST CANCER	53
SUPPLEMENTAL FIGURE 1: CONSENSUS CLUSTERING DEFINES TWO DISTINCT MOLECULAR SUBTYPES OF INVASIVE BLADDER CANCER	56
SUPPLEMENTAL FIGURE 2: CLINICAL VARIABLES ARE NOT SIGNIFICANTLY ASSOCIATED WITH DISEASE SPECIFIC OR OVERALL SURVIVAL AND PREVIOUS MUSCLE INVASIVE SIGNATURES ARE NOT PROGNOSTIC IN THE MSKCC DATASET.....	57

SUPPLEMENTAL FIGURE 3: MAKERS OF LUMINAL BREAST CANCER ARE CO-EXPRESSED WITH MARKERS OF UROTHELIAL DIFFERENTIATION	60
SUPPLEMENTAL FIGURE 4: BASAL-LIKE BLADDER CANCER POSSESSES TUMOR INITIATING CELL TRAITS AND IS MOLECULAR SIMILAR TO BASAL BREAST CANCER.	62
SUPPLEMENTAL FIGURE 5: BASAL, LUMINAL, CALUDIN LOW AND ONCOGENIC BREAST CANCER SIGNATURES ARE ASSOCIATED WITH INTRINSIC MOLECULAR SUBTYPES OF BLADDER CANCER.....	63
FIGURE 13: SENSITIVE TO CDK4/6 INHIBITION BY MUTATIONAL STATUS.....	69

LIST OF TABLES

TABLE 1: COMPARISON OF MUSCLE INVASIVE SUBTYPES	23
TABLE 2: DATASET CHARACTERISTICS	42
TABLE 3: MSKCC - UNIVARIABLE COX REGRESSION ANALYSIS OF DISEASE SPECIFIC SURVIVAL	43

LIST OF ABBREVIATIONS

BCG	Bacillus Calmette-Guerin
CCND1	cyclin D1
CCNE1	cyclin E1
CDK1A	cyclin-dependent kinase inhibitor 1A
CDK2A	cyclin-dependent kinase inhibitor 2A
CIS	carcinoma in situ
EMT	epithelial-mesenchymal transition
FGFR3	fibroblast growth factor receptor 3
GSEA	Gene Set Enrichment Analysis
HG	high grade
HMWK	High Molecular Weight Keratin
HRAS	Harvey rat sarcoma viral oncogene homolog
IPA	Ingenuity Pathway Analysis
KDM6A	lysine (K)-specific demethylase 6A
LG	low grade
LMWK	Low Molecular Weight Keratin
MAD	Mean Absolute Deviation
MSKCC	Memorial Sloan Kettering Cancer Center
PAM	Prediction Analysis for Microarrays
PTEN	phosphatase and tensin homolog
RB1	retinoblastoma 1
SAM	Significance Analysis of Microarrays

TCGA	The Cancer Genome Atlas
TP53	tumor protein p53
TURBT	Transurethral Resection of Bladder Tumor

Chapter 1: Bladder Cancer Pathology and Histologic Subtypes

1.1 Epidemiology

Bladder cancer is the 4th most commonly diagnosed cancer in men and 8th deadliest in the United States with an estimated 74,690 (56,390 in men and 18,300 in women) new cases and 15,580 (11,170 in men and 4,410 in women) deaths for the year 2014 (1). Bladder cancer has the highest per patient treatment cost of any cancer, costing the US healthcare industry 3.7 billion dollars annually (2). This is of note since bladder cancer is predominately a disease of the elderly, specifically elderly men; the average age at diagnosis is 65-70 years with an incidence rate of 36.9 for men and 9.1 for women (per 100,000 people) (1). Although women are diagnosed at a lower frequency than men, they have a worse overall prognosis. Studies suggest that gender may be an independent risk factor for poor prognosis, with women having a poorer outcome (3, 4). However, other reports suggest that when corrected for demographics and clinical factors, women had equal survival outcomes to men (5).

In addition to gender differences associated with bladder cancer diagnosis, race specific differences exist as well (6-8). A direct comparison of five year survival between White and African American patients showed a 14 percentage point difference in five-year overall survival (1). The survival difference in bladder cancer between race is one

of the most different as compared to other tumor types This could partially be explained by white patients having a higher incidence of low grade tumors as compared to African Americans. (9). Additionally, the difference in survival has previously been attributed to difference in access to health care and late stage diagnosis. However, multiple studies have shown that poor outcome is not fully due to the aforementioned factors, and other, yet to be determined factors contribute to race specific survival differences (5, 7, 10, 11).

3.2 Risk Factors

There are multiple known risk factors for bladder cancer including smoking, occupational exposures, environmental exposures and infection. Smoking is the single largest risk factor for bladder cancer, increasing a person's risk 2-4 fold (9). Additionally, it has been estimated that 30%-50% of all bladder cancer cases are caused by cigarette smoking (9, 12). While the risk of smoking related bladder cancer has been correlated to the duration and intensity of smoking, there is also a correlation between the variety of tobacco used in the cigarettes and cancer risk; black tobacco has a 2-3 times high risk than Virginia or brightleaf tobacco (12). Currently, there is no defined mechanism of smoking related carcinogenesis in bladder cancer. It has been hypothesized that the absorption of carcinogens such as 2-naphthylamine and 4-aminobiphenyl, which are filtered through the urine via the bladder, could act as the causal agents. However, the risk of bladder cancer is only increased by inhaled tobacco and not other products such as cigar and chewing tobacco, suggesting a more complicated mechanism of carcinogen metabolism (13). In addition to the carcinogens from cigarettes, carcinogenic exposure at the workplace is also a contributing risk factor to bladder cancer.

After smoking, occupational exposures represent the second largest risk factor for the development of bladder cancer. It is believed that 20% of bladder cancer cases can be linked to occupational exposure from wide array of industries such as, textiles, dyes, and paint (14). Case and Hosker in 1954 reported that rubber workers in England and Wales, who were exposed to naphthylamines had increased risk of developing

bladder cancer (15). This has been followed up over the past decades by numerous studies demonstrating the link between occupational exposure to carcinogens and bladder cancer (12, 16). Aromatic amines such as, benzidine; benzidine; 4-aminobiphenyl; 2-naphthylamine; 4-chloro-o-toluidine have been shown to be the main contributors to occupational related carcinogenesis (12, 14).

In addition to occupational exposures, environmental exposure to arsenic is a significant contributor to the risk of development of bladder cancer. It was first noted that high levels of arsenic in drinking water was statistically associated with cancer in the 1960s by Tseng et. al. as part of a large population based study in Taiwan. The original intent of the project was to investigate the high rate of Blackfoot disease, a peripheral vascular disease, in association with arsenic levels, however incidental findings revealed a high rate of skin cancer among people with high exposure to arsenic. Arsenic concentration in the affect area's well water was measured at 1.097ppm, 100x greater than surrounding villages with arsenic free water (17). In additional follow up studies numerous groups identified multiple arsenic associated cancers, including bladder cancer (17-20). Currently analysis of bladder cancer risk associated with arsenic exposure suggests that a 10ug/L lifetime exposure would increase bladder cancer risk to 2 in 1,000, compared to the EPA risk range of 1 in 10,000 (21). Although epidemiologic data concerning high-dose exposure is consistent with increased bladder cancer risk, recent data suggests that using previously established predictive risk models may not be accurate for low-dose exposure (21).

Environmental exposures as a risk factor extend beyond chemical carcinogens to microorganisms. Although not typically seen in the United States, parasitic infection with

Schistosomiasis is endemic in Egypt and the more generally the Middle East. Schistosomiasis spreads through infected drinking water and can lead to weakness, diarrhea. There are four schistosomes that infect humans; *S. haematobium*, *S. Mansoni*, *S. Japonicum*, and *S. Mekongi*, of these, *S. Haematobium* is associated with increased risk of malignancy. Carcinomas of the intestine, liver and bladder have been linked to *S. Haematobium* infection (22). It is estimated that ~27% of all bladder cancer diagnosis in Egypt are associated with *S. Haematobium* infection (23). Bladder cancers associated with infection are more likely to be of the squamous cell carcinoma histologic subtype, whereas transitional cell carcinomas are more commonly diagnosed in the western world (23, 24). Although the mechanism of cancer initiation is unknown, multiple groups have shown that chronic infection, including urinary tract infections, may be a contributing risk factor to bladder cancer (25-27)

Taken together, bladder cancer represents a significant health concern for the elderly population and a large burden for the US healthcare industry. Although there are several known risk factors, including lifestyle, occupational and environmental factors, more research must be done to understand the mechanisms in which these contribute to the initiation and progression of bladder cancer.

1.3 Bladder Histology, Staging and Pathologic Subtypes

The urinary bladder has a multi-layered transitional epithelium (urothelium), of which the luminal most layer consists of umbrella cells. This specialized epithelium allows for a water-tight barrier and resistance to mechanical stress associated expansion and contraction of the bladder when filling and voiding urine. These unique features of the epithelium are in part conferred by the presence of urothelial plaques on the apical surface of cell. The plaques are protein complexes composed of two heterodimers bound to a heterotetramer of uroplakins (UP1a/UPK2 and UPK1b/UPK3) (28). Hu et. al. demonstrated that lost of the UPK3 significantly increased the cell's membrane permeability to both urea and water (29). Additionally, uroplakin loss is associated with decreased umbrella cell size and defects in the urinary tract (30).

Beneath the umbrella layer are the intermediate and basal layers. The basal cells has been proposed to be the progenitor cell for the urothelium and the potential cell of origin for bladder cancer (31-33). The basement membrane is a specialized extracellular matrix connecting the urothelial compartment to the lamina propria, which contains blood and lymphatic vasculature. The muscularis propria consists of three layers of muscle, which when contracted allows for the voiding of urine. The outer most layer of the bladder is the adventitia, this includes connective tissue and fat that lines the organ (Figure 1).

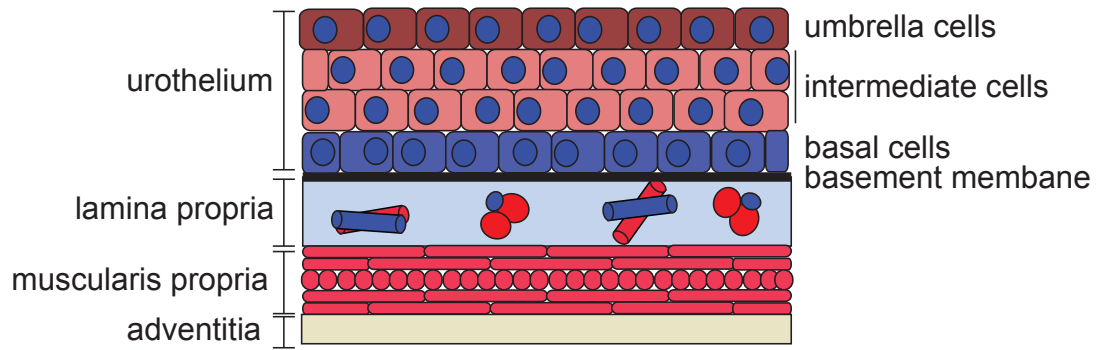


Figure 1: Bladder histology

A layer of transitional epithelial cells sits on top of a basement membrane, that separates the urothelium from the lamina propria. It is followed by a muscular layer (muscularis propria) and the adventitia.

Bladder cancer, which arises from the transformation of urothelial cells, is staged based on the degree of invasion into the underlying tissue (Figure 2). Pathologic stage is the most important prognostic factor for bladder cancer survival and is critical for informing treatment (9). Tumors diagnosed as Ta are tumors that are confined to the urothelium and do not invade into the lamina propria. These tumors can exist as either be low-grade (LG), papillary tumors, or high-grade (HG), carcinomas in situ (CIS). LG papillary tumors account for approximately 70% of tumors at diagnosis with HG tumors make up the remaining 30%. LG tumors have a good prognosis with a >95% five year survival, however need to be regularly monitored as reoccurrence is common in up to 80% of patients. Although high grade CIS are confined to the urothelium they are aggressive and may progress to invasive disease (1, 34).

Muscle invasive tumors ($\geq T2$) are almost exclusively HG and have a poor prognosis as compared to LG non-muscle invasive disease. Patients that are diagnosed with T2 tumors have a 63% five-year survival rate, which drops to 15% for patients diagnosed with T4, metastatic, or non-organ confined disease. Along with stage being critical to gauge prognosis, it also is an important factor in the determination of the course of treatment (1).

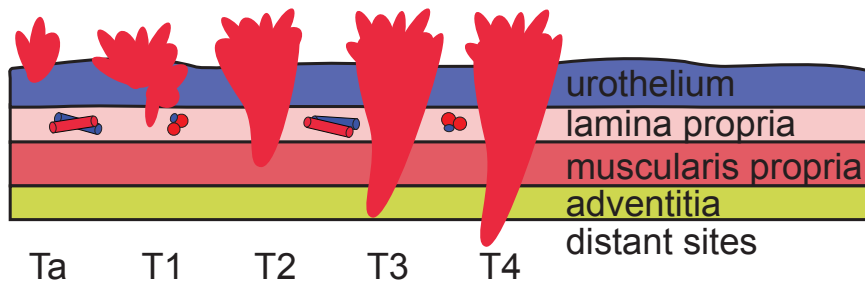


Figure 2: Bladder cancer staging

A diagram represents the degree of invasion as it relates to stage. Superficial tumors do not extend past the lamina propria (T0,T1). Once the tumor invades the muscularis propria they are considered invasive ($\geq T2$), tumors that have invaded neighboring organs or metastasized are classified as T4.

1.4 Bladder Cancer Treatment

As previously mentioned, the stage at diagnosis plays a critical role in determining the course of treatment. Currently the gold standard of care for non-muscle invasive bladder cancer is excision of the tumor via Transurethral Resection of Bladder Tumor (TURBT). During the procedure, the tumor is removed using a cystoscope inserted into the bladder through the urethra. Patients may, additionally, receive a one-time treatment with intravesical chemotherapy at the time of resection or a series of treatments over a period of multiple weeks. Patients that are deemed intermediate or high risk may also receive Bacillus Calmette-Guerin (BCG) treatment in combination with intravesical chemotherapy (35) (36). BCG is a live attenuated form of the bacterium *Mycobacterium bovis*. When the bacterium is instilled into the bladder it elicits an inflammatory response as well as triggers activation of the adaptive immune system (37, 38). It is proposed that this stimulation of the immune system helps to clear residual cancer cells after TURBT.

Whereas TURBT and surveillance is the preferred approach for LG disease, first line therapy for HG muscle invasive disease is radical cystectomy, often in combination with cisplatin based chemotherapy. Currently the combination treatment of GC (gemcitabine and cisplatin) is currently the most widely used, however the 4 drug therapy, MVAC (methotrexate, vinblastine, adriamycin and cisplatin), has shown similar effectiveness (39, 40). Despite the progress that has been made in other cancer types to develop targeted therapies, the paradigm for treatment of bladder cancer has not

shifted over the past decades. Because of this, new approaches need to be taken to elucidate the underlying mechanisms of bladder cancer in order develop better instruments to treat the disease, rather than relying of solely on surgery and chemotherapy.

1.5 Summary

Bladder cancer is a heterogeneous disease with two main histologic subtypes, which have differing histology, treatment and prognosis. Bladder cancer represents a major health concern in the geriatric population and a burden on the healthcare industry. The main risk factors for bladder cancer: smoking and occupational exposures to aromatic amines, are preventable and hopefully with the decrease in smoking rates over the past decade there will be a commensurate decrease in bladder cancer incidence. This underscores the importance of new research and education initiatives in the area of disease prevention and treatment. Although early detection and advances in treatment have lead to increases in the five-year survival rate across all cancer types by 19% over the past 30 years, a similar increase has not been seen in bladder cancer as survival rates have only increased by 8% over this same time period (1). The further understanding of the genomic underpinnings of this disease may help to facilitate the discovery of novel targeted therapies to increase survival rates.

Chapter 2: Bladder Cancer Genetics and Molecular Subtyping

2.1 Bladder Cancer Genetics

As there is a dichotomy in pathologic/histologic subtypes between LG papillary and HG muscle invasive disease, these subtypes also have distinct genomic features (Figure 3). LG papillary tumors are characterized by activating mutations in the oncogenes fibroblast growth factor 3 (*FGFR3*) and Harvey rat sarcoma viral oncogene homolog (*HRAS*), whereas HG muscle invasive tumors more typically have mutations causing the inactivation of the Retinoblastoma (RB) and p53 pathways (34, 41, 42). Additionally, with the advent of next generation sequencing, new highly prevalent mutations have been discovered, most notably the alterations in genes involved in chromatin modification and remodeling (43, 44).

FGFR3 is a receptor tyrosine kinase (RTK) that when activated, dimerizes and regulates cellular processes involved in proliferation, migration and survival (45). It has been observed that *FGFR3* activating mutations occur in up to 80% of LG tumors, making it the most frequent alteration in bladder cancer (34). The most frequent *FGFR3* mutation found in bladder cancer is S249C, which occurs within the extracellular domain, allowing for its constitutive dimerization and activation (46). Although *FGFR3* mutations do exist in HG tumors they do so at much less lower frequency, 5 -12% (43, 44) (34). One pathway *FGFR3* maybe signaling through in bladder cancer is the Ras-

MAPK pathway. Evidence for this is that *RAS* mutations are frequent in bladder occurring in 11-15%% of tumors, however they are mutually exclusive with *FGFR3* mutations (34).

In addition to *FGFR3* and *HRAS*, activation of the phosphatidylinositol 3-kinase (PI3K) pathway through mutations and copy number alteration of phosphatidylinositol-4,5-bisphosphate 3-kinase, catalytic subunit alpha (*PIK3CA*) has also been correlated with LG tumors (47-49). Interestingly, loss of phosphatase and tensin homolog (*PTEN*), which activates the PI3K pathway, is more associated in muscle invasive disease. This implicates the PI3K pathway in both LG and HG tumorigenesis, however each subtype has distinct pathway alterations, which are not mutually exclusive (48, 50).

Recently it has been noted that a significant number of chromatin modifying genes are mutated in bladder cancer, of which lysine (K)-specific demethylase 6A (*KDM6A*), also know as *UTX*, has been associated with LG tumors (44). Gui et. al. observed *KDM6A* mutations in ~30% of non-muscle invasive cases, where as the rate was only 15% in muscle invasive cases. Taken as a whole, LG bladder cancer has distinct genomic features, of which are a number that are potentially targetable.

As with LG bladder cancer, HG disease is associated with a unique set of genomic alterations. HG bladder tumors are enriched for mutations in the tumor suppressor gene Tumor Protein p65 (*TP53*) and inactivation of the RB pathway (34, 43). *TP53* is the most commonly mutated gene in HG bladder cancer with recent studies showing that mutations occurring in as many as 40% of bladder tumors (43, 44). Disruption of *TP53* leads to genomic instability though loss of cell cycle checkpoint

control in response to DNA damage (51). Additionally, bladder cancer is the first known tumor type to have mutations in the cyclin-dependant kinase inhibitor 1A (*CDKN1A*), p21, (14%).

HG bladder cancer also has a high rate of RB pathway alterations with multiple genes within the pathway either mutated or having copy number alteration (Figure 4). *RB1* is mutated in 13% of tumors sequenced by the TCGA and had copy number loss in an additional 14% of tumors. Immediately upstream of RB are the cyclin dependent kinases CDK4/6 and CDK2, and their regulators cyclin D1 and cyclin E1, which are encoded by *CCND1* and *CCNE1* respectively. Therefore, in bladder cancer, the focal amplification of *CCND1* (10%) and *CCNE1* (12%) allow for increases in activity of CDK4/6 and CDK2 respectively. Unphosphorylated RB normally binds the E2F family of transcription factors and prevents them from interacting with DNA. Cyclin / CDK complexes work to phosphorylate RB and this phosphorylation promotes its dissociation from E2Fs allowing them to translocate to the nucleus and bind to the promoters of target genes inducing cell cycle progression and proliferation (52).

Another mechanism by which the RB pathway can become inactivated is through loss of cyclin-dependent kinase inhibitor 2A (*CDKN2A*), which encodes the proteins p16/INK4A and p14/ARF. *CDKN2A* is only mutated in 5% of bladder tumors, however, it is the most frequently altered gene by copy number alteration, with 47% of tumors in the TCGA have some degree of copy number loss. Loss *CDKN2A* removes the inhibition of CyclinD1/CDK4/6 complex and allows for the phosphorylation of RB.

Upon phosphorylation by CDK4/6 or CDK2, RB releases E2F and allows for its translocalization to the nucleus. In bladder cancer, it has been observed that high E2F3

expression is associated with HG/invasive disease, additionally in the TCGA dataset E2F3 is amplified in 20% of the tumors (43, 53).

As with LG disease, next generation sequencing efforts have identified chromatin modifying genes that are significantly mutated in HG disease. In the TCGA data, after *TP53*, the next 3 most significantly mutated genes were Histone-lysine N-methyltransferase (*MLL2*), AT-rich interactive domain-containing protein 1A (*ARID1A*), and *KDM6A*. Gui et. al. has previously reported that *ARID1A* mutations are present in both HG and LG disease in roughly equal numbers, additionally *KDM6A* were present in both HG and LG, however it was significantly enriched within the LG tumors (44).

Both LG and HG bladder tumors have distinct but not necessarily mutually exclusive genomic alterations. These mutations and copy number events can lead to unique mRNA profiles both between and within the histologic bladder subtypes. These attempts to profile the tumors will be discussed in the remainder of this chapter.

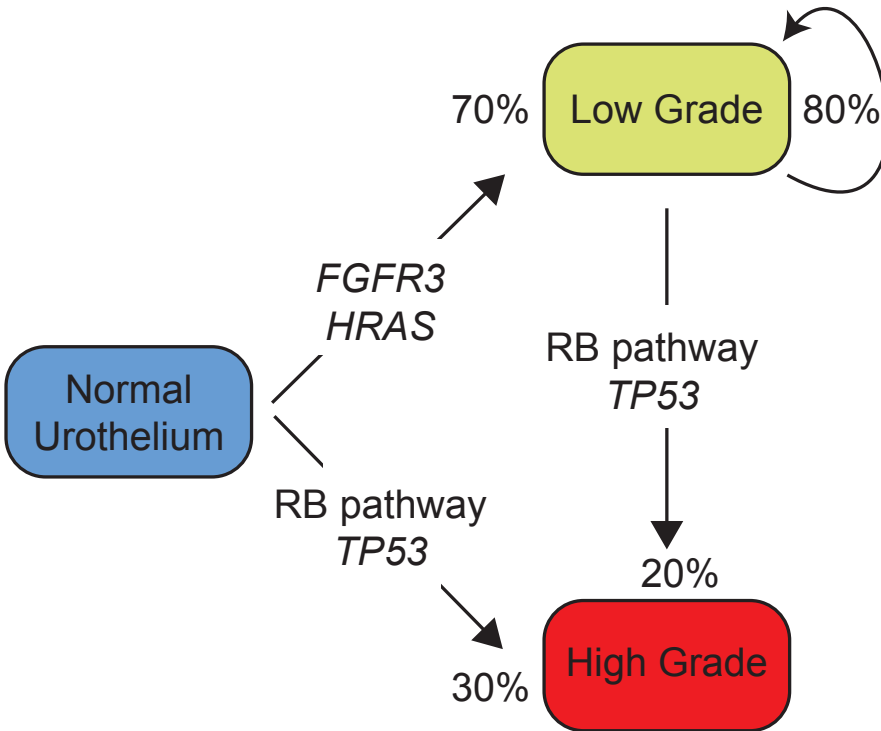


Figure 3: Genomic alteration in bladder cancer

Schematic of pathologic subtypes and predominate genomic alterations in each group. Percentages represent proportion of tumors at diagnosis, followed by recurrence/progression rate.

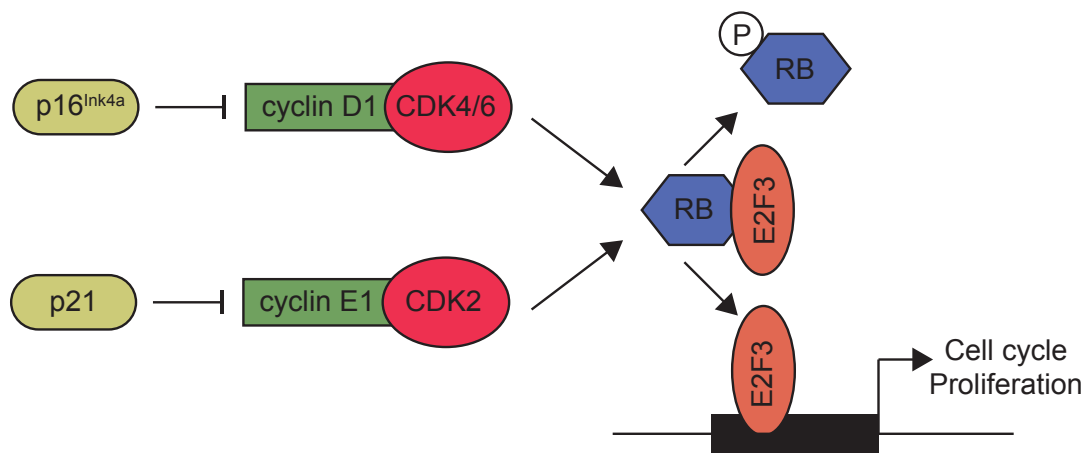


Figure 4: RB signaling pathway

Diagram of the RB signaling pathway. p21 and p16 inhibit CDK4/6 and CDK2 activity, respectively. Upon activation, the CDKs phosphorylate RB causing its disassociation with E2F3 allowing for E2F3 translocation to the nucleolus. E2F3 is then able to bind the promoter of its target genes inducing cell cycle progression and proliferation.

2.2 Molecular Signatures of Bladder Cancer

As previously discussed, LG non-invasive, and HG invasive, tumors have distinct genomic alterations. In addition to genomic alterations, numerous groups have reported on distinct gene expression patterns (54-60). In 2005, Blaveri et. al. reported that, using hierarchical clustering, muscle invasive and superficial tumors could be distinguished based on gene expression pattern. They then went on to identify a gene signature that can discriminate between superficial and muscle invasive disease, as well as signatures for prognosis and the classification of tumors as transitional cell carcinoma or squamous cell carcinoma (58). Similar approaches used by Sanchez-Carbayo et. al. resulted in gene profiles for the same two groups, superficial and invasive; however, they additionally reported generation of a signature of progression and metastasis by using patients with lymph node metastases and poor survival outcomes (56).

The Höglund group over the past 5 years has published a series of papers in which they have performed DNA and RNA analysis on a cohort of muscle invasive and superficial tumors. These papers initially identified two subtypes that they termed MS1 and MS2 which correlated highly with LG and HG histology respectively. The MS1 group contained increased FGFR3 mutations and was relatively genomically stable, whereas the MS2 group was enriched for TP53 mutations and high numbers of focal genomic amplifications (61). The group then went on to integrate the copy number, mutation and RNA data to identify five molecular clusters, of which three were primarily composed of invasive tumors (62). This was followed up using microarray data to identify five RNA based molecular subtypes of bladder cancer (Urobasal A, Genomically

Unstable, Infiltrate, Urobasal B, and SSC-like) . One of these subtypes encompassed the MS1 group previously described in Lindgren et. al., however the MS2 group was divided into 4 additional subtypes (63). Overall, Urobasal B and SCC-like have similar gene expression patterns, differing in the Urobasal B subtype having an increase in an FGFR3 signature. The increase in FGFR3 signature in the Urobasal B subtype may be the result of the Urobasal B subtype having a higher number of non-invasive tumors, whereas the SCC-like subtype has a majority invasive tumors (63). While the subtypes appear to be prognostic, it is important to note that the poor performing subtypes, SCC-like and Urobasal B, have the highest percentage of muscle invasive tumors. In 2013, Sjö Dahl developed an immunohistological staining strategy using 20 markers to identify the aforementioned subtypes. This IHC based strategy was only able to accurately separate the Urobasal A, SCC-like, and genomically unstable tumors, the authors noted that the Urobasal B tumors were unable to be reproducibly identified.

The inability to distinguish these two subtypes may be a reflection of the fact that the Urobasal B and SSC-like groups overall gene expression patterns are very similar. One of the common features of the SCC-like and Urobasal B groups is increased expression of keratin 5 (*KRT5*) and 14 (*KRT14*). The Chan group has since reported that high expression of *KRT14* is correlated to poor prognosis in bladder cancer (64). Both of these studies were performed using cohorts of HG and LG tumors raising the question of whether stratification of only muscle invasive tumors along the lines of keratin or other gene expression signatures still provide prognostic value.

To this point gene expression profiling efforts have focused on the utilization of a combination of LG and HG tumors, however, since pathologists can reliably identify LG and HG tumors, molecular signatures of these two groups are not clinically useful.

Multiple groups have recently addressed the identification of clinically relevant subtypes within HG tumors (43, 65, 66). These studies used cohorts of only HG tumors to identify multiple subtypes within HG bladder tumors. Choi et. al. identified three subtypes, basal, luminal and p53-like. The basal subtype was associated with decreased overall survival and high expression of high molecular weight keratins, similar to the SCC-like and Urobasal B subtypes reported by Sjödaahl, whereas the luminal subtype had improved survival and enrichment for *FGFR3* mutations. The third subtype, p53-like, was chemoresistant and had expression patterns related to wild type p53 expression (66).

In parallel, the Cancer Genome Atlas identified four subtypes, two subtypes (clusters I and II) had increased expression of markers of urothelial differentiation and decreased expression of keratins compared to cluster III and IV (43) This pattern of keratin expression was also a hallmark the subtypes identified by Sjödaahl et. al. and the basal and luminal subtypes identified by Choi et. al. (63, 66). Additionally, TCGA cluster IV had increased expression of genes associated with immune/tumor infiltrating cells. This similar expression pattern was also present in the subtypes discovered by Choi (p53-like) and Sjödaahl (infiltrated). Sjödaahl noted that the tumors within the infiltrated group stained for increased numbers of T cells and myofibroblasts, raising the question of whether the differences in gene expression stem from intrinsic tumor cell differences or the gene expression patterns of the tumor microenvironment..

When comparing common features between these three studies, a picture emerges of 2-3 unique subtypes; 1) FGFR3 high, UPK high; 2) KRT high with squamous differentiation; 3) samples with increased tumor infiltrating cells. While these subtypes seem to be reproducible and have been suggested to be prognostic, there still remains a need to derive a clinically useful tool for discriminating the subtypes based on a minimal set of differentially expressed genes.

This dissertation presents work that defines subtypes similar to those previously mentioned, creates a prognostic gene expression based classifier, and more broadly correlates the expression patterns of bladder cancer to those seen in breast cancer.

	Sjödahl					Choi			TCGA			
	Urobasal A	Genomically Unstable	Infiltrated	Urobasal B	SCC-Like	Luminal	p53-Like	Basal	I	II	III	IV
FGFR3	Red	Green	Green	Green	Green	Red	Green	Green	Red	Red	Green	Green
UPK	Red	Red	Green	Green	Green	Red	Green	Green	Red	Red	Green	Green
KRT	Green	Green	Green	Red	Red	Green	Green	Red	Green	Green	Red	Red
Squamous Diff	Green	Green	Green	Green	Red	Green	Green	Red	Green	Green	Red	Red
Infiltrate Cells	Green	Green	Red	Green	Green	Green	Red	Green	Green	Green	Green	Red

Table 1: Comparison of muscle invasive subtypes

Summary

Taken together, evidence supports the notion that distinct genomic and transcriptional profiles characterize LG and HG disease. LG disease is characterized by alterations of *FGFR3*, *PIK3CA*, and *RAS* as well as decreased levels of markers of differentiation and proliferation as compared to HG disease. HG bladder tumors are genomically unstable as compared to LG tumors and have alterations in DNA-damage response and cell cycle control. Additionally, HG bladder cancer is heterogeneous with varying degrees in expression of *ERBB2*, *FGFR3* and genes involved in urothelial differentiation. While previous studies have identified molecular subtypes with some success, none have created a gene expression based predictor to differentiate molecular subtypes within HG muscle invasive bladder cancer.

Chapter 3: Intrinsic subtypes of high-grade bladder cancer reflect the hallmarks of breast cancer biology¹

3.1 Overview

We sought to define whether there are intrinsic molecular subtypes of high-grade bladder cancer. Consensus Clustering performed on gene expression data from a meta-dataset of high-grade, muscle invasive bladder tumors identified two intrinsic, molecular subsets of high-grade bladder cancer: “luminal” and “basal-like” that have characteristics of different stages of urothelial differentiation, reflect the luminal and basal-like molecular subtypes of breast cancer, and have clinically meaningful differences in outcome. A gene set predictor: Bladder cancer Analysis of Subtypes by Expression (BASE47) was defined by Prediction analysis of microarrays (PAM) and accurately classifies the subtypes. Our data demonstrate that there are at least two molecularly and clinically distinct subtypes of high-grade bladder cancer and validate the BASE47 as a subtype predictor. Future studies exploring the predictive value of the BASE47 subtypes for standard of care bladder cancer therapies as well as novel subtype-specific therapy is warranted.

¹ A version of this work has been previously published and was reprinted with permission from the publisher. Damrauer et. al. Intrinsic subtypes of high-grade bladder cancer reflect the hallmarks of breast cancer biology, PNAS, 111(8):3110-5,2014

3.2 Introduction

In the United States, urothelial carcinoma (UC) of the bladder is the fourth most common malignancy in men and eight most common in women with 74,690 new cases and 15,580 deaths expected in 2014 (1). Bladder cancer is heterogeneous and can be histologically divided into low-grade and high-grade disease. While low-grade tumors are almost invariably non-invasive (Ta), high-grade tumors can be classified based on whether tumors have invaded into the muscularis propria of the bladder: non-muscle invasive bladder cancer (NMIBC, Tis, Ta, T1) and muscle invasive bladder cancer (MIBC, \geq T2). Low-grade tumors are associated with a high rate of recurrence, yet an excellent overall prognosis with a 5-year survival in the range of 90%. In contrast, high-grade, muscle-invasive bladder cancer has a relatively poor 5-year overall survival: 68% when T2 and decreasing to 15% for non-organ confined disease (pT3 and pT4) (1, 34).

Along with divergent pathologies and prognosis, low-grade and high-grade UCs are associated with distinct genetic alterations. For example, low-grade UC is enriched for activating mutations in *FGFR3*, *PIK3CA* and inactivating *UTX* mutations, whereas high-grade, muscle-invasive tumors are enriched for *TP53* and *RB1* pathway alterations (41, 42, 44, 47, 62, 67-69).

Several reports have examined the gene expression profiles of primary bladder tumors. From these studies, it is apparent that low-grade, non-invasive and high-grade, muscle-invasive tumors harbor distinct gene expression patterns and that further molecular subsets can be found within low-grade and high-grade tumors (56-58, 61, 70). Moreover, a number of gene signatures have been developed that can predict

tumor stage, lymph node metastases, or bladder cancer progression (54-60). Taken together, there are established gene expression patterns that differentiate low-grade and high-grade tumors, however there is little data identifying intrinsic subtypes specifically within high-grade disease. We have identified two intrinsic, molecular subsets of high-grade bladder cancer: “luminal” and “basal-like” with differences in clinical outcome. In addition, we have developed a 47-gene predictor, “BASE47”, which can accurately classify high-grade UC into luminal and basal-like tumors. The molecular subtypes appear to reflect different stages of urothelial differentiation and strikingly recapitulate aspects of breast cancer biology, including a claudin-low subtype.

3.3 Results

Consensus Cluster reveals two distinct molecular subtypes of high-grade bladder cancer.

Previous studies examining the gene expression changes associated with bladder cancer have assessed both low and high grade tumors in aggregate (56-58, 63, 67, 71). We therefore looked exclusively for intrinsic subtypes of high-grade disease agnostic to clinical stage or outcome. We first created a meta-dataset of 262 high grade, muscle-invasive tumors, curated from four publically available datasets (57, 63, 71, 72)) (Table 2). In parallel, two independent sets of high-grade tumors from MSKCC and the TCGA were used as validation (MSKCC n=49, TCGA n=129) (69). In both the meta and MSKCC datasets, Consensus Cluster identified two groups (K=2) as the optimal number of molecular subtypes as defined by the criterion of subclass stability (Figure 5A, 5B 5C and Supplemental Figure 1A, 1B).

To validate that the gene expression changes that define the two subtypes are similar, we determined the correlation between the median gene expression (using all common genes between datasets) for each subtype (yellow = correlation, blue=anti-correlation) (Figure 5D). There appeared to be a high level of correlation between the meta-dataset Cluster 1 (K1) and MSKCC and TCGA Cluster 2 (K2) as well as the meta-dataset Cluster 2 (K2) and MSKCC and TCGA Cluster 1 (K1). Therefore, the intrinsic molecular subtypes defined by independent discovery in the two datasets are defined by highly concordant gene expression patterns and suggest that the subtypes are robust.

The intrinsic molecular subtypes of bladder cancer differentially express markers of urothelial differentiation.

To understand the gene expression patterns that differentiate the intrinsic subtypes of high-grade bladder cancer, we performed 2-class significance analysis of microarrays (SAM) comparing Cluster 1 and Cluster 2 from the meta-dataset. 2,393 genes were found to be differentially expressed (FDR cut off of 0) (Appendix A). The intrinsic molecular subtypes were characterized by gene expression patterns representative of urothelial differentiation. Cluster 1 (K1) of the meta-dataset, expressed high levels of the high molecular weight keratins [HMWK] (*KRT14*, *KRT5*, *KRT6B*) and *CD44*, which are expressed in urothelial basal cells (33, 73). In contrast, Cluster 2 (K2) expressed high levels of uroplakins (*UPK1B*, *UPK2*, *UPK3A*) as well as the low molecular weight keratin (LMWK), *KRT20* (Figure 5E), characteristic of urothelial umbrella cells (73). Moreover, the gene expression of *KRT5* was inversely correlated with both *UPK2* and *KRT20* across all tumors (Supplemental Figure S1D and S1E). Similar findings were seen in the MSKCC dataset (Supplemental Figure S1F-S1G).

Ingenuity Pathway Analysis (IPA) was used to understand if processes other than urothelial differentiation were associated with the intrinsic subtypes. IPA revealed that Cluster 1 (K1) tumors were enriched in gene pathways involving cancer, cell survival, as well as cell movement (Figure 5F). In aggregate, these findings demonstrate that the two molecular subtypes of high-grade, muscle-invasive bladder cancer represent different stages of urothelial differentiation, leading us to name Clusters 1 and 2 “Basal-like” and “Luminal”, respectively.

Bladder Cancer Analysis of Subtypes by Expression of 47 genes (BASE47)

accurately predicts basal-like and luminal subtypes.

We next sought to define a minimal set of genes that could accurately classify bladder tumors into the luminal and basal-like bladder intrinsic subtypes. To this end, we applied prediction analysis of microarrays (PAM) to our meta-dataset and derived a 47-gene signature (Appendix B) that could accurately classify basal-like and luminal tumors relative to Consensus Cluster calls (Figure 6). A pairwise comparison of the subtype classification by Consensus Cluster relative to classification by BASE47, showed a strong correlation in the Meta Dataset, MSKCC and TCGA datasets (both chi square $p < 0.001$).

BASE47 Subtypes correlate to previously published tumor subtypes

Two papers published concurrently with Damrauer et. al. reported multiple molecular subtypes within HG bladder cancer. To determine if our subtypes were similar to those published by the TCGA and Choi et. al. subtype calls on the TCGA dataset were obtained from aforementioned authors. The TCGA data set was then hierarchically clustered by the BASE47 gene list and each group's subtype calls were overlaid (Figure 7A). The number of tumors called basal or luminal by the BASE 47 were then graphed according to the calls from Choi et. al. and the TCGA (Figure 7C and 7D). Overall the subtypes are highly concordant, showing that the subtypes can be reproducibly discovered.

Intrinsic bladder subtypes have differential survival.

We next asked whether the intrinsic bladder subtypes, had prognostic significance. Basal-like tumors (as determined by BASE47) had a significantly decreased disease-specific and overall survival ($p=0.0194$ and $p=0.0198$ respectively) (Figure 8A). Moreover, of the clinicopathologic features available to us in the MSKCC dataset (TNM Stage, mixed histology, and gender), only BASE47 subtype was found to be significant for disease specific survival by univariate analysis (Table 3, and Supplemental Figure S2A). Furthermore, to assess the prognostic value of the BASE47 relative to published prognostic signatures derived from muscle-invasive, high-grade tumors, we generated “Good” and “Poor” prognosis calls on the MSKCC tumors using the published gene lists (56, 58) (Supplemental Figure S2B and S3C). However, neither gene signature held prognostic value (Supplemental Figure S2D and S2E). Therefore, the BASE47 intrinsic bladder subtypes not only reflect bladder cancer biology but have prognostic value.

Interestingly, while the BASE47 predictor was developed on muscle-invasive tumors, we also noted that when applied to a meta-dataset of superficial tumors, it classified a significant proportion them as basal-like (Figure 8C), suggesting that the intrinsic subtypes may exist in non-muscle invasive bladder cancer and that the BASE47 might serve as a prognostic marker of recurrence and / or progression in non-muscle invasive bladder cancer.

The intrinsic subtypes are associated with distinct genomic alterations.

The MSKCC tumors have been previously characterized for bladder cancer relevant genetic alterations (69). We examined the relative enrichment of these molecular events in the bladder subtypes (Figure 8D). Notably, *FGFR3* ($p < 0.001$) and *TSC1* ($p = 0.02$) mutations were significantly enriched in the luminal subtype while RB1 pathway alterations were significantly enriched in basal-like bladder cancer ($p = 0.009$).

Multiple studies have shown that females have a poorer bladder cancer specific outcome than males (74). There was a trend towards enrichment of basal-like tumors in female patients in the MSKCC dataset (Figure 8D, $p = 0.1137$), and a significantly higher incidence of basal-like bladder cancer in female patients in the meta-dataset with annotated gender and TCGA (Figure 8E and Figure 9). This enrichment of basal-like bladder cancer may in part explain the decreased cancer specific outcomes in women.

Additionally, the TCGA provided clinical data associated with race, grade and histology. Interestingly, the papillary histology that is classically associated with LG tumors, is enriched in the luminal subtype ($p = 0.018$). The luminal subtype was also enriched for low-grade tumors, muscle invasive tumors ($p = 0.011$). Basal tumors, as previously noted, were enriched for female patients as well as trended toward enrichment in African Americans ($p = 0.07$), where as luminal tumors were enriched for Asian patients ($p = 0.0004$) (Figure 9).

Basal-like bladder cancer is enriched for the signatures of basal-like breast cancer and tumor initiating cells (TIC).

A number of genes fundamental for breast development and breast cancer were co-regulated with genes that regulate urothelial development (Supplemental Figure S3,

breast cancer related genes: red, urothelial related genes: blue). Moreover, when Gene Set Enrichment Analysis (GSEA) was performed on the meta-dataset to identify gene sets enriched in the intrinsic subtypes, multiple breast cancer-related gene signatures were enriched in the basal-like bladder subtype as well as signatures related to mammary stem cells (Appendix C). Conversely, multiple breast cancer derived luminal gene signatures were enriched in the luminal bladder cancer subtype. In keeping with these findings, we saw that a previously published bladder TIC signature (33) was enriched in the basal-like subtype by both hierarchical clustering (chi squared $p = 2 \times 10^{-16}$) (Supplemental Figure S4A) as well as by GSEA (Supplemental Figure S4B) suggesting that basal-like bladder cancer possesses a more “stem-like” phenotype, similar to previous observations described in basal-like breast cancer (75).

The intrinsic bladder subtypes reflect the attributes of breast cancer subtypes

We next asked whether the basal-like and luminal bladder cancer subtypes correlated with any of the previously defined molecular subtypes of breast cancer (76, 77). To this end, we generated breast molecular subtype classifications (Basal, Her2-enriched, Luminal A, Luminal B, and Normal-like) on two independent sets of breast tumors (TCGA Breast (78) and UNC337 (79)) using the PAM50 nearest centroid classifier (80). To see whether the gene expression patterns of luminal and basal-like bladder cancer were reflected in the intrinsic breast subtypes, we correlated the centroid gene expression (using the breast intrinsic gene list) between the bladder (bladder tumors) and breast (breast tumors) subtypes (Figure 10A: yellow=correlation, blue=anti-correlation). Basal-like bladder cancer had positive correlations to basal-like breast as

well as normal-like breast whereas luminal bladder cancer had positive correlations to both lum A and lum B breast subtypes. A similar comparison using published gene expression data from The Cancer Genome Atlas (TCGA) showed that while there were other cross-cancer similarities, the molecular association between breast and bladder cancer was relatively strong (Supplemental Figure S4C). Finally, strikingly, when the PAM50 was applied to our meta-dataset of bladder tumors, there were positive correlations between basal-like bladder tumors and the basal centroid and luminal bladder tumors and the luminal A centroid (Supplemental Figures 4D and 4E).

To better visualize this association, we hierarchically clustered the bladder tumors using a comprehensive list of 1906 genes (1,426 were present in the meta-dataset) that have been previously shown to define the intrinsic subtypes of breast cancer (80). The breast specific gene list clustered the bladder tumors along the lines of basal-like and luminal bladder subtypes (chi squared $p=2.2e-16$) (Supplemental Figure 4F). Furthermore, gene signatures representative of basal-like and luminal breast cancer as well as well-defined breast cancer related oncogenic pathway signatures faithfully clustered basal-like and luminal bladder tumors in both datasets (Figure 10B and Supplemental Figure 5A). Basal-like bladder tumors displayed enhanced MYC and E2F3 pathway signatures while luminal tumors appeared enriched in the set of genes characteristic of the HER2 amplicon. These data in aggregate strongly demonstrate that the gene expression patterns that distinguish basal-like and luminal bladder cancer reflect the RNA expression patterns that define the intrinsic subtypes of breast cancer.

A subset of basal-like bladder tumors are claudin-low

The recently described claudin-low molecular subtype of breast cancer is characterized by low expression of the claudin tight junction proteins (claudins 3, 4, and 7) and upregulation of markers of EMT as well as stem cell-like features (79). Tumors from the meta-dataset were classified based on an 807 gene signature, which accurately defines claudin-low breast cancer (79). Overall, 16% of the meta-dataset tumors (Figure 5A) and 26% of the MSKCC tumors (Supplemental Figure S8) were identified as claudin-low. When clustered based on genes that define key molecular pathways in claudin-low breast tumors (Breast cancer subtype markers, EMT markers, and TIC markers) (Figure 11A and Supplemental Figure 5B), the claudin-low bladder tumors displayed expression patterns indicative of claudin-low breast tumors. Therefore, a subset of basal-like bladder tumors have claudin-low features.

3.4 Discussion

Using independent discovery in distinct datasets, we have defined two molecular subsets of high-grade urothelial carcinoma. The subtypes harbor molecular features that reflect different stages of urothelial differentiation. Luminal bladder cancers express markers of terminal urothelial differentiation such as those seen in umbrella cells (*UPK1B*, *UPK2*, *UPK3A*, and *KRT20*) while basal-like tumors express high levels of genes that typically mark urothelial basal cells (*KRT14*, *KRT5*, and *KRT6B*). The basal cell compartment is a common feature of most organs with stratified or pseudostratified epithelium. It is characterized by its proximity to the basal lamina and is thought to harbor multipotent tissue stem cells important for normal tissue homeostasis and orderly regeneration after injury. Because basal cells are a long-lived population, they are potentially more likely to incur multiple genomic alterations including changes in their chromatin landscape. In this regard it is interesting to note that there appears to be a relatively high prevalence of mutations in histone and chromatin modifying genes in urothelial carcinoma (44).

The luminal and basal-like subtypes of bladder cancer reflect many of the hallmarks of the intrinsic breast cancer subtypes. For example, a number of basal-like and luminal breast cancer specific gene signatures were enriched in the corresponding bladder subtype including bona fide luminal breast cancer pathways such as GATA3 and estrogen receptor signaling in the luminal bladder subtype. Moreover, the gene expression patterns that define luminal and basal-like bladder cancers corresponded highly with the gene expression patterns that define luminal (Lum A and Lum B) and

basal-like breast cancer. These similarities may reflect the presence of urothelial basal cells and their corollary, the basal/myoepithelial cells of the breast. In both tissues, these basal cells represent a multipotent “stem/progenitor cell” population (81, 82) and their similar functional roles may explain their similar molecular profile.

There were differences between the breast and bladder cancer intrinsic subtypes as well. For example, while we identify a claudin-low subtype of bladder cancer. In contrast to breast cancer in which claudin-low tumors arise from multiple intrinsic subtypes, all of the claudin-low bladder tumors were a subpopulation of the basal-like subtype. Furthermore, despite a subset of luminal bladder tumors having elevated expression of the HER2 amplicon, we did not see any significant correlation to the Her2-enriched breast subtype by our correlation matrix (Figure 10A).

Our study has created a gene signature, the BASE47, which accurately discriminates intrinsic bladder subtypes. Interestingly, even in superficial bladder tumors, there appears to be a significant number of basal-like tumors. While the characteristics of our meta-dataset did not allow us to determine whether the subtypes were prognostic or predicted the progression to muscle-invasive disease in superficial bladder tumors, these will be important questions to answer and have important clinical implications such as early cystectomy for patients with high-grade T1 disease. The ability to accurately classify basal-like and luminal bladder subtypes with only 47 genes (BASE47) should allow the adoption of the BASE47 to formalin-fixed, paraffin embedded (FFPE) tissues allowing its widespread use.

Female patients with UC have worse outcomes to males, even when controlled for other known prognostic variables, such as stage and grade (74). Interestingly, we

found that females have an increased incidence of basal-like bladder cancer, which is associated with a worse outcome. To what extent this increased prevalence of basal-like bladder tumors in women contributes to their poorer outcome remains unclear. Moreover, whether this association suggests that the pathogenesis of bladder cancer in females (i.e. chronic inflammation) is different should be of future interest.

In summary, the basal-like and luminal intrinsic subtypes of bladder cancer reflect many aspects of physiologic urothelial development as well as breast cancer biology. These findings underscore the notion that there are common themes underlying the development and maintenance of solid tumors that extend beyond overlapping mutational spectra. An appreciation of subtype heterogeneity has substantially furthered our understanding of breast cancer biology. Our results suggest that the intrinsic subtypes of high grade bladder cancer strikingly reflect many aspects of breast cancer. It will be particularly interesting to see whether the bladder subtypes, like the breast subtypes are useful for stratification for therapy.

3.5 Materials and Methods

Training Dataset Analysis – A meta-dataset was generated by combining the muscle invasive ($\geq T2$) UC samples from four publically available data sets (GSE13507, GSE31684, GSE32894, GSE5287) with clinical annotation provided by the Michor Lab (Dana-Farber Cancer Institute, Boston MA). The data were normalized, median centered by gene, and merged into a single dataset consisting of $n=262$ tumors. The Mean Absolute Deviation (MAD) was computed across samples by gene. Genes with a MAD score of >0.10 were selected for clustering analysis (7303 genes). Consensus hierarchical clustering was performed as described previously (83) with 90% resampling and 1000 iterations. Two Class significance analysis of microarrays (SAM; FDR=0) was performed to generate subtype-specific gene lists (84). The significant genes and corresponding fold changes as determined by SAM were analyzed by Ingenuity IPA (Ingenuity Systems, Redwood City, CA) for predicted pathway activation. Gene set enrichment analysis (GSEA) was performed comparing basal and luminal tumors against MSigDBv4.0c2 (85, 86).

Validation Datasets – Gene expression data were derived from 49 high-grade tumors from Memorial Sloan-Kettering Cancer Center (MSKCC) using Human HT-12 Expression BeadChip arrays (Illumina) as previously described (69). The MSKCC and TCGA datasets were normalized, median centered and the MAD was computed across samples by gene. Genes with a MAD score of >0.10 were selected for clustering analysis. Consensus clustering was performed identically to the

meta-dataset (83). The resulting subtypes assignments for K=2 using consensus cluster plus were used to validate the training dataset. Centroids were generated for both the Meta and MSKCC datasets using all common genes and correlations were calculated by 1-Pearson correlation. Copy number alterations and hotspot mutation analyses were determined as previously described(69).

Subtype Predictor – Prediction Analysis of Microarrays (PAM) was used to determine the minimal number of genes that could accurately predict subtype classification on the meta-dataset using the consensus clustering calls as the reference (87). The resulting 47-gene predictor (delta=6.3) was then used to classify the MSKCC samples (87). Tumors were then analyzed for enrichment of mutations or copy number alteration (69) by chi square or fisher's exact test when appropriate. Categorical survival analyses were performed using a log-rank test and visualized with Kaplan-Meier plots. The BASE47 was then applied to superficial tumors, which were excluded from the Meta dataset. The superficial were normalized and median centered as previously described and BASE47 calls were made using PAM.

Correlation to Breast Cancer – The breast cancer dataset from the Cancer Genome Atlas project (78) as well as a UNC dataset, UNC337 (GSE18229) mRNA datasets were log transformed and median centered. Breast and bladder subtypes were compared using a pearson correlation (visualized as 1-pearson) by the median gene expression of the breast cancer intrinsic gene list (80). Heatmaps were generated using the 1-pearson values. PAM50 calls were made on the individual data sets that

composed the meta dataset and the MSKCC dataset as described in (80). Breast cancer signature enrichment was performed as described in (88), samples were hierarchically clustered and visualized on a heatmap. Claudin low subtype calls were made as previously described (79).

3.6 Figures

Table 2: Dataset Characteristics

	Training Datasets (Meta)				Validation Dataset
	Als	Kim	Riester	Sjödahl	Iyer
GEO ID	GSE5287	GSE13507	GSE31684	GSE32894	cBioPortal
Clinical Characteristic	No.	No.	No.	No.	No.
Sex					
Male	NA	NA	57	68	35
Female	NA	NA	21	25	14
Stage					
pT0	0	23	5	116	4
pT1	0	80	10	97	6
pT2	0	31	17	85	5
pT3	0	19	42	7	17
pT4	30	11	19	1	16
NA	0	0	0	0	1

Table 3: MSKCC - Univariable Cox Regression Analysis of Disease Specific Survival

Variable	Comparison	HR	95% CI	p-value
BASE47	Basal vs Luminal	3.1722	1.144-8.798	0.0265
Stage	III vs II	3.188	0.040-25	0.27
	IV vs II	3.409	0.434-26.76	0.243
Mixed Histology		1.034	0.438-2.438	0.939
Gender		0.98838	0.376-2.592	0.981

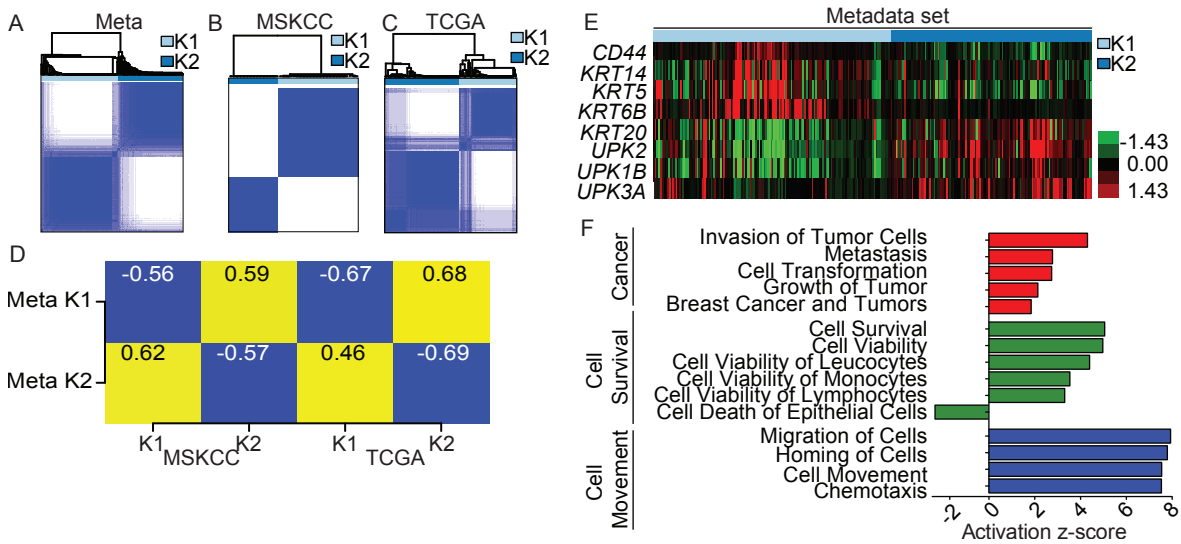


Figure 5: Discovery of two distinct subtypes of bladder cancer

(A) Consensus Clustering was performed on 262 muscle-invasive tumors, curated from four publicly available datasets (Meta dataset), yielding two subtypes. **(B)** Consensus Clustering was independently performed on a dataset of high-grade bladder tumors obtained from MSKCC (n=49) as well as the **(D)** TCGA dataset (n=129). **(C)** The median gene expression of all common genes between the datasets were compared and the Pearson correlation was plotted (yellow=correlation, blue=anti-correlation). Numerical values represent the Pearson correlation. **(E)** Gene expression of epithelial and urothelial markers were visualized by heatmap, supervised by consensus cluster plus calls in the meta-dataset. KRT5 mRNA expression was plotted **(F)** Significantly differentially expressed genes between K1 and K2 from the meta-dataset and their respective fold change, as determined by 2-class SAM (3,374 genes, FDR=0) were analyzed for predicted pathway enrichment by Ingenuity Pathway Analysis (IPA). Selected significant pathways enriched in K1 are represented.

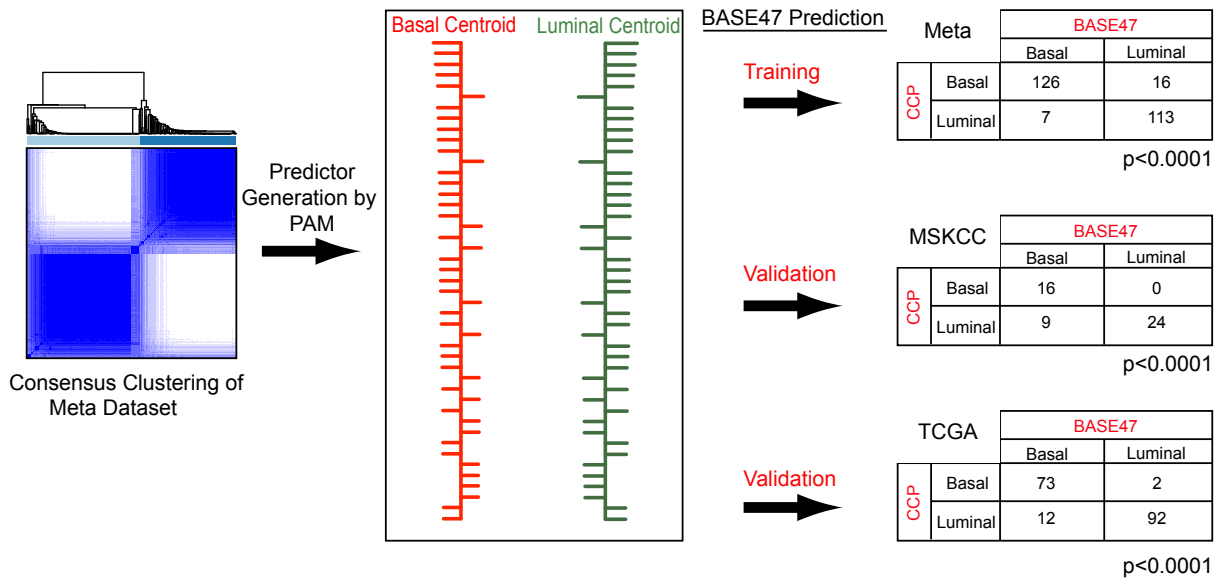
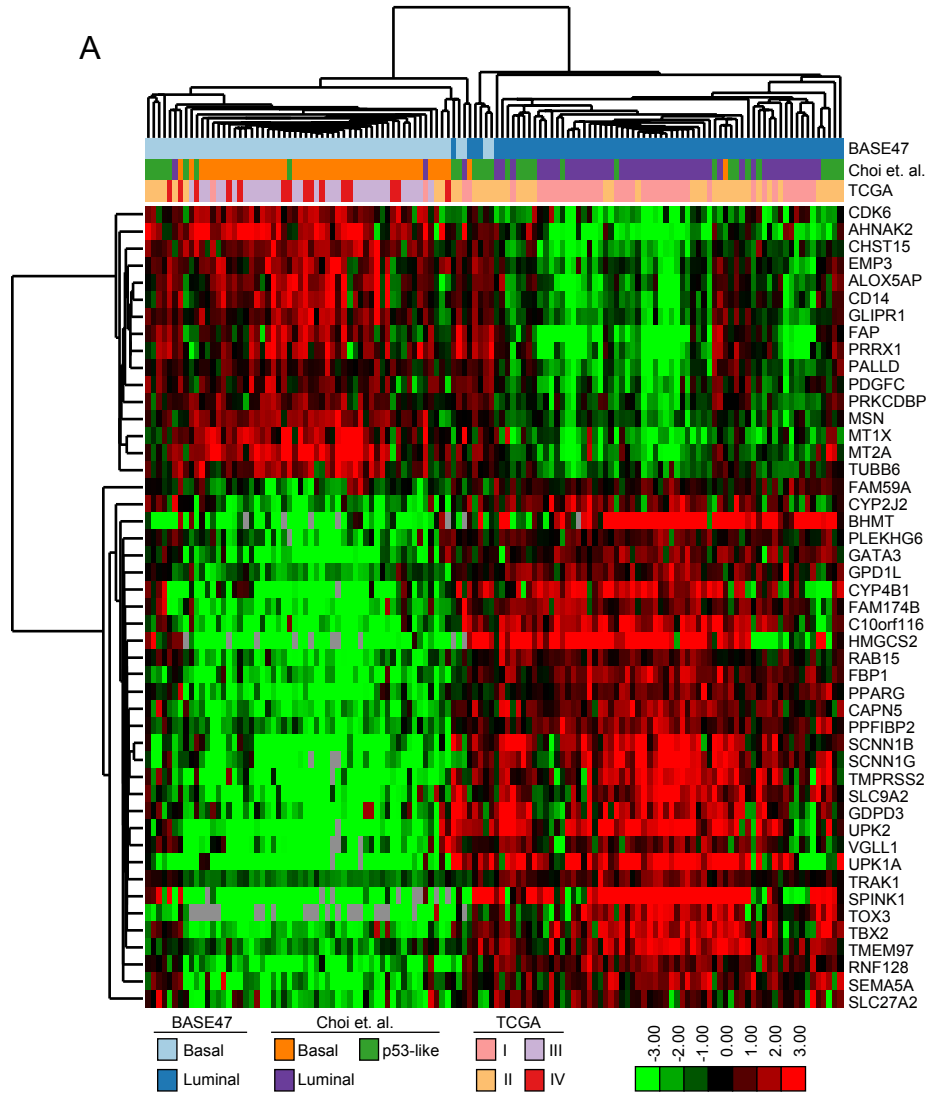
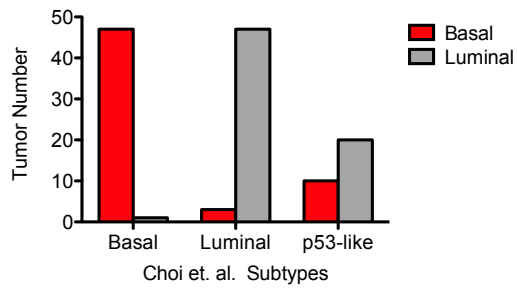


Figure 6: Generation of the BASE47 subtype predictor

(A) Prediction Analysis of Microarrays (PAM) was performed using the basal-like and luminal subtype calls generated by consensus cluster plus. A predictor consisting of 47 genes was generated that accurately predict the subtypes from the meta-dataset training set ($p < 0.001$) as well as a MSKCC validation dataset (45/47 genes present) ($p < 0.001$). **(B)** The BASE47 gene list was used to cluster the MSKCC dataset, showing two distinct expression profiles. BASE47 genes are listed along the right.



B BASE47 Calls vs. Choi Calls



C BASE47 Calls vs. TCGA Calls

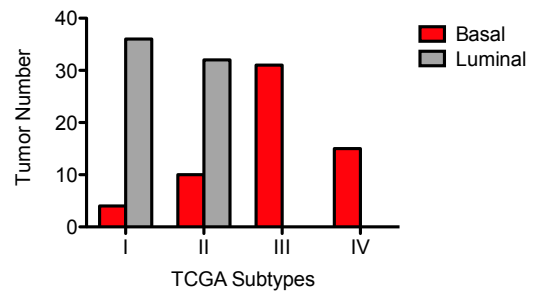


Figure 7: BASE47 calls are similar to previously published calls for the TCGA

dataset (A) Consensus clustering of the TCGA dataset by BASE47 gene signature.

Graphs representing the number of basal and luminal tumors and how they were classed according to (B) Choi et. al. and (C) the TCGA.

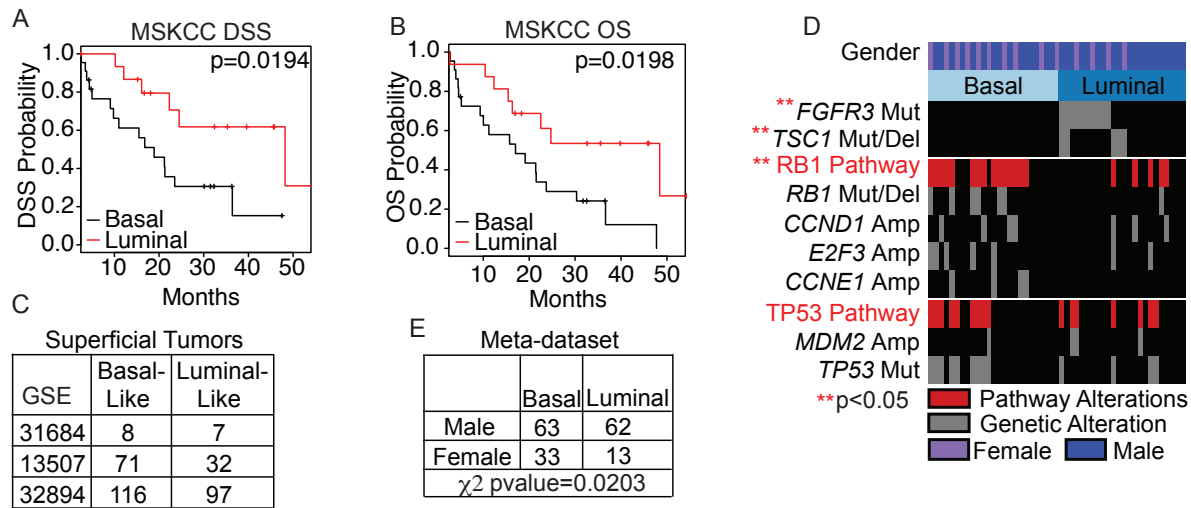


Figure 8: Luminal and basal bladder cancer have differential survival and are associated with distinct genomic alterations

A Kaplan-Meier plot for muscle-invasive tumors from the MSKCC set (\geq pT2) was generated for **(A)** disease specific and **(B)** overall survival. Basal-like tumors ($n=22$) had a significantly decreased disease free and overall survival as compared to luminal tumors ($n=16$) ($p=0.0194$ and $p=0.0081$ respectively). **(C)** Superficial tumors, which were not included in the generation of BASE47, were subjected to BASE47 subtype prediction. **(D)** Sequencing was performed on common mutations in bladder cancer. *FGFR3* and *TSC1* alterations were significantly enriched in luminal bladder cancer whereas alterations of the *RB1* pathway were enriched in basal-like bladder cancer. *TP53* alterations were distributed evenly in both subtypes. **(E)** Basal-like and luminal tumors from the meta-dataset were annotated for gender (2/4 datasets). Basal-like bladder cancer was significantly enriched in female patients (chi square p value=0.0203).

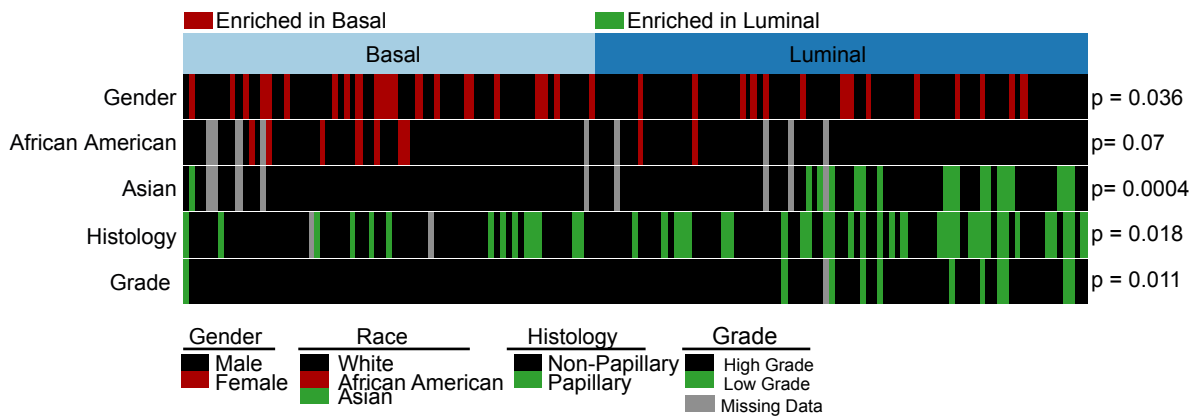


Figure 9: Basal and luminal bladder cancer have distinct clinical features.

Clinical data for the TCGA tumors were correlated to the basal and luminal subtype calls. Basal bladder cancer was enriched for female patients ($p=0.036$) trended toward enrichment in African American patients ($p=0.07$) Luminal bladder cancer was enriched for Asian patients ($p=0.0004$), as well as papillary histology ($p=0.018$) and low grade tumors ($p=0.011$).

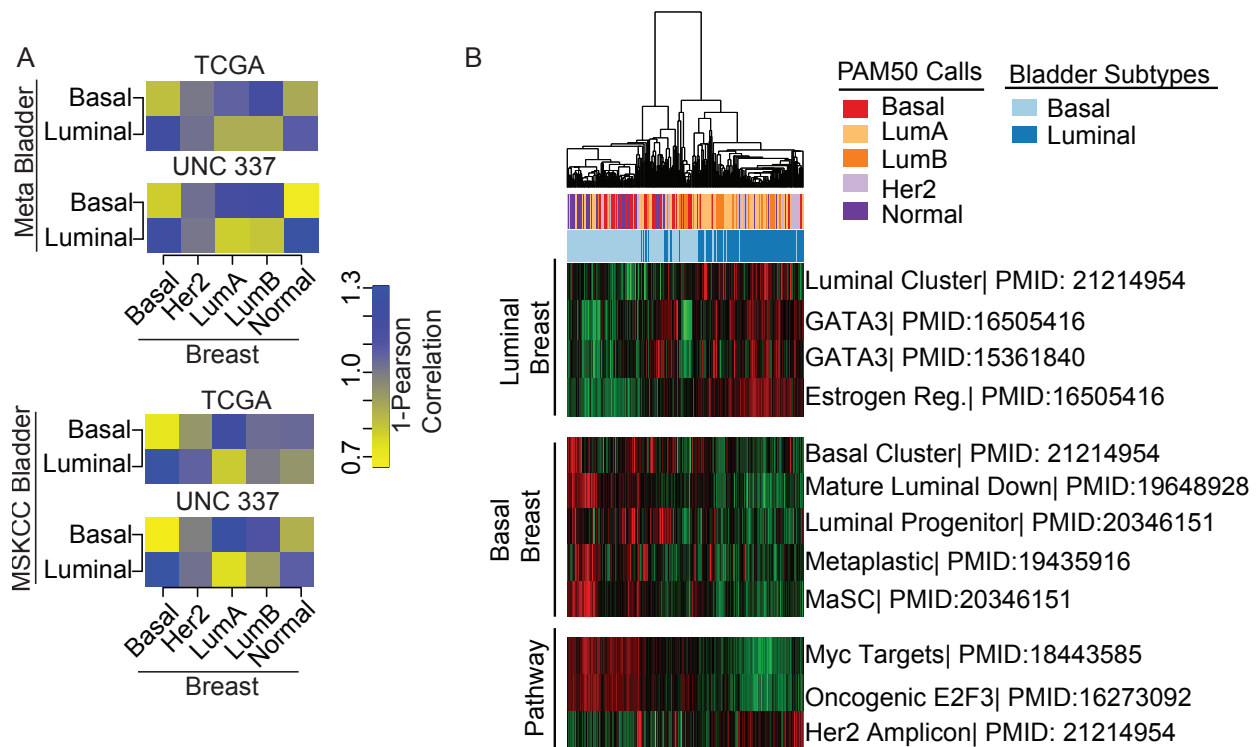


Figure 10: Basal-like and luminal bladder cancer correlate to the intrinsic molecular subtypes of breast cancer

(A) Median gene expression of genes present in the breast cancer specific intrinsic gene list were determined for each bladder and breast subtype and 1-pearson correlation was calculated comparing bladder subtypes (bladder tumors) to breast subtypes (breast tumors) in both the Breast TCGA and UNC337 datasets. **(B)** Waterfall plots representing the correlation of basal-like (black) and luminal (red) bladder tumors to the Basal and **(C)** Luminal A breast cancer centroid as determined by the PAM50. **(D)** The meta-dataset of bladder tumors were clustered by genes that defined the intrinsic subtypes of breast cancer. Tracks indicated bladder cancer subtypes as well as

subtypes predicted by the breast cancer PAM50 bioclassifier. **(E)** The meta dataset tumors were run against previously published breast cancer related gene sets and the resulting pathway scores were clustered by hierarchical clustering and heatmaps were generated for visualization.

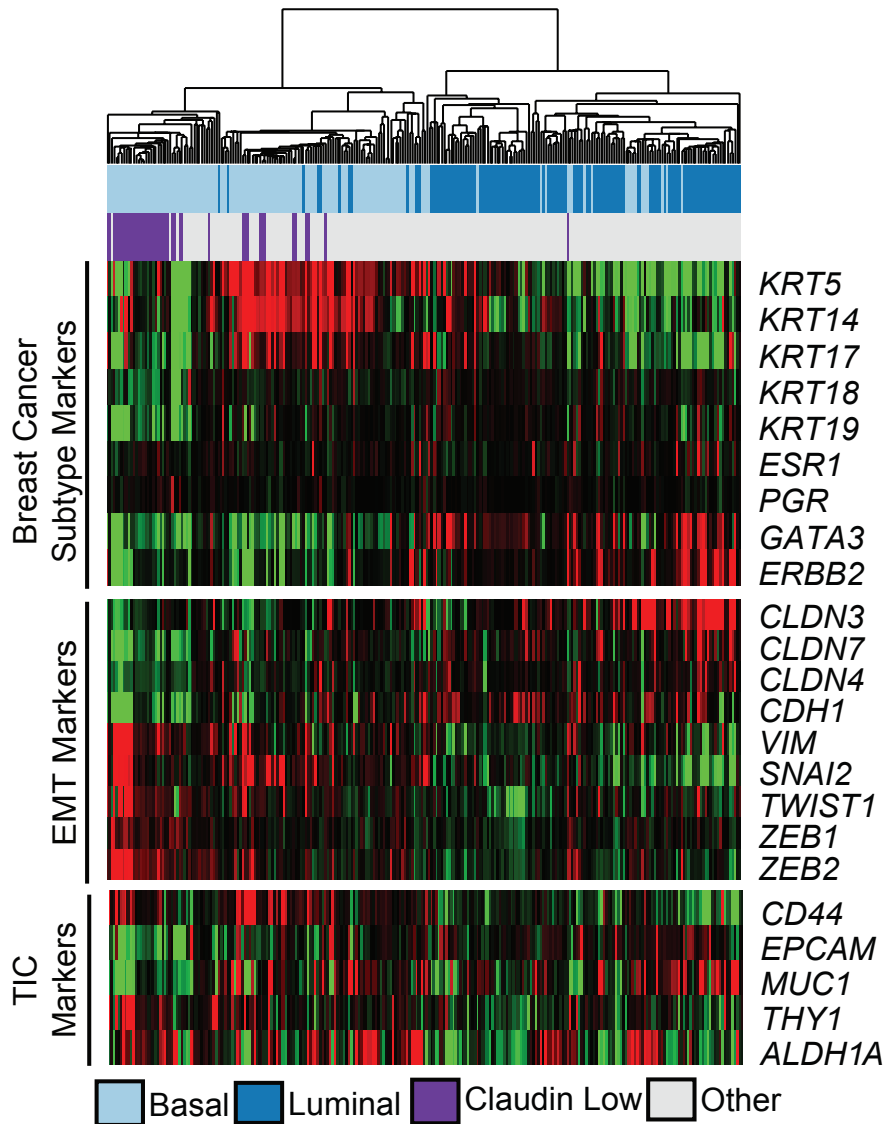


Figure 11: A subset of basal-like bladder tumors are claudin-low

(A) The meta dataset was hierarchically clustered using representative genes known to define claudin-low breast tumors. Claudin low subtype designation was performed using a previously defined 807 gene signature. (B) A Kaplan-Meier plot was generated comparing disease specific survival and (C) overall survival of the basal, luminal and claudin low subtypes.

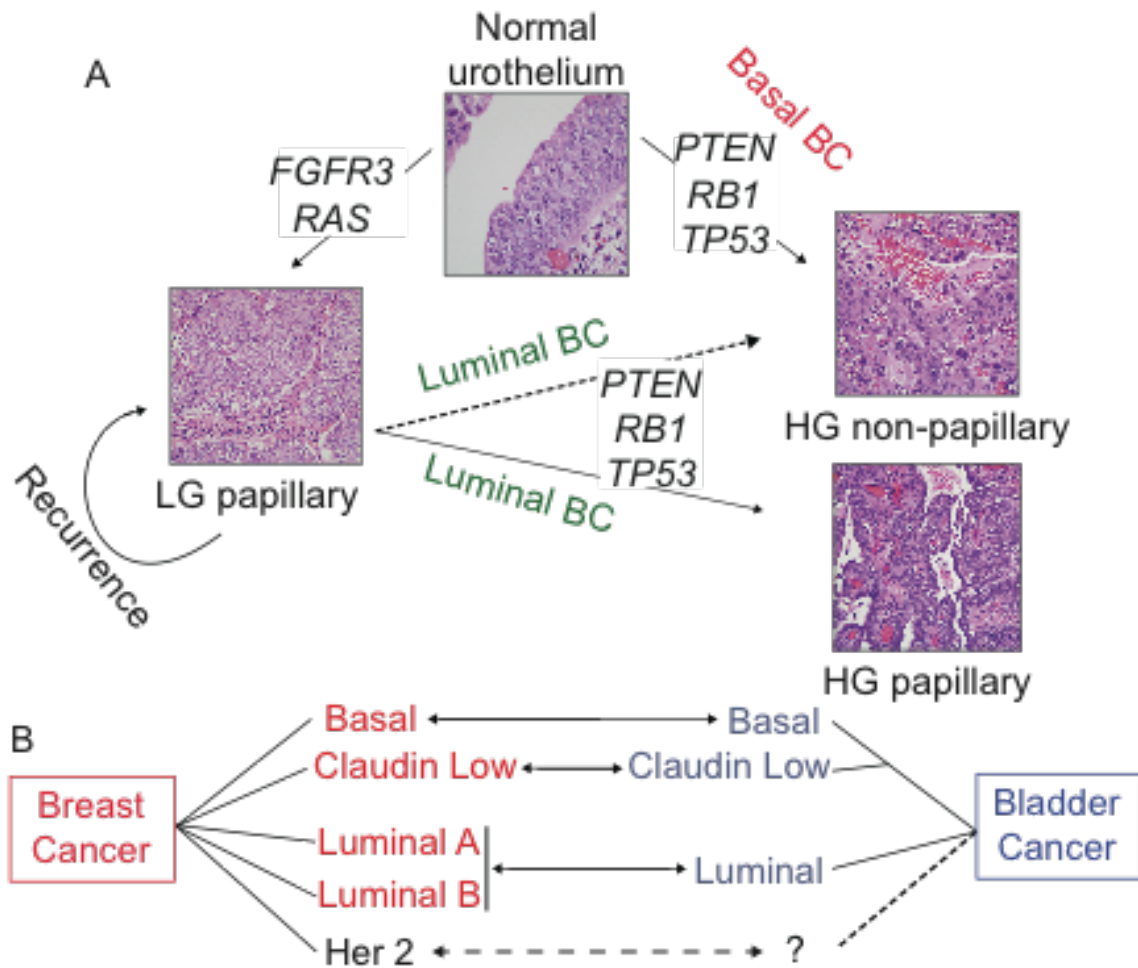
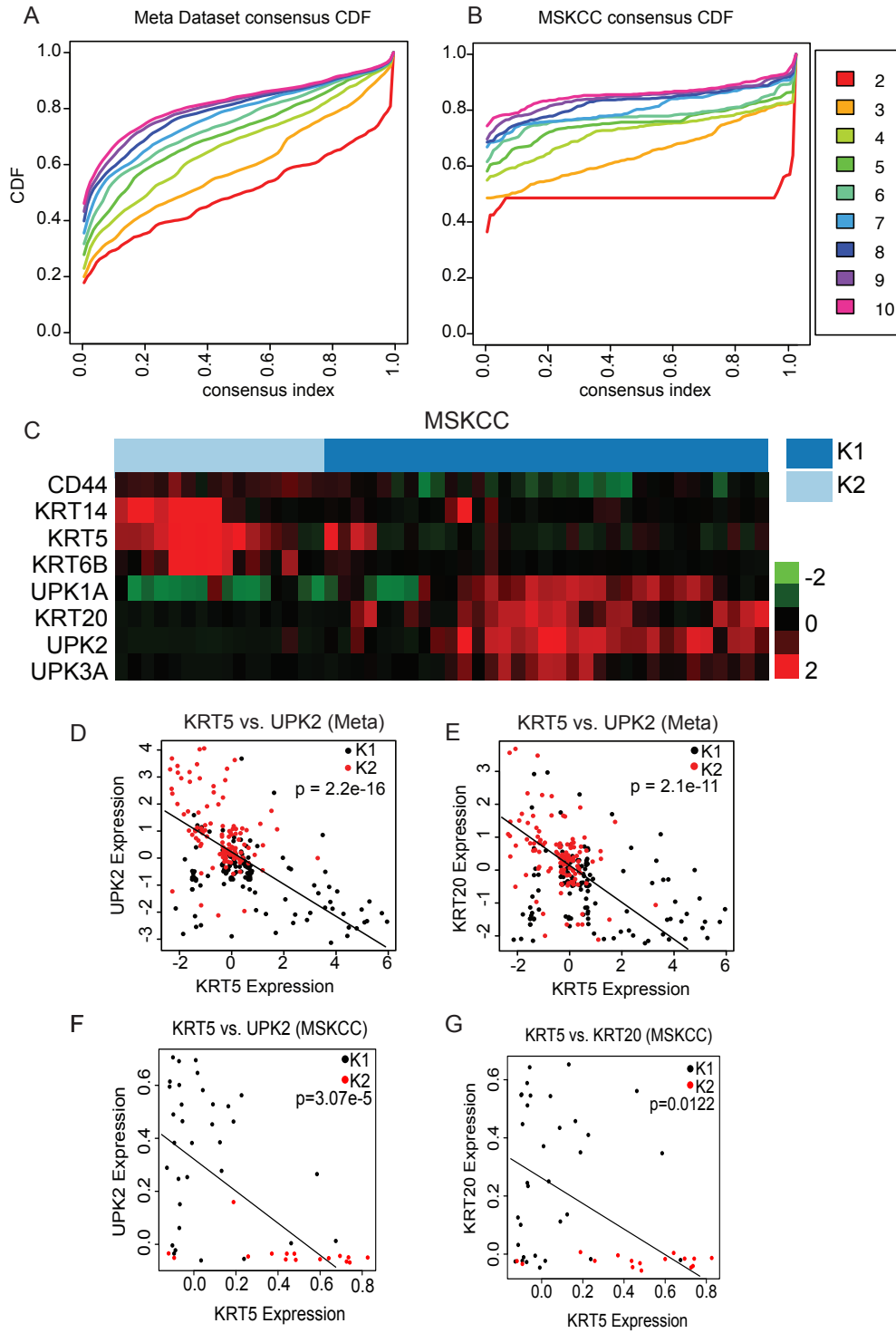


Figure 12: Proposed model of urothelial tumorigenesis and relationships to intrinsic subtypes of breast cancer

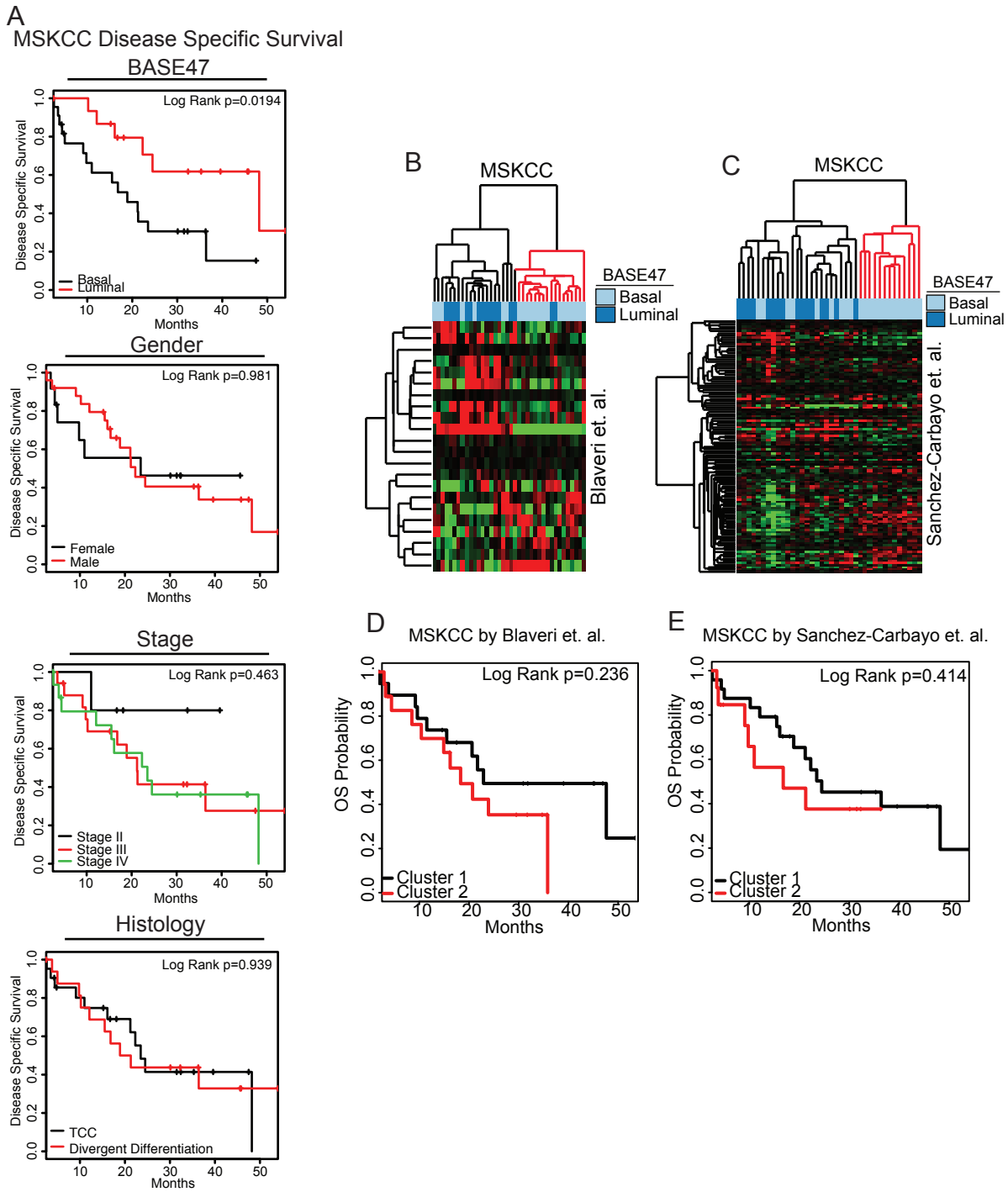
(A) Low-grade (LG) and high-grade (HG) urothelial carcinoma are associated with specific genetic alterations. Low-grade papillary tumors often incur FGFR3, RAS, and receptor tyrosine kinase alterations, while high-grade tumors are characterized by loss of tumor suppressor genes such as PTEN, TP53, and RB1 pathway alterations. While most LG tumors recur as LG, a small proportion will progress to HG tumors in association with PTEN, TP53, and RB1 pathways alterations. We propose that LG tumors that progress are likely to be papillary, HG tumors of the luminal molecular

subtype. De novo HG tumors are likely to be basal-like in expression subtype. Whether luminal, non-papillary tumors arise from LG tumors is unclear. **(B)** Diagram showing the proposed relationship between intrinsic subtypes of breast and bladder cancers.

3.7 Supplemental Figures

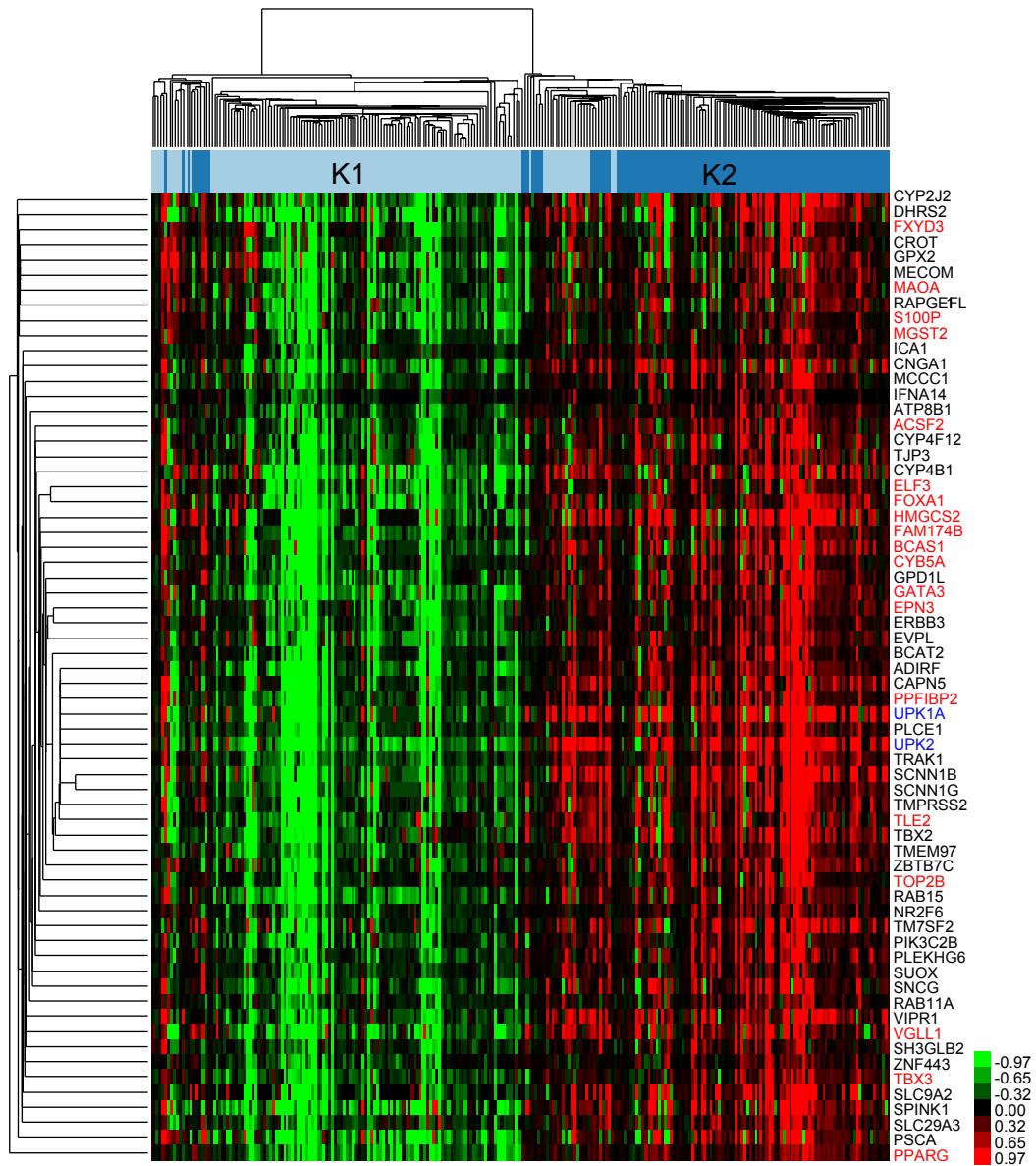


Supplemental Figure 1: Consensus Clustering defines two distinct molecular subtypes of invasive bladder cancer (A) Consensus Cumulative Distribution Function (CDF) plot were generated by Consensus Cluster Plus clustering on the Meta-dataset and the (B) MSKCC dataset. (C) Genes representative of epithelial and urothelial differentiation were used to generate a heatmap, supervised by subtype in the MSKCC dataset. KRT5 mRNA expression was plotted against UPK2 and KRT20 expression in the (D, E) Meta-dataset and (F, G) MSKCC dataset.



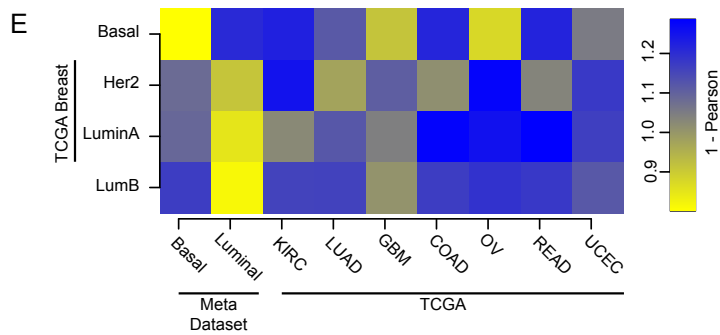
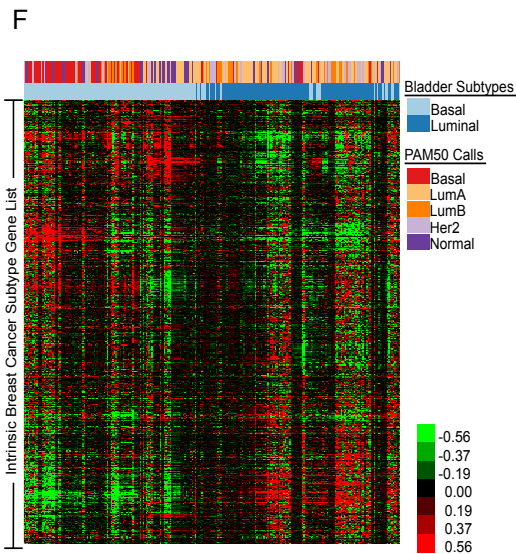
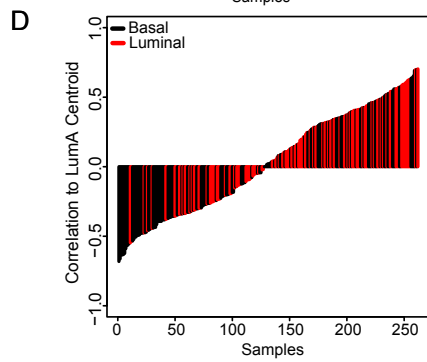
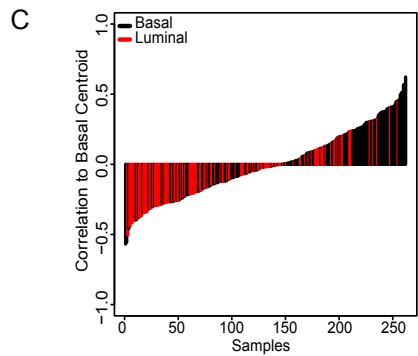
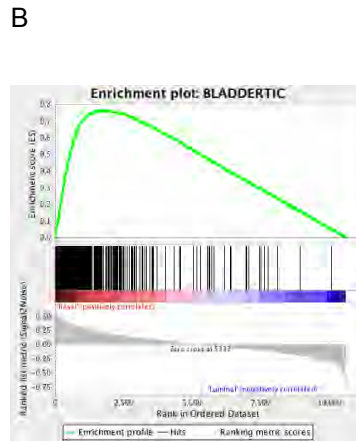
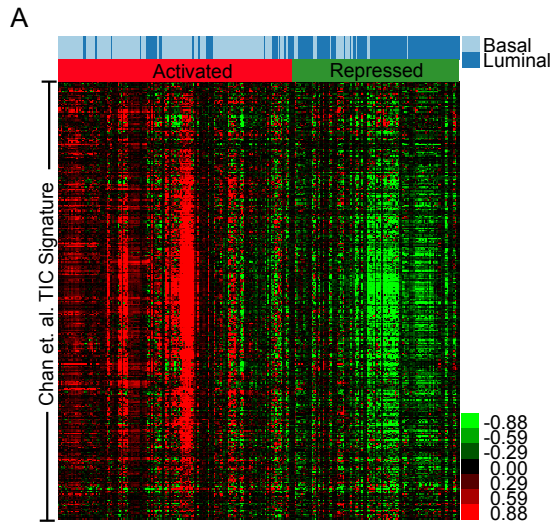
Supplemental Figure 2: Clinical variables are not significantly associated with disease specific or overall survival and previous muscle invasive signatures are not prognostic in the MSKCC dataset. (A) Kaplan-Meier plots for disease specific

survival were generated based on gender, stage and whether a tumor was pure urothelial or of mixed differentiation. **(B)** The MSKCC dataset was hierarchically clustered by prognostic signatures from Blaveri et. al. and **(C)** Sanchez-Carbayo et. al. **(D,E)** The tumors were then classified based on the two major clusters (black and red) and Kaplan-Meier plots were made to determine the prognostic value of these signatures.

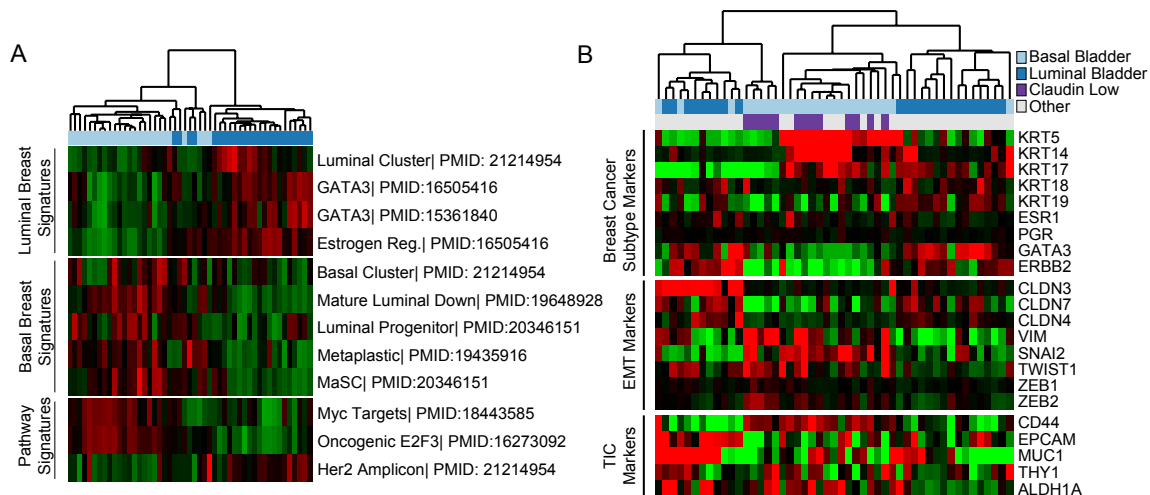


Text Color
 Breast Cancer Related
 Urothelial Related

Supplemental Figure 3: Makers of luminal breast cancer are co-expressed with markers of urothelial differentiation Hierarchical clustering was performed on all significantly differentially expressed (2-class SAM) genes from the Meta-dataset. The node containing the urothelial makers of differentiation, UPK2 and UPK1A, was isolated and overlapped with the Parker et. al. breast cancer intrinsic gene list. A significant number of genes within the node overlapped the breast cancer gene list (19/65 genes, chi squared p value=0.006).



Supplemental Figure 4: Basal-like bladder cancer possesses tumor initiating cell traits and is molecular similar to basal breast cancer. (A) A 467-gene signature of bladder TIC expression (330/467 genes present in the meta-dataset) was used to hierarchically cluster the tumors from the meta-dataset. **(B)** GSEA was performed using the bladder TIC gene set. The basal subtype was significantly enriched for the TIC signature (nominal p value=0.006). **(C)** The intrinsic breast cancer gene list was used to correlate basal, her2, Lum A and Lum B breast tumors from the TCGA to the basal and luminal bladder cancer subtypes from the Meta-dataset tumors as well as 7 additional tumors from The Cancer Genome Atlas (TCGA). **(D)** Waterfall plots representing the correlation of basal-like (black) and luminal (red) bladder tumors to the Basal and **(E)** Luminal A breast cancer centroid as determined by the PAM50. **(F)** The meta-dataset of bladder tumors were clustered by genes that defined the intrinsic subtypes of breast cancer. Tracks indicated bladder cancer subtypes as well as subtypes predicted by the breast cancer PAM50 bioclassifier.



Supplemental Figure 5: Basal, luminal, Claudin Low and oncogenic breast cancer signatures are associated with intrinsic molecular subtypes of bladder cancer. (A)

The MSKCC datasets tumors were run against previously published breast cancer related gene sets (88) and the resulting pathway scores were clustered by hierarchical clustering and heatmaps were generated for visualization. **(B)** The MSKCC dataset was hierarchically clustered using representative genes known to define claudin-low breast tumors. Claudin low subtype designation was performed using an 807 gene signature.

Chapter 4: Future Directions

4.1 BASE47 as a prognostic tool

Bladder cancer is a heterogeneous disease, histologically and molecularly. We have shown, using multiple independent datasets, that there are at least two molecular subtypes within HG, muscle invasive bladder cancer that are associated with distinct transcriptional and genomic patterns, clinical factors and survival. Additionally, these subtypes, basal and luminal bladder cancer, share molecular feature with basal and luminal breast cancer, respectively. However, two critical questions remain that need to be addressed in order for these subtypes to become clinically valuable: can the BASE47 be adapted to a clinically relevant platform and are there expression differences between the subtypes that can be exploited for the development of targeted therapies.

The prognostic ability of the BASE47 creates the potential for it to be a clinically relevant tool. Our current study allowed us to assess the BASE47's prognostic ability on muscle invasive disease; however, future work to determine its ability to predict reoccurrence and progression of non-muscle invasive and muscle invasive disease alike, is a critical need. This new information will be key in the determination of therapy for patients; one could envision a patient who presents with a HG non-invasive tumor, which is classified as basal, undergoing a more aggressive therapeutic regimen, whereas a patient with a luminal tumor would undergo a more conservative approach.

However for this to come to fruition a mechanism for making this assessment on these tumors in a clinical setting must be created. To this end, we have been working to transition the BASE47 to the NanoString platform.

NanoString, which is the basis for the FDA approved Prosigna assay for breast cancer, utilizes a fluorescently labeled cDNA oligo code-set for accurate quantification of gene expression from formalin fixed paraffin embedded (FFPE) samples, as well as fresh frozen tumor (89, 90).

We are currently assembling a new dataset of previously unanalyzed tumors and the corresponding clinical data. All tumors have both fresh frozen and FFPE material, allowing us to validate NanoString derived BASE47 calls from FFPE against the gold standard of fresh frozen tumors run on microarray. RNA will be extracted from fresh frozen tumor samples and analyzed via microarray. The BASE47 will then be applied to the dataset to make subtype calls. In order to develop gene level cutoffs for the NanoString assay, RNA from FFPE samples will be extracted and gene expression of the BASE47 genes will be determined by NanoString. The subtype assignments derived from the microarray will then be applied to the NanoString gene expression data to determine the proper expression cutoffs, allowing us to make future BASE47 calls de novo from NanoString data. Once the NanoString assay has been validated, we will be able to use FFPE samples address the larger questions such as the ability of the BASE47 assess overall prognosis and recurrence in both non-invasive and invasive disease, as well as determine correlations between subtypes and response to therapy.

4.2 BASE47 as a predictive tool

In addition to understanding the relationship between the subtypes of bladder cancer and their response to therapy, the expression differences between the subtypes may aid in the development of novel targeted therapy. This is of critical importance as there are currently no FDA approved targeted therapies for bladder cancer, additionally as this is a disease of elderly population many patients are unable to undergo traditional cisplatin based therapy do to toxicity related complications. Current small molecule inhibitors which are approved or in clinical trial for other disease types may show effectiveness within either basal or luminal bladder cancer.

Luminal bladder cancer has over expression of the *ERBB2* oncogene as compared to basal bladder cancer, this suggests that using a targeted therapy such as Trastuzumab may be an appropriate therapy. Trastuzumab is an antibody against the Her2 receptor and is FDA approved for use in Her2+ breast cancer as well as metastatic gastric and gastroesophageal cancers in which Her2 is overexpressed by amplification or IHC staining.

Additionally, a large proportion of luminal tumors have overexpression of *FGFR3*. Currently, there are 25 open clinical trials for Dovitinib, a small molecular inhibitor targetign *FGFR3*, one of which is a Phase II trial for urothelial carcinoma (NCT01732107). However, the inclusion criteria restricts the study to only non-invasive disease, T1 or less. Our data suggest invasive tumors may also drive a benefit from this therapy and that the BASE47 maybe an appropriate tool for predicting sensitive to *FGFR3* inhibition.

The development of targeted therapy for basal bladder cancer is of utmost importance as basal bladder cancer has a worse prognosis, compared to luminal bladder cancer. CDK6 ranked as one of the most differentially regulated genes between basal and luminal bladder cancer. CDK6, along with CDK4 play a key role in RB mediated cell cycle progression. Palbociclib, a CDK4/6 inhibitor developed by Pfizer, is currently in Phase III clinical trials for metastatic breast cancer (NCT01942135). In a Phase II clinical trial, Palbociclib in combination with letrozole increased patient progression free survival to 20.2 months from 10.2 for letrozole alone. This therapy shows promise and should be further investigated in basal bladder cancer. However, when carrying out such a trial, it should be noted that basal tumors also contain downstream alteration such as *RB1* mutations that would render tumors resistant to CDK4/6 inhibition. The selection of patients for the trial that have increased expression of CDK4/6 along with tumors that have *CCND1* amplifications present, yet in the absence of *RB1* mutations would be critical for the success of this trial. Based on a mutational analysis of the TCGA data, ~30% of patients would meet the criteria and be deemed to have potentially sensitive tumor (Figure 13).

Overall, the adoption of the BASE47 to a clinically useful platform would result in the better classification of bladder tumors. This would also allow for the use of differential gene expression patterns between basal and luminal tumors to inform treatment options and the application of novel targeted therapies for bladder cancer.

More generally, the subtype classification of basal and luminal may not be confined to bladder and breast cancer. In other tumor types, such as prostate, it has been demonstrated that mutations in luminal vs. basal epithelial cells lead to tumors

molecularly distinct tumors in mice (91). This suggests that the basal and luminal subtypes may be more broadly applicable to tumors of epithelial origin. As more data become available with the completion of the TCGA, these questions can be addressed.

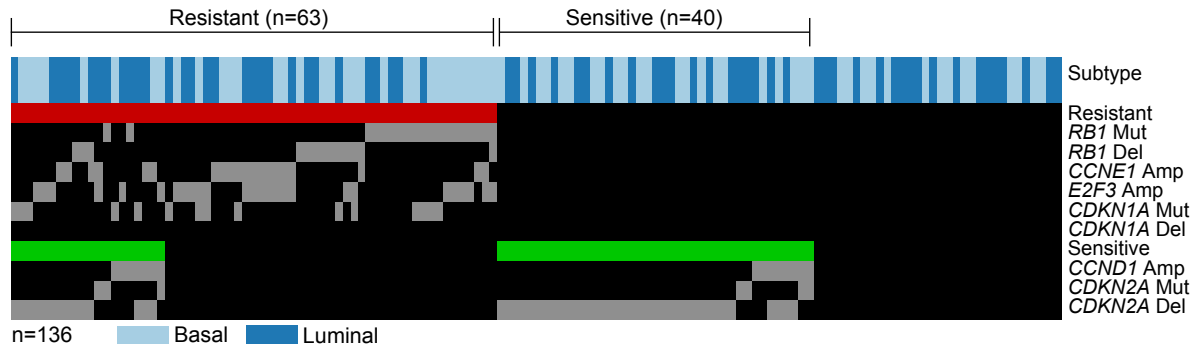


Figure 13: Sensitive to CDK4/6 inhibition by mutational status TCGA tumors were classified based on non-silent mutations and copy number alterations (+2,-2 threshold) which would dictate sensitivity to CDK4/6 inhibition.

APPENDIX A: SAM GENE LIST

Two Class SAM					
Basal vs Luminal					
FDR=0					
Basal Postive Genes					
Gene ID	Score(d)	Numerator(r)	Denominator(s+s0)	Fold Change	q-value(%)
CHST15	9.2814	0.8233	0.0887	1.7694	0
EMP3	9.0764	0.6595	0.0727	1.5795	0
CORO1C	8.9796	0.4885	0.0544	1.4030	0
AHNAK2	8.8714	1.1001	0.1240	2.1437	0
CLIC4	8.8713	0.5196	0.0586	1.4336	0
CDK6	8.8580	0.6742	0.0761	1.5958	0
MSN	8.8440	0.6955	0.0786	1.6194	0
SACS	8.7394	0.4444	0.0508	1.3607	0
PDGFC	8.6196	0.6549	0.0760	1.5745	0
PALLD	8.6056	0.6431	0.0747	1.5617	0
GLIPR1	8.5678	0.6666	0.0778	1.5873	0
MT1X	8.5583	1.0428	0.1218	2.0602	0
TUBB6	8.4656	0.6735	0.0796	1.5949	0
OSMR	8.3502	0.4951	0.0593	1.4094	0
PRKCDBP	8.3327	0.7246	0.0870	1.6525	0
CD14	8.3009	0.7561	0.0911	1.6889	0
DEGS1	8.2501	0.5680	0.0689	1.4825	0
PRRX1	8.2416	0.8125	0.0986	1.7563	0
FLNA	8.2207	0.3313	0.0403	1.2581	0
LRIG1	8.2050	0.5522	0.0673	1.4663	0
DPYD	8.1710	0.5668	0.0694	1.4813	0
ANXA5	8.1057	0.5642	0.0696	1.4786	0
PTGS1	8.0881	0.4751	0.0587	1.3900	0
ALOX5AP	8.0850	0.8974	0.1110	1.8627	0
NOD2	8.0651	0.5727	0.0710	1.4874	0
FAP	8.0510	0.8080	0.1004	1.7507	0

DSE	8.0472	0.6558	0.0815	1.5755	0
CERK	8.0371	0.4124	0.0513	1.3309	0
TNC	8.0014	0.7539	0.0942	1.6863	0
MPP1	7.9554	0.4775	0.0600	1.3924	0
TLR1	7.9506	0.5870	0.0738	1.5021	0
MT2A	7.9128	1.0304	0.1302	2.0426	0
TNFAIP6	7.8870	0.8055	0.1021	1.7478	0
SNAI2	7.7733	0.6866	0.0883	1.6095	0
RRAS	7.7132	0.5138	0.0666	1.4278	0
FAS	7.6969	0.3831	0.0498	1.3042	0
KCTD12	7.6850	0.3398	0.0442	1.2656	0
KIAA0922	7.6503	0.3637	0.0475	1.2867	0
ST3GAL6	7.6146	0.4015	0.0527	1.3209	0
CD44	7.5969	0.6129	0.0807	1.5294	0
CD86	7.5965	0.4063	0.0535	1.3253	0
MT1M	7.5890	0.6517	0.0859	1.5710	0
C1S	7.5704	0.5821	0.0769	1.4970	0
SIRPA	7.5670	0.5281	0.0698	1.4421	0
PTRF	7.5612	0.6157	0.0814	1.5323	0
ITGA5	7.5139	0.6457	0.0859	1.5645	0
ZEB2	7.5106	0.4296	0.0572	1.3469	0
LY96	7.5041	0.6479	0.0863	1.5669	0
LAMP2	7.5035	0.3944	0.0526	1.3144	0
HCK	7.5000	0.5660	0.0755	1.4804	0
EFEMP1	7.4420	0.6804	0.0914	1.6026	0
PRNP	7.4413	0.6518	0.0876	1.5711	0
CAV1	7.4015	0.5795	0.0783	1.4944	0
TGFBI	7.3419	0.7521	0.1024	1.6843	0
SLA	7.3285	0.4087	0.0558	1.3275	0
ATXN1	7.3284	0.3510	0.0479	1.2754	0
AXL	7.3205	0.5626	0.0769	1.4770	0
FPR3	7.3200	0.5754	0.0786	1.4901	0
CSF1R	7.2959	0.6776	0.0929	1.5995	0
IL15RA	7.2578	0.3527	0.0486	1.2769	0
FCGR2A	7.2285	0.4669	0.0646	1.3822	0
SAMSN1	7.2264	0.4559	0.0631	1.3717	0
NMT2	7.2259	0.3821	0.0529	1.3032	0
SPI1	7.2232	0.4340	0.0601	1.3510	0
IFITM2	7.2164	0.5625	0.0780	1.4769	0
SERPINA3	7.2059	1.0643	0.1477	2.0912	0
NCF2	7.1870	0.4859	0.0676	1.4005	0

RNASE6	7.1834	0.5212	0.0726	1.4351	0
SYNC	7.1736	0.4816	0.0671	1.3963	0
RGS2	7.1545	0.6432	0.0899	1.5618	0
C1QA	7.1505	0.5197	0.0727	1.4337	0
AP1S2	7.1447	0.4771	0.0668	1.3919	0
NFIL3	7.1411	0.4430	0.0620	1.3594	0
TMEM45A	7.1406	0.8884	0.1244	1.8512	0
FCER1G	7.1327	0.7079	0.0992	1.6334	0
SPHK1	7.1262	0.6289	0.0882	1.5464	0
TIMP2	7.1075	0.5160	0.0726	1.4299	0
WIPF1	7.1020	0.4574	0.0644	1.3731	0
C5AR1	7.0874	0.5552	0.0783	1.4693	0
CD163	7.0846	0.6525	0.0921	1.5719	0
STX2	7.0776	0.5387	0.0761	1.4526	0
PMEPA1	7.0768	0.5351	0.0756	1.4490	0
SLC7A7	7.0715	0.6146	0.0869	1.5311	0
MYO5A	7.0573	0.3959	0.0561	1.3158	0
GPR68	7.0536	0.5586	0.0792	1.4728	0
MS4A4A	7.0394	0.4172	0.0593	1.3353	0
ZNF532	7.0112	0.3303	0.0471	1.2573	0
TYMP	7.0039	0.5545	0.0792	1.4687	0
GAS1	6.9774	0.6863	0.0984	1.6092	0
KIAA0226L	6.9665	0.3042	0.0437	1.2348	0
COL5A2	6.9605	0.6867	0.0987	1.6096	0
CASP1	6.9602	0.6038	0.0868	1.5197	0
RAB27A	6.9595	0.2611	0.0375	1.1984	0
NXN	6.9541	0.5560	0.0800	1.4702	0
SRGN	6.9539	0.7493	0.1077	1.6809	0
SLAMF8	6.9537	0.4721	0.0679	1.3871	0
FYB	6.9528	0.4456	0.0641	1.3619	0
COL6A2	6.9404	0.4685	0.0675	1.3837	0
SERPINA1	6.9360	0.5955	0.0859	1.5110	0
CDA	6.9349	0.5734	0.0827	1.4880	0
ADCY7	6.9074	0.2671	0.0387	1.2034	0
NR3C1	6.8989	0.2131	0.0309	1.1592	0
DACT1	6.8890	0.4660	0.0676	1.3812	0
ROR2	6.8864	0.4555	0.0661	1.3712	0
SLC15A3	6.8851	0.5382	0.0782	1.4522	0
GPM6B	6.8793	0.3320	0.0483	1.2588	0
CRYAB	6.8787	0.5798	0.0843	1.4946	0
CALD1	6.8774	0.4996	0.0726	1.4138	0

IFI30	6.8592	0.5322	0.0776	1.4461	0
RBP1	6.8556	0.7022	0.1024	1.6270	0
MT1E	6.8510	0.4840	0.0707	1.3987	0
CYBB	6.8452	0.5222	0.0763	1.4361	0
AEBP1	6.8409	0.7326	0.1071	1.6617	0
RAC2	6.8390	0.6109	0.0893	1.5272	0
EPB41L2	6.8381	0.3403	0.0498	1.2660	0
MAF	6.8314	0.3870	0.0567	1.3077	0
CPVL	6.8311	0.5740	0.0840	1.4886	0
IL32	6.8308	0.5541	0.0811	1.4683	0
ARL4C	6.8301	0.2877	0.0421	1.2207	0
VIM	6.8054	0.5817	0.0855	1.4966	0
CLEC4A	6.7943	0.5519	0.0812	1.4661	0
GREM1	6.7931	0.7757	0.1142	1.7120	0
IL10RA	6.7914	0.4803	0.0707	1.3951	0
FMOD	6.7908	0.4972	0.0732	1.4115	0
FBN1	6.7870	0.3327	0.0490	1.2594	0
COL5A1	6.7822	0.7246	0.1068	1.6524	0
GLT8D2	6.7811	0.5695	0.0840	1.4840	0
C1QB	6.7789	0.7567	0.1116	1.6896	0
SH2B3	6.7785	0.4460	0.0658	1.3622	0
AK4	6.7696	0.5303	0.0783	1.4442	0
C3AR1	6.7654	0.3862	0.0571	1.3069	0
SERPING1	6.7648	0.5716	0.0845	1.4862	0
ECI2	6.7631	0.4441	0.0657	1.3605	0
IFI16	6.7605	0.6147	0.0909	1.5312	0
PLAUR	6.7525	0.5263	0.0779	1.4402	0
ACTN1	6.7433	0.5075	0.0753	1.4216	0
LILRB2	6.7378	0.4870	0.0723	1.4015	0
IFITM3	6.7148	0.5888	0.0877	1.5040	0
RGS1	6.6982	0.7142	0.1066	1.6405	0
GFPT2	6.6752	0.5807	0.0870	1.4956	0
VSNL1	6.6744	0.6152	0.0922	1.5317	0
OAT	6.6726	0.6061	0.0908	1.5222	0
EVI2A	6.6575	0.4457	0.0669	1.3620	0
SULF1	6.6477	0.8334	0.1254	1.7819	0
MN1	6.6473	0.4121	0.0620	1.3307	0
COL6A1	6.6440	0.7122	0.1072	1.6383	0
COL16A1	6.6390	0.6128	0.0923	1.5292	0
TNFSF4	6.6385	0.3936	0.0593	1.3136	0
LAPTM5	6.6369	0.5950	0.0897	1.5105	0

ITGB2	6.6353	0.6867	0.1035	1.6096	0
SLC2A3	6.6274	0.6342	0.0957	1.5521	0
MNDA	6.6233	0.4457	0.0673	1.3620	0
MT1F	6.6170	0.5914	0.0894	1.5067	0
BIN1	6.6150	0.5051	0.0764	1.4192	0
TYROBP	6.6041	0.6766	0.1024	1.5983	0
FGL2	6.5663	0.6007	0.0915	1.5164	0
IL15	6.5439	0.3058	0.0467	1.2361	0
NCKAP1L	6.5365	0.3399	0.0520	1.2657	0
EDNRA	6.5326	0.4344	0.0665	1.3514	0
NNMT	6.5239	0.5137	0.0787	1.4277	0
CLIP4	6.5221	0.3528	0.0541	1.2770	0
PRDM1	6.5206	0.2645	0.0406	1.2013	0
MAFB	6.5144	0.5047	0.0775	1.4188	0
CCL8	6.4903	0.7202	0.1110	1.6475	0
CLEC5A	6.4860	0.4141	0.0638	1.3324	0
AIF1	6.4801	0.5297	0.0817	1.4437	0
PDLIM3	6.4767	0.5873	0.0907	1.5024	0
HIF1A	6.4752	0.3747	0.0579	1.2965	0
ADAM19	6.4648	0.6289	0.0973	1.5464	0
TRPS1	6.4621	0.2330	0.0361	1.1753	0
ZYX	6.4567	0.3480	0.0539	1.2728	0
CFI	6.4479	0.4757	0.0738	1.3906	0
VSIG4	6.4464	0.4185	0.0649	1.3365	0
ISG20	6.4460	0.6310	0.0979	1.5486	0
HPSE	6.4419	0.3638	0.0565	1.2868	0
EGR2	6.4352	0.6068	0.0943	1.5228	0
LGALS1	6.4275	0.6131	0.0954	1.5296	0
MS4A6A	6.4025	0.5895	0.0921	1.5048	0
GNLY	6.3943	0.4349	0.0680	1.3518	0
IL1RAP	6.3892	0.3639	0.0569	1.2869	0
COL1A2	6.3851	0.6517	0.1021	1.5710	0
POSTN	6.3829	0.7819	0.1225	1.7194	0
RUNX3	6.3794	0.5953	0.0933	1.5107	0
IGSF6	6.3751	0.4710	0.0739	1.3861	0
BNC2	6.3726	0.3212	0.0504	1.2494	0
SOCS1	6.3667	0.3263	0.0512	1.2538	0
PSMB9	6.3648	0.4899	0.0770	1.4044	0
HS3ST3A1	6.3582	0.6183	0.0972	1.5351	0
CYBRD1	6.3550	0.5285	0.0832	1.4424	0
HEG1	6.3480	0.3560	0.0561	1.2798	0

ACOT9	6.3463	0.3536	0.0557	1.2778	0
ATP8B2	6.3421	0.2192	0.0346	1.1641	0
NID2	6.3344	0.4058	0.0641	1.3248	0
GEM	6.3334	0.3734	0.0590	1.2954	0
CREB5	6.3216	0.2910	0.0460	1.2235	0
TGFB3	6.3169	0.4858	0.0769	1.4004	0
CXCL10	6.3153	0.8965	0.1419	1.8615	0
HBEGF	6.3087	0.5001	0.0793	1.4143	0
SRPX	6.3071	0.7440	0.1180	1.6748	0
CCR1	6.3026	0.3272	0.0519	1.2546	0
CYTIP	6.2984	0.4641	0.0737	1.3795	0
THEMIS2	6.2965	0.2876	0.0457	1.2206	0
KCNMB1	6.2932	0.5240	0.0833	1.4380	0
BLVRA	6.2866	0.3738	0.0595	1.2958	0
GPR183	6.2678	0.5576	0.0890	1.4718	0
COL6A3	6.2477	0.6403	0.1025	1.5587	0
CTGF	6.2429	0.5909	0.0946	1.5061	0
ISLR	6.2340	0.3993	0.0641	1.3189	0
GAS6	6.2325	0.4122	0.0661	1.3307	0
IL7R	6.2190	0.5910	0.0950	1.5063	0
OLFML3	6.2175	0.4827	0.0776	1.3974	0
DPYSL2	6.2154	0.4308	0.0693	1.3480	0
KIAA0247	6.2133	0.3182	0.0512	1.2468	0
PLEK	6.2108	0.6584	0.1060	1.5784	0
IFITM1	6.2065	0.6296	0.1014	1.5472	0
FMO1	6.2064	0.4497	0.0725	1.3658	0
IRAK3	6.2012	0.4595	0.0741	1.3751	0
IGFBP6	6.1972	0.6547	0.1057	1.5743	0
PAM	6.1825	0.3991	0.0646	1.3187	0
CEP112	6.1824	0.2221	0.0359	1.1664	0
PTP4A1	6.1793	0.2399	0.0388	1.1809	0
CXCL11	6.1774	0.7020	0.1136	1.6267	0
WARS	6.1742	0.5324	0.0862	1.4463	0
FERMT2	6.1556	0.4817	0.0783	1.3964	0
TPM1	6.1455	0.3770	0.0614	1.2987	0
TGFB1I1	6.1436	0.2931	0.0477	1.2253	0
SPON2	6.1365	0.3888	0.0634	1.3093	0
C7orf10	6.1357	0.4440	0.0724	1.3604	0
MMP9	6.1229	0.8715	0.1423	1.8295	0
ZBED2	6.1176	0.5682	0.0929	1.4827	0
DOCK10	6.1025	0.4382	0.0718	1.3549	0

EVI2B	6.0985	0.5183	0.0850	1.4322	0
HLA-G	6.0923	0.4328	0.0710	1.3499	0
C1R	6.0916	0.4838	0.0794	1.3985	0
OGFRL1	6.0888	0.3285	0.0540	1.2557	0
DPT	6.0829	0.4225	0.0695	1.3402	0
TMEM158	6.0750	0.7037	0.1158	1.6287	0
BMP2K	6.0743	0.1757	0.0289	1.1295	0
PHLDA1	6.0700	0.6438	0.1061	1.5625	0
FN1	6.0681	0.2929	0.0483	1.2251	0
COPZ2	6.0666	0.3108	0.0512	1.2404	0
ROBO1	6.0660	0.4241	0.0699	1.3417	0
CEBPB	6.0645	0.3770	0.0622	1.2986	0
PRR16	6.0632	0.2640	0.0435	1.2008	0
SLC39A14	6.0632	0.4009	0.0661	1.3203	0
PIK3CD	6.0577	0.2992	0.0494	1.2305	0
TLR2	6.0518	0.2493	0.0412	1.1887	0
STK17B	6.0472	0.2557	0.0423	1.1940	0
MT1H	6.0457	0.3561	0.0589	1.2800	0
GPR65	6.0438	0.4294	0.0710	1.3466	0
ZEB1	6.0389	0.2274	0.0377	1.1707	0
DIXDC1	6.0387	0.2227	0.0369	1.1669	0
SOD2	6.0373	0.3979	0.0659	1.3176	0
HLA-F	6.0352	0.4759	0.0788	1.3908	0
RAB31	6.0290	0.4530	0.0751	1.3689	0
KRT6B	6.0274	0.8162	0.1354	1.7608	0
SGK1	6.0249	0.4906	0.0814	1.4050	0
SGCB	6.0249	0.2152	0.0357	1.1609	0
LST1	6.0173	0.3784	0.0629	1.2999	0
GALNT10	6.0164	0.3382	0.0562	1.2642	0
TLR8	6.0126	0.2791	0.0464	1.2135	0
SLC43A3	6.0102	0.2837	0.0472	1.2174	0
PNMA1	6.0085	0.2756	0.0459	1.2105	0
COPS8	6.0081	0.2062	0.0343	1.1537	0
ACVR1	6.0019	0.3285	0.0547	1.2557	0
PTPLA	5.9979	0.5398	0.0900	1.4538	0
ECM2	5.9973	0.2751	0.0459	1.2101	0
ARSJ	5.9906	0.3227	0.0539	1.2507	0
PDLIM4	5.9806	0.2369	0.0396	1.1785	0
TRIM22	5.9794	0.4805	0.0804	1.3953	0
CCDC109B	5.9793	0.3912	0.0654	1.3115	0
EIF5A2	5.9783	0.2949	0.0493	1.2268	0

F3	5.9757	0.6102	0.1021	1.5265	0
GZMB	5.9693	0.6703	0.1123	1.5914	0
ITGA4	5.9584	0.2860	0.0480	1.2193	0
DSG3	5.9499	0.8449	0.1420	1.7962	0
GZMA	5.9443	0.6568	0.1105	1.5765	0
WISP1	5.9293	0.4097	0.0691	1.3284	0
NT5E	5.9186	0.5729	0.0968	1.4875	0
DNAJB4	5.9174	0.2978	0.0503	1.2293	0
FAM198B	5.9137	0.4160	0.0703	1.3342	0
PLSCR4	5.9109	0.4046	0.0685	1.3238	0
ADAP2	5.9038	0.3639	0.0616	1.2869	0
KITLG	5.8963	0.3167	0.0537	1.2455	0
PLEKHO1	5.8945	0.3530	0.0599	1.2772	0
EMILIN1	5.8903	0.4965	0.0843	1.4108	0
THBS1	5.8848	0.5655	0.0961	1.4799	0
EGR3	5.8793	0.2903	0.0494	1.2229	0
LOX	5.8712	0.5949	0.1013	1.5104	0
PDGFRB	5.8710	0.4706	0.0802	1.3857	0
MYO1B	5.8697	0.3885	0.0662	1.3090	0
CAV2	5.8685	0.3885	0.0662	1.3091	0
LAT2	5.8662	0.3237	0.0552	1.2516	0
RAB23	5.8639	0.2435	0.0415	1.1838	0
GFOD1	5.8634	0.3748	0.0639	1.2967	0
TSPAN4	5.8628	0.3770	0.0643	1.2986	0
CDH11	5.8574	0.5844	0.0998	1.4994	0
STOM	5.8470	0.3441	0.0588	1.2693	0
CTSC	5.8447	0.3593	0.0615	1.2828	0
ECM1	5.8419	0.3809	0.0652	1.3022	0
FAM129A	5.8376	0.4339	0.0743	1.3509	0
KAL1	5.8366	0.3272	0.0561	1.2546	0
COL3A1	5.8342	0.5395	0.0925	1.4534	0
RRAD	5.8253	0.4010	0.0688	1.3204	0
COLEC12	5.8184	0.5547	0.0953	1.4689	0
MYL9	5.7986	0.4316	0.0744	1.3487	0
BCAT1	5.7981	0.5299	0.0914	1.4439	0
COL8A2	5.7966	0.3267	0.0564	1.2541	0
PLAU	5.7924	0.6304	0.1088	1.5480	0
PDPN	5.7899	0.5698	0.0984	1.4843	0
BCL2A1	5.7830	0.4462	0.0772	1.3625	0
ANXA6	5.7759	0.2601	0.0450	1.1975	0
PRPS1	5.7751	0.2725	0.0472	1.2079	0

IFFO1	5.7746	0.2988	0.0518	1.2302	0
DYRK3	5.7705	0.2475	0.0429	1.1872	0
CXCL1	5.7695	0.6865	0.1190	1.6094	0
PTPN12	5.7649	0.3131	0.0543	1.2424	0
AGPAT4	5.7636	0.3556	0.0617	1.2795	0
LAMA4	5.7614	0.3786	0.0657	1.3001	0
IFIH1	5.7581	0.4158	0.0722	1.3340	0
DOCK2	5.7563	0.4760	0.0827	1.3909	0
IL6	5.7491	0.6178	0.1075	1.5345	0
MFAP5	5.7488	0.6213	0.1081	1.5383	0
PLA2G7	5.7481	0.4906	0.0853	1.4050	0
PCDH7	5.7475	0.3927	0.0683	1.3129	0
MFGE8	5.7461	0.4768	0.0830	1.3916	0
ITGA1	5.7433	0.3090	0.0538	1.2388	0
ACOX2	5.7183	0.4011	0.0701	1.3205	0
PARVB	5.7112	0.2212	0.0387	1.1657	0
COL18A1	5.7091	0.2456	0.0430	1.1856	0
ENTPD1	5.7084	0.3246	0.0569	1.2523	0
MSC	5.6964	0.3454	0.0606	1.2705	0
ZFPM2	5.6848	0.3400	0.0598	1.2658	0
MBNL1	5.6835	0.2273	0.0400	1.1706	0
AFAP1	5.6830	0.3474	0.0611	1.2723	0
NINJ2	5.6777	0.3907	0.0688	1.3111	0
ELL2	5.6765	0.3537	0.0623	1.2778	0
FXVD6	5.6746	0.4063	0.0716	1.3252	0
IDO1	5.6703	0.7465	0.1317	1.6777	0
RAMP1	5.6582	0.3462	0.0612	1.2712	0
CD300A	5.6544	0.3767	0.0666	1.2984	0
DOK2	5.6541	0.2119	0.0375	1.1582	0
KRT5	5.6537	1.0668	0.1887	2.0947	0
ITGAM	5.6490	0.4182	0.0740	1.3362	0
DPYSL3	5.6478	0.5530	0.0979	1.4671	0
IL1R2	5.6404	0.3580	0.0635	1.2817	0
IFIT1	5.6358	0.4465	0.0792	1.3627	0
GCNT1	5.6339	0.2992	0.0531	1.2305	0
CCL5	5.6332	0.6534	0.1160	1.5728	0
LY86	5.6249	0.3962	0.0704	1.3160	0
SP110	5.6213	0.3092	0.0550	1.2390	0
ZNF281	5.6152	0.2747	0.0489	1.2097	0
CTSK	5.5749	0.6329	0.1135	1.5507	0
TCF7L1	5.5658	0.3055	0.0549	1.2358	0

TPM2	5.5638	0.3640	0.0654	1.2870	0
CD248	5.5632	0.4988	0.0897	1.4130	0
NUAK1	5.5620	0.4135	0.0744	1.3320	0
CSGALNACT2	5.5600	0.1758	0.0316	1.1296	0
CHST7	5.5589	0.3405	0.0613	1.2662	0
COL11A1	5.5561	0.5785	0.1041	1.4933	0
RGS4	5.5522	0.4433	0.0799	1.3598	0
FLI1	5.5494	0.2020	0.0364	1.1503	0
ATP6V1B2	5.5465	0.2761	0.0498	1.2109	0
COL1A1	5.5431	0.6219	0.1122	1.5389	0
BHLHE40	5.5376	0.4648	0.0839	1.3801	0
TEAD4	5.5369	0.2858	0.0516	1.2191	0
MAP1B	5.5324	0.2885	0.0522	1.2214	0
HTRA1	5.5300	0.4869	0.0881	1.4015	0
OLFML2B	5.5131	0.4788	0.0869	1.3936	0
ALDH2	5.5128	0.4709	0.0854	1.3860	0
ANXA1	5.5099	0.5734	0.1041	1.4881	0
CD53	5.5047	0.3788	0.0688	1.3002	0
PTPN22	5.4997	0.2423	0.0441	1.1829	0
NKG7	5.4965	0.5470	0.0995	1.4610	0
SSFA2	5.4961	0.3183	0.0579	1.2469	0
GULP1	5.4941	0.2420	0.0441	1.1827	0
FYN	5.4863	0.2788	0.0508	1.2132	0
TNFAIP3	5.4860	0.4652	0.0848	1.3805	0
IQGAP2	5.4856	0.2702	0.0493	1.2059	0
NCK1	5.4806	0.3056	0.0558	1.2359	0
NAB1	5.4805	0.3067	0.0560	1.2368	0
EXOG	5.4782	0.5691	0.1039	1.4836	0
BTK	5.4749	0.3471	0.0634	1.2720	0
PDE4B	5.4739	0.3883	0.0709	1.3089	0
RNASE2	5.4725	0.3160	0.0577	1.2449	0
PANX1	5.4725	0.2508	0.0458	1.1899	0
TRPV2	5.4692	0.3587	0.0656	1.2822	0
CHSY1	5.4688	0.2211	0.0404	1.1656	0
IFI44	5.4652	0.5693	0.1042	1.4838	0
CCL2	5.4553	0.5797	0.1063	1.4946	0
CD84	5.4509	0.2080	0.0382	1.1551	0
TM6SF1	5.4496	0.2640	0.0485	1.2008	0
FBLN2	5.4490	0.4154	0.0762	1.3337	0
FCGR2B	5.4455	0.3323	0.0610	1.2590	0
MMP12	5.4450	0.8126	0.1492	1.7563	0

EMP1	5.4441	0.4655	0.0855	1.3808	0
CCND2	5.4431	0.4337	0.0797	1.3507	0
NAP1L3	5.4329	0.3606	0.0664	1.2840	0
CD37	5.4298	0.3992	0.0735	1.3187	0
JAK2	5.4264	0.2788	0.0514	1.2132	0
TAGLN	5.4264	0.3901	0.0719	1.3105	0
CDC25B	5.4214	0.4587	0.0846	1.3743	0
OLFML1	5.4209	0.3766	0.0695	1.2983	0
CXCL9	5.4199	0.7784	0.1436	1.7153	0
SERPINB2	5.4151	0.7397	0.1366	1.6699	0
FSCN1	5.4148	0.5021	0.0927	1.4163	0
MT1G	5.4131	0.6228	0.1150	1.5398	0
NRP1	5.4130	0.3588	0.0663	1.2823	0
KIAA1644	5.4084	0.2758	0.0510	1.2107	0
FKBP5	5.3968	0.3991	0.0740	1.3187	0
MYLK	5.3953	0.4155	0.0770	1.3338	0
CCPG1	5.3946	0.2470	0.0458	1.1867	0
P4HA2	5.3888	0.2908	0.0540	1.2233	0
LPXN	5.3848	0.4376	0.0813	1.3543	0
KLF9	5.3839	0.4473	0.0831	1.3635	0
VCAN	5.3821	0.5551	0.1031	1.4693	0
SERPINB4	5.3815	0.8234	0.1530	1.7695	0
PAPPA	5.3793	0.4752	0.0883	1.3901	0
CAP2	5.3729	0.4638	0.0863	1.3792	0
SAV1	5.3714	0.2587	0.0482	1.1964	0
RND3	5.3708	0.4429	0.0825	1.3593	0
CXCL12	5.3682	0.4100	0.0764	1.3287	0
PCOLCE2	5.3646	0.5252	0.0979	1.4391	0
TGM2	5.3620	0.4035	0.0752	1.3227	0
ST8SIA4	5.3614	0.1927	0.0359	1.1429	0
RAB3IL1	5.3601	0.4027	0.0751	1.3220	0
BMP1	5.3594	0.2101	0.0392	1.1568	0
OSTM1	5.3593	0.2318	0.0433	1.1743	0
STX11	5.3499	0.3833	0.0716	1.3043	0
CELF2	5.3449	0.2201	0.0412	1.1648	0
TBXAS1	5.3426	0.3761	0.0704	1.2978	0
RTN1	5.3419	0.3337	0.0625	1.2602	0
STAT1	5.3400	0.4746	0.0889	1.3895	0
COL10A1	5.3398	0.6675	0.1250	1.5883	0
S100A10	5.3397	0.4654	0.0872	1.3807	0
SNX10	5.3350	0.3688	0.0691	1.2913	0

ITGAV	5.3321	0.3263	0.0612	1.2538	0
FLRT2	5.3252	0.3039	0.0571	1.2345	0
NREP	5.3169	0.4496	0.0846	1.3656	0
ST6GALNAC5	5.3139	0.2515	0.0473	1.1905	0
HK3	5.3070	0.3371	0.0635	1.2632	0
PTHLH	5.3048	0.6411	0.1209	1.5595	0
MILR1	5.2997	0.2302	0.0434	1.1730	0
NABP1	5.2797	0.3576	0.0677	1.2813	0
PRRX2	5.2791	0.3953	0.0749	1.3152	0
LAMA3	5.2728	0.4582	0.0869	1.3738	0
COL15A1	5.2728	0.4399	0.0834	1.3565	0
RGS20	5.2703	0.5117	0.0971	1.4258	0
LCP1	5.2683	0.4451	0.0845	1.3614	0
LILRB3	5.2651	0.2907	0.0552	1.2232	0
AMPD3	5.2567	0.1526	0.0290	1.1116	0
LAP3	5.2532	0.3131	0.0596	1.2424	0
ANTXR1	5.2508	0.2782	0.0530	1.2127	0
DKK3	5.2478	0.3879	0.0739	1.3085	0
UCHL1	5.2474	0.5389	0.1027	1.4529	0
GOS2	5.2450	0.5349	0.1020	1.4488	0
IL8	5.2447	0.8499	0.1621	1.8024	0
DUSP14	5.2446	0.2991	0.0570	1.2303	0
ARHGAP24	5.2411	0.1421	0.0271	1.1035	0
FPR1	5.2383	0.4477	0.0855	1.3638	0
TPST1	5.2370	0.3380	0.0645	1.2640	0
VEGFC	5.2358	0.4168	0.0796	1.3350	0
CD68	5.2325	0.2740	0.0524	1.2092	0
DCLK1	5.2309	0.2382	0.0455	1.1795	0
C1orf54	5.2305	0.3346	0.0640	1.2610	0
FUT8	5.2281	0.3273	0.0626	1.2547	0
DCBLD2	5.2273	0.5436	0.1040	1.4576	0
PDZRN3	5.2270	0.2110	0.0404	1.1575	0
LUM	5.2246	0.5518	0.1056	1.4660	0
AOAH	5.2228	0.2677	0.0512	1.2039	0
PAPSS2	5.2114	0.3910	0.0750	1.3113	0
MOB3B	5.2092	0.2735	0.0525	1.2087	0
RIN3	5.2057	0.1510	0.0290	1.1103	0
COL5A3	5.2032	0.2689	0.0517	1.2049	0
BATF3	5.2019	0.2491	0.0479	1.1884	0
CST7	5.2019	0.3751	0.0721	1.2970	0
TDO2	5.2018	0.3655	0.0703	1.2883	0

FGD6	5.1996	0.2584	0.0497	1.1961	0
DDR2	5.1941	0.3562	0.0686	1.2800	0
PCOLCE	5.1938	0.4768	0.0918	1.3916	0
CTSB	5.1920	0.3444	0.0663	1.2697	0
CXCL2	5.1909	0.5582	0.1075	1.4724	0
CCDC88A	5.1893	0.2024	0.0390	1.1506	0
NRP2	5.1802	0.1529	0.0295	1.1118	0
CSRP1	5.1801	0.2744	0.0530	1.2095	0
40061	5.1774	0.2303	0.0445	1.1731	0
ALDH1A1	5.1749	0.5796	0.1120	1.4944	0
THY1	5.1650	0.4205	0.0814	1.3384	0
BGN	5.1641	0.3972	0.0769	1.3169	0
OLR1	5.1587	0.5731	0.1111	1.4878	0
IL13RA1	5.1560	0.2877	0.0558	1.2207	0
EXT1	5.1549	0.3499	0.0679	1.2744	0
IMPDH1	5.1532	0.1962	0.0381	1.1457	0
FAM216A	5.1509	0.3006	0.0584	1.2317	0
DNAJB5	5.1479	0.1577	0.0306	1.1155	0
FLNC	5.1408	0.5782	0.1125	1.4930	0
TRAM2	5.1353	0.3111	0.0606	1.2407	0
MAP7D1	5.1327	0.2423	0.0472	1.1829	0
TNFRSF1B	5.1318	0.3398	0.0662	1.2655	0
TWIST1	5.1313	0.3566	0.0695	1.2804	0
ARSB	5.1298	0.1694	0.0330	1.1246	0
RHOG	5.1297	0.2464	0.0480	1.1863	0
RAB32	5.1245	0.3327	0.0649	1.2594	0
EVC	5.1241	0.2011	0.0392	1.1495	0
ADAMDEC1	5.1213	0.5426	0.1059	1.4566	0
KLF10	5.1200	0.2065	0.0403	1.1539	0
CD97	5.1183	0.3184	0.0622	1.2469	0
SLC24A3	5.1143	0.3648	0.0713	1.2877	0
LY6E	5.1139	0.5521	0.1080	1.4662	0
ARHGAP22	5.1127	0.2992	0.0585	1.2305	0
S100A3	5.1108	0.5422	0.1061	1.4562	0
ADA	5.1099	0.4400	0.0861	1.3566	0
FILIP1L	5.1096	0.3423	0.0670	1.2678	0
CXCL13	5.1038	0.5794	0.1135	1.4942	0
RASA3	5.1022	0.1601	0.0314	1.1174	0
IFIT3	5.1021	0.4047	0.0793	1.3238	0
FHL3	5.0935	0.2183	0.0429	1.1633	0
CD38	5.0924	0.4364	0.0857	1.3532	0

IL2RB	5.0900	0.4158	0.0817	1.3340	0
KIRREL	5.0821	0.1720	0.0338	1.1266	0
SLCO2B1	5.0798	0.3775	0.0743	1.2991	0
EHD2	5.0776	0.3124	0.0615	1.2418	0
SEC23A	5.0766	0.1697	0.0334	1.1248	0
ELOVL4	5.0736	0.4136	0.0815	1.3320	0
CDC42EP1	5.0722	0.2206	0.0435	1.1653	0
HDAC4	5.0697	0.2589	0.0511	1.1966	0
WAS	5.0683	0.4201	0.0829	1.3381	0
DIO2	5.0655	0.4535	0.0895	1.3694	0
HERC5	5.0603	0.5093	0.1006	1.4233	0
KDELC1	5.0544	0.2531	0.0501	1.1918	0
ANGPTL2	5.0525	0.4441	0.0879	1.3605	0
HPS5	5.0400	0.1588	0.0315	1.1164	0
SERPINF1	5.0399	0.4506	0.0894	1.3666	0
PRR5L	5.0392	0.2947	0.0585	1.2266	0
KLF13	5.0384	0.3257	0.0646	1.2533	0
CHN1	5.0381	0.3803	0.0755	1.3016	0
CD4	5.0372	0.2290	0.0455	1.1721	0
MMP11	5.0333	0.6959	0.1383	1.6199	0
PCNXL4	5.0268	0.2164	0.0430	1.1618	0
CLEC11A	5.0259	0.3899	0.0776	1.3103	0
CILP	5.0247	0.4054	0.0807	1.3244	0
ROR1	5.0241	0.1963	0.0391	1.1458	0
TIMP1	5.0235	0.3916	0.0780	1.3119	0
MAPKAPK2	5.0213	0.1709	0.0340	1.1257	0
STAT4	5.0211	0.3608	0.0719	1.2841	0
CD82	5.0163	0.2798	0.0558	1.2140	0
MYC	5.0146	0.5171	0.1031	1.4311	0
CD69	5.0146	0.5219	0.1041	1.4358	0
CD7	5.0145	0.4027	0.0803	1.3220	0
MFSD12	5.0138	0.1639	0.0327	1.1203	0
TPM4	5.0098	0.2709	0.0541	1.2066	0
EHBP1	5.0079	0.2669	0.0533	1.2032	0
RCN3	5.0075	0.4318	0.0862	1.3489	0
RGS10	5.0051	0.2235	0.0447	1.1676	0
ANXA2	4.9963	0.3486	0.0698	1.2733	0
PLEKHO2	4.9955	0.2698	0.0540	1.2057	0
MRC2	4.9859	0.1925	0.0386	1.1427	0
OLFML2A	4.9854	0.3960	0.0794	1.3158	0
CNTN1	4.9846	0.3400	0.0682	1.2658	0

MITF	4.9832	0.1543	0.0310	1.1129	0
BIRC3	4.9804	0.3344	0.0671	1.2608	0
RECQL	4.9762	0.1925	0.0387	1.1427	0
IL27RA	4.9751	0.3180	0.0639	1.2466	0
NOX4	4.9747	0.3140	0.0631	1.2432	0
LAIR1	4.9717	0.2022	0.0407	1.1505	0
COL7A1	4.9711	0.5856	0.1178	1.5006	0
VCAM1	4.9702	0.3541	0.0712	1.2782	0
GUCY1B3	4.9684	0.1769	0.0356	1.1305	0
DUSP22	4.9664	0.2124	0.0428	1.1586	0
CLEC7A	4.9663	0.2156	0.0434	1.1612	0
MAOB	4.9632	0.1940	0.0391	1.1440	0
PMAIP1	4.9623	0.3802	0.0766	1.3015	0
FCGR3B	4.9545	0.3452	0.0697	1.2704	0
SLC38A6	4.9543	0.2655	0.0536	1.2021	0
MXRA5	4.9397	0.5379	0.1089	1.4519	0
LRRC17	4.9364	0.3092	0.0626	1.2390	0
MYO1F	4.9321	0.2396	0.0486	1.1807	0
SLMO1	4.9320	0.3017	0.0612	1.2326	0
TREM2	4.9286	0.2804	0.0569	1.2146	0
PTPRC	4.9242	0.2474	0.0502	1.1871	0
BNC1	4.9211	0.3327	0.0676	1.2594	0
PCNX	4.9176	0.2368	0.0482	1.1784	0
ADAMTS2	4.9098	0.1810	0.0369	1.1337	0
CXCR4	4.9057	0.4160	0.0848	1.3342	0
SLC39A8	4.9035	0.2867	0.0585	1.2199	0
RASSF4	4.8980	0.1875	0.0383	1.1388	0
GLRX	4.8961	0.3341	0.0682	1.2606	0
DCN	4.8958	0.5062	0.1034	1.4203	0
CALU	4.8933	0.2932	0.0599	1.2253	0
PTMS	4.8906	0.3221	0.0659	1.2502	0
CASP4	4.8853	0.1872	0.0383	1.1386	0
STAB1	4.8846	0.3573	0.0731	1.2810	0
KCNJ8	4.8816	0.2788	0.0571	1.2132	0
IER3	4.8807	0.4921	0.1008	1.4065	0
ILK	4.8794	0.2210	0.0453	1.1655	0
CYTH4	4.8774	0.4113	0.0843	1.3299	0
CNN2	4.8746	0.2528	0.0519	1.1915	0
JAG1	4.8739	0.3528	0.0724	1.2770	0
HLA-DPA1	4.8639	0.5132	0.1055	1.4272	0
OPTN	4.8632	0.2796	0.0575	1.2138	0

SLIT2	4.8627	0.3626	0.0746	1.2858	0
SFRP4	4.8617	0.4333	0.0891	1.3503	0
ESD	4.8569	0.2288	0.0471	1.1719	0
NUDT11	4.8559	0.3392	0.0699	1.2650	0
ETF1	4.8456	0.1744	0.0360	1.1285	0
P2RY13	4.8422	0.2596	0.0536	1.1972	0
TFPI2	4.8359	0.5316	0.1099	1.4456	0
ABL2	4.8352	0.1758	0.0364	1.1296	0
RECK	4.8310	0.2137	0.0442	1.1597	0
GUCY1A3	4.8291	0.3415	0.0707	1.2671	0
EMR2	4.8280	0.3391	0.0702	1.2649	0
LCP2	4.8276	0.2367	0.0490	1.1783	0
TSC22D3	4.8261	0.2718	0.0563	1.2073	0
SLC2A5	4.8261	0.3476	0.0720	1.2724	0
RASSF9	4.8228	0.2481	0.0514	1.1877	0
PLK2	4.8224	0.2462	0.0511	1.1861	0
PKD2	4.8213	0.1995	0.0414	1.1483	0
MXRA7	4.8196	0.1869	0.0388	1.1383	0
STXBP1	4.8184	0.2152	0.0447	1.1609	0
MMD	4.8150	0.3526	0.0732	1.2769	0
PLGRKT	4.8134	0.2853	0.0593	1.2186	0
TNS1	4.8058	0.2099	0.0437	1.1566	0
AQP9	4.8045	0.5309	0.1105	1.4449	0
NCOR2	4.8031	0.2417	0.0503	1.1824	0
CDV3	4.8012	0.2329	0.0485	1.1752	0
ADCY9	4.7911	0.2033	0.0424	1.1514	0
SERPINB1	4.7889	0.3990	0.0833	1.3186	0
SPP1	4.7880	0.6523	0.1362	1.5717	0
TMEM176A	4.7816	0.3740	0.0782	1.2959	0
PRF1	4.7815	0.3172	0.0663	1.2459	0
UBTD1	4.7779	0.2619	0.0548	1.1991	0
CPE	4.7743	0.4012	0.0840	1.3206	0
RBMS3	4.7721	0.1431	0.0300	1.1043	0
IL2RG	4.7698	0.1811	0.0380	1.1338	0
PFKFB3	4.7698	0.2806	0.0588	1.2147	0
KIAA1598	4.7683	0.3288	0.0690	1.2560	0
IRF7	4.7668	0.3261	0.0684	1.2536	0
PI3	4.7617	0.9720	0.2041	1.9615	0
EFR3A	4.7536	0.1926	0.0405	1.1428	0
LRRC32	4.7465	0.3786	0.0798	1.3001	0
CAPN2	4.7460	0.2652	0.0559	1.2018	0

HLA-DQA1	4.7447	0.6101	0.1286	1.5264	0
TPP1	4.7399	0.2656	0.0560	1.2021	0
PLAGL1	4.7386	0.2825	0.0596	1.2163	0
NXPE3	4.7245	0.1685	0.0357	1.1239	0
PTX3	4.7193	0.2904	0.0615	1.2230	0
NPC1	4.7144	0.2617	0.0555	1.1989	0
ETV5	4.7134	0.2187	0.0464	1.1637	0
PIP4K2A	4.7050	0.1612	0.0343	1.1182	0
RHOC	4.6952	0.2364	0.0504	1.1781	0
IRF8	4.6928	0.4319	0.0920	1.3490	0
PTPRG	4.6907	0.1974	0.0421	1.1467	0
LEPRE1	4.6898	0.2653	0.0566	1.2019	0
SERPINE2	4.6880	0.5760	0.1229	1.4907	0
TLR6	4.6843	0.1854	0.0396	1.1371	0
LMCD1	4.6838	0.3633	0.0776	1.2864	0
GRAMD4	4.6812	0.2324	0.0496	1.1748	0
MCTP1	4.6812	0.2001	0.0427	1.1488	0
PLN	4.6807	0.2892	0.0618	1.2220	0
IRF1	4.6799	0.3652	0.0780	1.2880	0
GZMH	4.6756	0.4266	0.0912	1.3441	0
SYNM	4.6724	0.3600	0.0771	1.2835	0
SAMD4A	4.6684	0.2014	0.0431	1.1498	0
SASH3	4.6680	0.2822	0.0605	1.2161	0
LYN	4.6672	0.2984	0.0639	1.2297	0
MCL1	4.6648	0.2342	0.0502	1.1763	0
AKIP1	4.6644	0.1859	0.0399	1.1375	0
SLCO1B3	4.6632	0.4928	0.1057	1.4072	0
HSD11B1	4.6585	0.2608	0.0560	1.1981	0
LILRB4	4.6569	0.3185	0.0684	1.2470	0
LRP1	4.6547	0.1659	0.0357	1.1219	0
SIGLEC1	4.6522	0.2141	0.0460	1.1600	0
GPSM3	4.6455	0.2946	0.0634	1.2265	0
PLA2G4C	4.6444	0.2998	0.0645	1.2309	0
NQO2	4.6421	0.2495	0.0537	1.1888	0
PLXNC1	4.6390	0.1522	0.0328	1.1113	0
ATP8B4	4.6264	0.2772	0.0599	1.2118	0
DDX60	4.6163	0.3604	0.0781	1.2838	0
RSAD2	4.6160	0.4705	0.1019	1.3856	0
CD47	4.6149	0.2650	0.0574	1.2017	0
PDLIM7	4.6144	0.1756	0.0381	1.1294	0
IL2RA	4.5992	0.1558	0.0339	1.1141	0

KCTD15	4.5990	0.2666	0.0580	1.2030	0
FBXL7	4.5953	0.1690	0.0368	1.1243	0
CD74	4.5946	0.4215	0.0917	1.3393	0
TCF4	4.5929	0.3120	0.0679	1.2414	0
PI15	4.5890	0.2688	0.0586	1.2048	0
SGCD	4.5872	0.1836	0.0400	1.1357	0
IL6ST	4.5863	0.1218	0.0266	1.0881	0
EMR1	4.5849	0.2154	0.0470	1.1610	0
PLOD1	4.5824	0.2648	0.0578	1.2015	0
RELB	4.5787	0.2141	0.0468	1.1600	0
ACP5	4.5698	0.4143	0.0907	1.3326	0
NINJ1	4.5674	0.2936	0.0643	1.2257	0
ANK2	4.5664	0.1558	0.0341	1.1140	0
ARHGAP25	4.5656	0.2941	0.0644	1.2261	0
JAM2	4.5642	0.3018	0.0661	1.2326	0
SCG5	4.5637	0.4681	0.1026	1.3833	0
CTLA4	4.5602	0.2224	0.0488	1.1666	0
CNN1	4.5589	0.4730	0.1038	1.3880	0
SLC12A8	4.5587	0.3679	0.0807	1.2905	0
ARNTL	4.5473	0.1888	0.0415	1.1398	0
CLIC2	4.5459	0.1963	0.0432	1.1457	0
TUBA4A	4.5459	0.4183	0.0920	1.3363	0
TPD52L1	4.5445	0.2908	0.0640	1.2233	0
SLC16A2	4.5434	0.1772	0.0390	1.1307	0
PELO	4.5418	0.2042	0.0450	1.1521	0
MFI2	4.5402	0.1927	0.0425	1.1429	0
ARFGAP3	4.5395	0.2088	0.0460	1.1558	0
ST5	4.5384	0.2039	0.0449	1.1518	0
KLHL2	4.5287	0.2407	0.0532	1.1816	0
GBP1	4.5278	0.4063	0.0897	1.3253	0
HDAC9	4.5223	0.1370	0.0303	1.0996	0
HCFC2	4.5206	0.1662	0.0368	1.1221	0
ELOVL5	4.5201	0.2799	0.0619	1.2141	0
MALT1	4.5170	0.1742	0.0386	1.1284	0
TANK	4.5078	0.1741	0.0386	1.1283	0
PDZD2	4.5018	0.1984	0.0441	1.1474	0
BACH2	4.4973	0.1516	0.0337	1.1108	0
TINF2	4.4853	0.2693	0.0600	1.2052	0
LHFP	4.4851	0.2900	0.0647	1.2226	0
TNFSF12	4.4833	0.2622	0.0585	1.1993	0
WWTR1	4.4821	0.1708	0.0381	1.1257	0

GHR	4.4716	0.3297	0.0737	1.2568	0
PTAFR	4.4705	0.1853	0.0414	1.1370	0
FSTL1	4.4678	0.2868	0.0642	1.2200	0
SAMD9	4.4654	0.4258	0.0954	1.3434	0
LYZ	4.4628	0.4656	0.1043	1.3809	0
CCDC91	4.4622	0.2062	0.0462	1.1536	0
TAP2	4.4612	0.2358	0.0528	1.1775	0
GLI2	4.4596	0.1546	0.0347	1.1131	0
B2M	4.4595	0.2144	0.0481	1.1602	0
HOXD11	4.4586	0.3175	0.0712	1.2461	0
CD48	4.4582	0.4331	0.0971	1.3501	0
DFNA5	4.4469	0.4853	0.1091	1.3999	0
DCHS1	4.4417	0.1539	0.0347	1.1126	0
HLA-A	4.4416	0.2843	0.0640	1.2178	0
LAG3	4.4291	0.3861	0.0872	1.3069	0
F2R	4.4235	0.1701	0.0385	1.1252	0
PLOD2	4.4147	0.3581	0.0811	1.2817	0
MAMLD1	4.4103	0.1972	0.0447	1.1465	0
IL21R	4.4060	0.2158	0.0490	1.1613	0
ME1	4.4051	0.3817	0.0866	1.3029	0
PRSS23	4.4037	0.2990	0.0679	1.2303	0
SYT11	4.4021	0.3511	0.0797	1.2755	0
FHL1	4.4020	0.3486	0.0792	1.2733	0
NLRP3	4.4012	0.3025	0.0687	1.2333	0
ACTG2	4.3993	0.5735	0.1304	1.4882	0
SH3BGRL3	4.3988	0.2419	0.0550	1.1825	0
NIN	4.3965	0.1390	0.0316	1.1011	0
AMD1	4.3955	0.2006	0.0456	1.1491	0
MSR1	4.3940	0.1504	0.0342	1.1099	0
VRK2	4.3897	0.2180	0.0497	1.1631	0
HES2	4.3811	0.3889	0.0888	1.3094	0
TFPI	4.3781	0.3309	0.0756	1.2578	0
LAIR2	4.3778	0.2672	0.0610	1.2035	0
TRAF3	4.3739	0.1449	0.0331	1.1056	0
SEMA3A	4.3736	0.2203	0.0504	1.1650	0
GZMK	4.3722	0.4913	0.1124	1.4058	0
IFNG	4.3670	0.3751	0.0859	1.2969	0
FADS3	4.3661	0.1667	0.0382	1.1225	0
ACTR3	4.3658	0.2114	0.0484	1.1578	0
NFIX	4.3603	0.3382	0.0776	1.2642	0
STAT3	4.3574	0.1755	0.0403	1.1294	0

DENND5A	4.3547	0.2334	0.0536	1.1756	0
CD40	4.3544	0.2238	0.0514	1.1678	0
ATP2B4	4.3465	0.2323	0.0534	1.1747	0
SELPLG	4.3454	0.1588	0.0366	1.1164	0
IFI44L	4.3413	0.5796	0.1335	1.4944	0
CALB2	4.3367	0.2658	0.0613	1.2023	0
FRMD4B	4.3365	0.1294	0.0298	1.0938	0
NAMPT	4.3359	0.3451	0.0796	1.2702	0
HLX	4.3324	0.1760	0.0406	1.1297	0
CD80	4.3258	0.1584	0.0366	1.1161	0
SYDE1	4.3209	0.2013	0.0466	1.1497	0
TNF	4.3196	0.2950	0.0683	1.2269	0
PPFIBP1	4.3185	0.1796	0.0416	1.1326	0
GIMAP4	4.3181	0.3503	0.0811	1.2748	0
KLK6	4.3170	0.6892	0.1597	1.6124	0
ICOS	4.3164	0.3022	0.0700	1.2330	0
CLIP3	4.3131	0.3445	0.0799	1.2697	0
FSTL3	4.3096	0.3381	0.0785	1.2641	0
NAALADL1	4.3075	0.2013	0.0467	1.1497	0
SERPINB7	4.3072	0.3539	0.0822	1.2780	0
ARL2BP	4.3027	0.1820	0.0423	1.1345	0
CYP26B1	4.2990	0.3163	0.0736	1.2451	0
PGM1	4.2990	0.3201	0.0745	1.2484	0
MMP7	4.2965	0.7792	0.1814	1.7162	0
AIM2	4.2964	0.4227	0.0984	1.3405	0
YBX3	4.2938	0.2344	0.0546	1.1764	0
ADAMTS6	4.2903	0.1475	0.0344	1.1077	0
PLIN3	4.2876	0.1994	0.0465	1.1483	0
CD33	4.2855	0.2042	0.0477	1.1521	0
BAG3	4.2831	0.2426	0.0566	1.1831	0
RARB	4.2805	0.1729	0.0404	1.1273	0
SDC2	4.2788	0.2479	0.0579	1.1875	0
VAV1	4.2784	0.2066	0.0483	1.1540	0
IFI6	4.2777	0.4441	0.1038	1.3605	0
DSC3	4.2770	0.4510	0.1055	1.3670	0
BTN3A3	4.2736	0.2617	0.0612	1.1989	0
HSPA13	4.2731	0.1480	0.0346	1.1080	0
SOAT1	4.2689	0.1971	0.0462	1.1464	0
ANGPT1	4.2687	0.2484	0.0582	1.1879	0
LYL1	4.2646	0.2479	0.0581	1.1875	0
SYNDIG1	4.2636	0.2361	0.0554	1.1778	0

MAPRE2	4.2619	0.2522	0.0592	1.1910	0
MAP3K6	4.2576	0.2236	0.0525	1.1676	0
THBS2	4.2522	0.5205	0.1224	1.4344	0
CHRD1	4.2489	0.2355	0.0554	1.1773	0
KCTD9	4.2461	0.2058	0.0485	1.1533	0
ACTA2	4.2452	0.3481	0.0820	1.2729	0
AGTPBP1	4.2423	0.1660	0.0391	1.1220	0
PTPRZ1	4.2413	0.3179	0.0750	1.2465	0
RNF19B	4.2408	0.2121	0.0500	1.1584	0
SOX9	4.2386	0.4610	0.1088	1.3765	0
OSM	4.2377	0.4005	0.0945	1.3199	0
CD8A	4.2353	0.3246	0.0766	1.2523	0
CYTH1	4.2345	0.1474	0.0348	1.1076	0
LAMC2	4.2300	0.4382	0.1036	1.3549	0
CDK14	4.2273	0.2258	0.0534	1.1694	0
ELMO1	4.2249	0.1675	0.0396	1.1231	0
IL33	4.2216	0.3794	0.0899	1.3008	0
KLHL21	4.2176	0.1924	0.0456	1.1427	0
PPP3CC	4.2164	0.1724	0.0409	1.1269	0
C9orf91	4.2153	0.1893	0.0449	1.1402	0
IFI35	4.2130	0.3065	0.0727	1.2367	0
CD2	4.2074	0.4301	0.1022	1.3474	0
KLRD1	4.2073	0.2157	0.0513	1.1613	0
TSPAN7	4.2033	0.4062	0.0966	1.3252	0
SERPINB9	4.2010	0.1748	0.0416	1.1288	0
MAP7D3	4.2008	0.1424	0.0339	1.1037	0
SERPINB3	4.2000	0.7036	0.1675	1.6285	0
SPOCK1	4.1996	0.4905	0.1168	1.4049	0
GAS7	4.1988	0.2676	0.0637	1.2038	0
STON1	4.1987	0.2050	0.0488	1.1527	0
HMGA2	4.1975	0.1666	0.0397	1.1224	0
IL36G	4.1972	0.4212	0.1004	1.3390	0
PTGER2	4.1971	0.2302	0.0548	1.1730	0
PSTPIP1	4.1960	0.2092	0.0499	1.1561	0
HSPA12A	4.1943	0.2865	0.0683	1.2197	0
GGT5	4.1939	0.1681	0.0401	1.1236	0
HLA-DRA	4.1936	0.4266	0.1017	1.3441	0
COL17A1	4.1927	0.5320	0.1269	1.4460	0
FAM49B	4.1920	0.2144	0.0511	1.1602	0
IFIT2	4.1828	0.3810	0.0911	1.3023	0
OGN	4.1820	0.3098	0.0741	1.2396	0

SERPINB13	4.1811	0.5377	0.1286	1.4517	0
JAM3	4.1810	0.2998	0.0717	1.2310	0
POLR3G	4.1809	0.1331	0.0318	1.0966	0
WNT5B	4.1789	0.2571	0.0615	1.1951	0
CANX	4.1778	0.1860	0.0445	1.1376	0
MEF2C	4.1762	0.2161	0.0517	1.1616	0
APBB2	4.1754	0.1207	0.0289	1.0873	0
MYO10	4.1729	0.3134	0.0751	1.2427	0
ARRB2	4.1685	0.2152	0.0516	1.1608	0
CFH	4.1667	0.3279	0.0787	1.2552	0
SECTM1	4.1619	0.1692	0.0407	1.1244	0
FAT2	4.1603	0.4367	0.1050	1.3535	0
S100A8	4.1564	0.7005	0.1685	1.6250	0
TLN1	4.1527	0.2019	0.0486	1.1502	0
SCO2	4.1512	0.2343	0.0564	1.1763	0
CNN3	4.1507	0.2418	0.0583	1.1825	0
SLCO3A1	4.1503	0.1763	0.0425	1.1300	0
BDKRB1	4.1480	0.1906	0.0459	1.1412	0
AVEN	4.1469	0.2018	0.0487	1.1501	0
RBMS2	4.1468	0.1900	0.0458	1.1408	0
IL18RAP	4.1458	0.2457	0.0593	1.1857	0
ZBP1	4.1452	0.2100	0.0507	1.1567	0
TAP1	4.1433	0.3446	0.0832	1.2698	0
TNFRSF9	4.1430	0.1601	0.0386	1.1173	0
HLA-B	4.1421	0.3595	0.0868	1.2830	0
GIMAP6	4.1420	0.2793	0.0674	1.2136	0
CYLD	4.1355	0.1607	0.0389	1.1179	0
CRISPLD2	4.1340	0.3645	0.0882	1.2874	0
ZCCHC24	4.1276	0.2774	0.0672	1.2120	0
ITK	4.1169	0.3068	0.0745	1.2370	0
SEC14L2	4.1118	0.2028	0.0493	1.1509	0
FTSJ1	4.1104	0.1390	0.0338	1.1012	0
SH3PXD2A	4.1097	0.2962	0.0721	1.2279	0
SEC61B	4.1046	0.1359	0.0331	1.0988	0
SCRG1	4.1030	0.2861	0.0697	1.2193	0
PPP3CA	4.1026	0.1504	0.0367	1.1099	0
RUNX1T1	4.1020	0.1993	0.0486	1.1481	0
CISD1	4.1019	0.1763	0.0430	1.1300	0
PRUNE2	4.0977	0.1526	0.0372	1.1116	0
KLK11	4.0973	0.5018	0.1225	1.4160	0
PCSK5	4.0960	0.3065	0.0748	1.2367	0

MEOX2	4.0951	0.1882	0.0460	1.1394	0
ITPR2	4.0928	0.1602	0.0391	1.1175	0
PTPRO	4.0899	0.1757	0.0430	1.1295	0
CCL20	4.0885	0.5787	0.1415	1.4935	0
CD300C	4.0859	0.1709	0.0418	1.1257	0
MUSK	4.0850	0.1823	0.0446	1.1347	0
DUSP1	4.0849	0.4305	0.1054	1.3477	0
TGFB2	4.0849	0.1462	0.0358	1.1066	0
FGR	4.0812	0.2851	0.0699	1.2185	0
SH3BGRL	4.0803	0.2811	0.0689	1.2151	0
ALDH1B1	4.0796	0.2091	0.0513	1.1560	0
HLA-DQB1	4.0770	0.4001	0.0981	1.3196	0
LILRA2	4.0751	0.1996	0.0490	1.1484	0
RNASE1	4.0745	0.3066	0.0753	1.2368	0
CLUAP1	4.0731	0.1469	0.0361	1.1072	0
ADAM12	4.0728	0.1578	0.0388	1.1156	0
KRT16	4.0685	0.5152	0.1266	1.4292	0
CSPG4	4.0665	0.2502	0.0615	1.1893	0
ZFHX4	4.0650	0.2288	0.0563	1.1719	0
SPSB1	4.0633	0.2015	0.0496	1.1499	0
PDP1	4.0588	0.2535	0.0625	1.1921	0
IFI27	4.0582	0.5451	0.1343	1.4591	0
TXNDC15	4.0563	0.1463	0.0361	1.1067	0
UBE2L6	4.0554	0.2705	0.0667	1.2063	0
LPAR1	4.0537	0.2104	0.0519	1.1570	0
KIAA0930	4.0521	0.1458	0.0360	1.1064	0
STRN3	4.0489	0.1725	0.0426	1.1270	0
RNF130	4.0428	0.2466	0.0610	1.1864	0
DOK3	4.0405	0.1214	0.0301	1.0878	0
GPR124	4.0397	0.2501	0.0619	1.1893	0
IGF2BP2	4.0392	0.4128	0.1022	1.3312	0
CD93	4.0378	0.2678	0.0663	1.2040	0
SERPINH1	4.0367	0.2642	0.0655	1.2010	0
DSC2	4.0348	0.4011	0.0994	1.3205	0
GPR37	4.0334	0.2718	0.0674	1.2073	0
GYPC	4.0314	0.2327	0.0577	1.1750	0
MGAT2	4.0294	0.1717	0.0426	1.1264	0
PLP2	4.0266	0.2332	0.0579	1.1754	0
EREG	4.0265	0.2456	0.0610	1.1855	0
MARCO	4.0220	0.3190	0.0793	1.2475	0
TXNRD1	4.0205	0.2547	0.0634	1.1931	0

ST8SIA1	4.0187	0.1795	0.0447	1.1325	0
CAB39	4.0174	0.1845	0.0459	1.1364	0
CD209	4.0171	0.2665	0.0663	1.2029	0
ELK3	4.0170	0.1036	0.0258	1.0744	0
MMP14	4.0169	0.1881	0.0468	1.1393	0
DDX58	4.0139	0.2131	0.0531	1.1592	0
TMEM38B	4.0084	0.1768	0.0441	1.1304	0
CTSL1	4.0075	0.2558	0.0638	1.1940	0
COL4A2	4.0070	0.2485	0.0620	1.1880	0
GABRP	4.0045	0.4682	0.1169	1.3834	0
EVA1B	4.0037	0.1768	0.0442	1.1304	0
DPP4	4.0035	0.3249	0.0811	1.2525	0
IFIT5	4.0027	0.1665	0.0416	1.1223	0
RAP2C	4.0022	0.1813	0.0453	1.1339	0
PTTG2	4.0017	0.1852	0.0463	1.1369	0
TMX4	3.9967	0.1967	0.0492	1.1460	0
ITGAX	3.9964	0.2213	0.0554	1.1658	0
FAM65B	3.9956	0.3329	0.0833	1.2595	0
EPYC	3.9955	0.3276	0.0820	1.2550	0
PTPRD	3.9950	0.1486	0.0372	1.1085	0
COX7A1	3.9941	0.2842	0.0712	1.2177	0
IL12RB1	3.9923	0.1288	0.0323	1.0934	0
GSN	3.9900	0.1607	0.0403	1.1178	0
ITGB5	3.9885	0.2638	0.0661	1.2006	0
ADAM23	3.9880	0.2448	0.0614	1.1849	0
SETBP1	3.9870	0.2963	0.0743	1.2280	0
MMP3	3.9849	0.5230	0.1313	1.4370	0
MCFD2	3.9847	0.1553	0.0390	1.1137	0
MFAP4	3.9837	0.5445	0.1367	1.4585	0
RFTN1	3.9831	0.2680	0.0673	1.2041	0
GIMAP5	3.9799	0.2728	0.0685	1.2081	0
C12orf5	3.9785	0.2099	0.0528	1.1566	0
MACF1	3.9747	0.1302	0.0327	1.0944	0
GOLT1B	3.9743	0.1951	0.0491	1.1448	0
DENND1A	3.9738	0.1587	0.0399	1.1163	0
NRG1	3.9735	0.2095	0.0527	1.1563	0
LRP8	3.9703	0.2126	0.0535	1.1588	0
ENPEP	3.9664	0.2137	0.0539	1.1597	0
RRAS2	3.9645	0.2286	0.0577	1.1717	0
MOXD1	3.9641	0.3413	0.0861	1.2669	0
LMF2	3.9621	0.1941	0.0490	1.1440	0

GPNMB	3.9577	0.4176	0.1055	1.3357	0
MMP2	3.9547	0.2072	0.0524	1.1544	0
PIK3CG	3.9543	0.2246	0.0568	1.1684	0
FHOD3	3.9508	0.3365	0.0852	1.2627	0
CORO1A	3.9486	0.3089	0.0782	1.2388	0
GFI1	3.9482	0.2125	0.0538	1.1587	0
SPEG	3.9457	0.1148	0.0291	1.0828	0
SAT1	3.9446	0.2611	0.0662	1.1984	0
UAP1L1	3.9444	0.2006	0.0509	1.1492	0
IL18R1	3.9427	0.2148	0.0545	1.1606	0
SSBP2	3.9409	0.2006	0.0509	1.1491	0
NID1	3.9403	0.1602	0.0407	1.1174	0
NEIL3	3.9400	0.1999	0.0507	1.1486	0
DBN1	3.9374	0.3223	0.0819	1.2503	0
RALB	3.9356	0.1740	0.0442	1.1282	0
SEC14L1	3.9350	0.1591	0.0404	1.1166	0
MAP4K4	3.9335	0.2187	0.0556	1.1636	0
CYR61	3.9334	0.3601	0.0916	1.2835	0
CDC42EP3	3.9325	0.1779	0.0452	1.1312	0
ZNF365	3.9267	0.3987	0.1015	1.3183	0
SORBS3	3.9229	0.2222	0.0567	1.1665	0
CCL21	3.9211	0.3221	0.0822	1.2502	0
TREM1	3.9208	0.2782	0.0710	1.2127	0
WWC3	3.9193	0.1980	0.0505	1.1471	0
KPNA3	3.9188	0.2004	0.0511	1.1490	0
PLAC8	3.9169	0.4298	0.1097	1.3471	0
OSBPL8	3.9160	0.1628	0.0416	1.1194	0
NTM	3.9149	0.3139	0.0802	1.2430	0
PNP	3.9137	0.2235	0.0571	1.1676	0
CREM	3.9131	0.1641	0.0419	1.1205	0
GPX7	3.9090	0.3357	0.0859	1.2620	0
ACTB	3.9075	0.1954	0.0500	1.1451	0
TUBA1A	3.9021	0.1856	0.0476	1.1373	0
GBE1	3.9011	0.2285	0.0586	1.1717	0
CSRP2	3.9001	0.2779	0.0713	1.2124	0
WNT2	3.8986	0.2810	0.0721	1.2150	0
TRPC1	3.8967	0.2127	0.0546	1.1589	0
APOE	3.8911	0.4350	0.1118	1.3519	0
JUN	3.8863	0.3546	0.0913	1.2787	0
SAP30	3.8843	0.2206	0.0568	1.1652	0
FGFBP1	3.8835	0.6333	0.1631	1.5511	0

SPTSSA	3.8829	0.2297	0.0592	1.1726	0
BDKRB2	3.8814	0.1704	0.0439	1.1254	0
PPP1R12A	3.8803	0.2021	0.0521	1.1504	0
GRK5	3.8776	0.1656	0.0427	1.1217	0
SGPP1	3.8766	0.1625	0.0419	1.1192	0
EPHA3	3.8726	0.1901	0.0491	1.1408	0
SNCAIP	3.8713	0.3558	0.0919	1.2797	0
C1QTNF1	3.8704	0.2223	0.0574	1.1666	0
GTF2H1	3.8698	0.1610	0.0416	1.1181	0
HAS2	3.8692	0.2113	0.0546	1.1578	0
DRAP1	3.8687	0.1856	0.0480	1.1373	0
GM2A	3.8644	0.2393	0.0619	1.1804	0
CDKN3	3.8628	0.2846	0.0737	1.2180	0
RIN2	3.8617	0.1981	0.0513	1.1472	0
FBLN5	3.8610	0.2600	0.0673	1.1975	0
IGFBP7	3.8547	0.2741	0.0711	1.2093	0
ICAM1	3.8538	0.1430	0.0371	1.1042	0
40062	3.8526	0.2224	0.0577	1.1667	0
STRA6	3.8489	0.1897	0.0493	1.1406	0
MFNG	3.8440	0.2505	0.0652	1.1896	0
OMD	3.8437	0.1728	0.0449	1.1272	0
STK17A	3.8407	0.1199	0.0312	1.0867	0
FKBP10	3.8402	0.1918	0.0500	1.1422	0
ACTR10	3.8382	0.1429	0.0372	1.1041	0
GAL3ST4	3.8350	0.1535	0.0400	1.1123	0
CD72	3.8345	0.2091	0.0545	1.1560	0
CD302	3.8335	0.1647	0.0430	1.1209	0
SLC11A1	3.8334	0.3513	0.0917	1.2757	0
CD1D	3.8326	0.1867	0.0487	1.1382	0
MATK	3.8320	0.1993	0.0520	1.1481	0
LMOD1	3.8319	0.2059	0.0537	1.1534	0
PDCD1LG2	3.8281	0.1177	0.0307	1.0850	0
SPARC	3.8278	0.3162	0.0826	1.2450	0
PLCL1	3.8277	0.1065	0.0278	1.0766	0
ASAP1	3.8272	0.1951	0.0510	1.1448	0
IFNGR1	3.8260	0.2243	0.0586	1.1682	0
PRKCQ	3.8202	0.2132	0.0558	1.1592	0
HLA-DMB	3.8196	0.3576	0.0936	1.2812	0
ATP10D	3.8188	0.1610	0.0422	1.1181	0
NAP1L1	3.8176	0.1565	0.0410	1.1146	0
MEOX1	3.8174	0.2070	0.0542	1.1543	0

CCL18	3.8163	0.2487	0.0652	1.1882	0
PKIG	3.8163	0.1113	0.0292	1.0802	0
COL13A1	3.8162	0.1720	0.0451	1.1266	0
HIPK3	3.8106	0.1246	0.0327	1.0902	0
RASL12	3.8055	0.2440	0.0641	1.1843	0
TAF4B	3.8040	0.1742	0.0458	1.1284	0
FOLR2	3.8016	0.2550	0.0671	1.1933	0
LIF	3.7967	0.2048	0.0539	1.1525	0
MEF2A	3.7939	0.1177	0.0310	1.0850	0
PILRA	3.7939	0.1800	0.0474	1.1329	0
CNIH	3.7938	0.2034	0.0536	1.1514	0
DNM1	3.7932	0.1796	0.0474	1.1326	0
KYNU	3.7926	0.3778	0.0996	1.2994	0
LYST	3.7896	0.1179	0.0311	1.0852	0
HEXB	3.7850	0.1624	0.0429	1.1191	0
KLK5	3.7844	0.3846	0.1016	1.3055	0
GSTO1	3.7819	0.1906	0.0504	1.1412	0
ARHGEF4	3.7814	0.1755	0.0464	1.1294	0
P2RY10	3.7803	0.1626	0.0430	1.1193	0
LAMP3	3.7776	0.3087	0.0817	1.2386	0
BACE1	3.7776	0.1197	0.0317	1.0865	0
GLI3	3.7758	0.1738	0.0460	1.1280	0
F8	3.7747	0.1499	0.0397	1.1095	0
CD59	3.7692	0.1730	0.0459	1.1274	0
CLEC10A	3.7682	0.1599	0.0424	1.1172	0
RELN	3.7672	0.1923	0.0511	1.1426	0
RARRES3	3.7657	0.5208	0.1383	1.4348	0
ITGBL1	3.7656	0.1835	0.0487	1.1356	0
IL24	3.7654	0.2733	0.0726	1.2086	0
MPP6	3.7635	0.2706	0.0719	1.2063	0
CYTH3	3.7631	0.1135	0.0302	1.0818	0
LAMA2	3.7609	0.1884	0.0501	1.1395	0
MMP13	3.7605	0.4406	0.1172	1.3572	0
CSDC2	3.7581	0.1515	0.0403	1.1107	0
HSD17B6	3.7575	0.2961	0.0788	1.2279	0
NOTCH1	3.7564	0.2464	0.0656	1.1862	0
HEPH	3.7560	0.2794	0.0744	1.2137	0
SLC25A46	3.7549	0.1875	0.0499	1.1388	0
SH3BP4	3.7527	0.2048	0.0546	1.1525	0
TRIP12	3.7507	0.1602	0.0427	1.1174	0
XAF1	3.7497	0.3430	0.0915	1.2684	0

PER2	3.7482	0.1977	0.0527	1.1469	0
SLC46A3	3.7463	0.2311	0.0617	1.1738	0
THRA	3.7463	0.2099	0.0560	1.1566	0
DYNC1LI1	3.7450	0.1221	0.0326	1.0883	0
STK38L	3.7428	0.1361	0.0364	1.0990	0
CPED1	3.7419	0.2515	0.0672	1.1904	0
RHCG	3.7413	0.2973	0.0795	1.2289	0
CDH13	3.7398	0.2630	0.0703	1.2000	0
ABCA12	3.7383	0.2219	0.0594	1.1663	0
SMTN	3.7352	0.1465	0.0392	1.1069	0
TRAF5	3.7346	0.1851	0.0496	1.1369	0
IQGAP1	3.7343	0.1699	0.0455	1.1250	0
CLTB	3.7288	0.1434	0.0384	1.1045	0
ITGAL	3.7264	0.2663	0.0715	1.2027	0
ACTC1	3.7263	0.3334	0.0895	1.2600	0
CD3D	3.7263	0.3763	0.1010	1.2980	0
CLEC2B	3.7221	0.2593	0.0697	1.1969	0
KIAA1199	3.7217	0.3952	0.1062	1.3151	0
PRDM8	3.7173	0.2587	0.0696	1.1964	0
CCL7	3.7162	0.1489	0.0401	1.1088	0
FHOD1	3.7134	0.2002	0.0539	1.1489	0
SOCS3	3.7102	0.2200	0.0593	1.1647	0
NTN1	3.7069	0.1518	0.0409	1.1109	0
RGS19	3.7063	0.1643	0.0443	1.1206	0
GRP	3.7053	0.2249	0.0607	1.1687	0
SDCBP	3.7043	0.2287	0.0617	1.1718	0
MRAS	3.7042	0.1356	0.0366	1.0986	0
FOSL1	3.7019	0.2922	0.0789	1.2245	0
IL18BP	3.7000	0.1706	0.0461	1.1255	0
IGF1	3.6997	0.2462	0.0666	1.1861	0
EDIL3	3.6957	0.1155	0.0313	1.0834	0
NSMF	3.6956	0.1984	0.0537	1.1474	0
CNTNAP1	3.6937	0.1987	0.0538	1.1477	0
CPA4	3.6889	0.3223	0.0874	1.2503	0
ACAP1	3.6888	0.2499	0.0677	1.1891	0
CPA3	3.6885	0.3797	0.1030	1.3011	0
SLC47A1	3.6867	0.2032	0.0551	1.1513	0
NR4A3	3.6850	0.1377	0.0374	1.1002	0
PTPN1	3.6795	0.1496	0.0407	1.1093	0
GNA12	3.6764	0.1461	0.0397	1.1066	0
KLK7	3.6720	0.4318	0.1176	1.3490	0

TRIM21	3.6694	0.1840	0.0501	1.1360	0
CD52	3.6688	0.4008	0.1092	1.3202	0
SDS	3.6684	0.1849	0.0504	1.1367	0
NACC2	3.6660	0.1904	0.0519	1.1411	0
HSPA1A	3.6660	0.4838	0.1320	1.3984	0
PRKCB	3.6641	0.1980	0.0540	1.1471	0
KLK10	3.6638	0.2618	0.0715	1.1990	0
TNFRSF12A	3.6613	0.3954	0.1080	1.3153	0
MMP1	3.6546	0.5486	0.1501	1.4627	0
MICAL2	3.6536	0.1489	0.0408	1.1087	0
P2RY6	3.6485	0.1440	0.0395	1.1050	0
HSPB2	3.6470	0.1463	0.0401	1.1067	0
TGM1	3.6470	0.3129	0.0858	1.2422	0
FXD5	3.6468	0.2633	0.0722	1.2002	0
STK10	3.6440	0.1558	0.0427	1.1140	0
ASB1	3.6439	0.1901	0.0522	1.1409	0
MTHFD2	3.6385	0.2332	0.0641	1.1754	0
WWC2	3.6380	0.1007	0.0277	1.0723	0
FBXL2	3.6354	0.1889	0.0520	1.1399	0
COL4A1	3.6351	0.2261	0.0622	1.1697	0
ARHGEF3	3.6308	0.1903	0.0524	1.1410	0
MCTS1	3.6282	0.1926	0.0531	1.1428	0
GCNT2	3.6273	0.1575	0.0434	1.1153	0
KIAA1033	3.6266	0.1646	0.0454	1.1209	0
SP140	3.6265	0.1618	0.0446	1.1187	0
TBC1D2	3.6256	0.2374	0.0655	1.1789	0
CKAP4	3.6239	0.2049	0.0565	1.1526	0
SP100	3.6233	0.1395	0.0385	1.1015	0
PLS3	3.6227	0.2091	0.0577	1.1560	0
IL11	3.6144	0.2194	0.0607	1.1642	0
POPDC3	3.6138	0.3099	0.0858	1.2396	0
SPRR1B	3.6125	0.4845	0.1341	1.3991	0
AZI2	3.6111	0.1372	0.0380	1.0998	0
BTG1	3.6104	0.2049	0.0568	1.1526	0
SLC35G2	3.6079	0.2243	0.0622	1.1682	0
ACOT7	3.6069	0.1975	0.0548	1.1467	0
GALNT6	3.6057	0.2250	0.0624	1.1688	0
CACNA2D3	3.6012	0.1521	0.0422	1.1112	0
LIMS2	3.5998	0.1521	0.0423	1.1112	0
CDH2	3.5992	0.4150	0.1153	1.3333	0
LILRA5	3.5983	0.1775	0.0493	1.1309	0

SNX24	3.5982	0.1444	0.0401	1.1053	0
IGFLR1	3.5967	0.2179	0.0606	1.1630	0
ELMO2	3.5967	0.0989	0.0275	1.0710	0
SSH1	3.5953	0.1494	0.0416	1.1091	0
RAB38	3.5902	0.4031	0.1123	1.3224	0
ANXA3	3.5872	0.4118	0.1148	1.3303	0
CXCL5	3.5872	0.4226	0.1178	1.3404	0
PPP4R4	3.5859	0.1572	0.0438	1.1151	0
NCS1	3.5841	0.1981	0.0553	1.1472	0
APP	3.5817	0.1947	0.0544	1.1445	0
ADORA3	3.5768	0.1747	0.0488	1.1287	0
MAPK9	3.5738	0.1430	0.0400	1.1042	0
MUC16	3.5710	0.4169	0.1168	1.3351	0
APOBEC3A	3.5672	0.3166	0.0887	1.2454	0
CXCL6	3.5640	0.4772	0.1339	1.3920	0
EMILIN2	3.5614	0.2539	0.0713	1.1924	0
ARHGEF10	3.5603	0.2371	0.0666	1.1786	0
NCF4	3.5602	0.1972	0.0554	1.1465	0
LAMP5	3.5593	0.1968	0.0553	1.1462	0
SMOX	3.5589	0.2066	0.0580	1.1540	0
CARD10	3.5575	0.2464	0.0693	1.1862	0
TPST2	3.5569	0.1966	0.0553	1.1460	0
DENND3	3.5543	0.1506	0.0424	1.1100	0
FCN1	3.5522	0.3602	0.1014	1.2836	0
SLAMF7	3.5502	0.1804	0.0508	1.1332	0
GATA6	3.5498	0.1347	0.0379	1.0979	0
EYA4	3.5494	0.1326	0.0374	1.0962	0
ST6GALNAC4	3.5490	0.1369	0.0386	1.0995	0
TNIP1	3.5480	0.1765	0.0497	1.1301	0
SLC22A4	3.5476	0.1886	0.0532	1.1396	0
PIGK	3.5458	0.1586	0.0447	1.1162	0
SEC24D	3.5454	0.1809	0.0510	1.1336	0
ST6GAL1	3.5420	0.1979	0.0559	1.1470	0
RUSC2	3.5400	0.1243	0.0351	1.0900	0
DENND5B	3.5372	0.1862	0.0526	1.1377	0
SOD3	3.5353	0.1825	0.0516	1.1349	0
MCAM	3.5346	0.1057	0.0299	1.0760	0
CASQ2	3.5339	0.2348	0.0664	1.1767	0
GPC4	3.5334	0.2805	0.0794	1.2146	0
BEST1	3.5333	0.1148	0.0325	1.0828	0
PITX1	3.5328	0.3162	0.0895	1.2450	0

TIAM2	3.5327	0.1470	0.0416	1.1072	0
SLC22A3	3.5324	0.1436	0.0407	1.1047	0
PPEF1	3.5307	0.1594	0.0451	1.1168	0
TPPP3	3.5263	0.1793	0.0508	1.1323	0
AP3S1	3.5256	0.1762	0.0500	1.1299	0
PSMB8	3.5245	0.2056	0.0583	1.1531	0
GPR132	3.5157	0.1054	0.0300	1.0758	0
LBH	3.5152	0.1255	0.0357	1.0909	0
ME2	3.5140	0.1613	0.0459	1.1183	0
OSBPL1A	3.5134	0.1980	0.0564	1.1471	0
DZIP1	3.5110	0.1676	0.0477	1.1232	0
HLA-E	3.5088	0.2156	0.0614	1.1612	0
ADAMTS3	3.5040	0.1260	0.0360	1.0913	0
OXCT1	3.5038	0.1832	0.0523	1.1354	0
OLFM1	3.5038	0.2712	0.0774	1.2068	0
NT5DC3	3.5034	0.1846	0.0527	1.1365	0
SLC17A9	3.5021	0.1574	0.0449	1.1152	0
IKZF1	3.5001	0.2185	0.0624	1.1635	0
SFRP1	3.5000	0.3686	0.1053	1.2911	0
PJA2	3.4990	0.1549	0.0443	1.1133	0
S100A7	3.4953	0.7545	0.2159	1.6871	0
CDH3	3.4915	0.4423	0.1267	1.3588	0
NAV3	3.4904	0.0967	0.0277	1.0693	0
LITAF	3.4895	0.2022	0.0580	1.1505	0
MFF	3.4868	0.1871	0.0536	1.1384	0
ARHGAP4	3.4843	0.2456	0.0705	1.1856	0
MAP1A	3.4841	0.1607	0.0461	1.1178	0
LHFPL2	3.4787	0.1771	0.0509	1.1306	0
DES	3.4765	0.2947	0.0848	1.2266	0
PPP2CB	3.4759	0.1282	0.0369	1.0930	0
MPHOSPH9	3.4740	0.1340	0.0386	1.0974	0
LARP6	3.4720	0.2316	0.0667	1.1741	0
OLFM4	3.4717	0.4854	0.1398	1.4000	0
RASGRP1	3.4694	0.2412	0.0695	1.1819	0
L1CAM	3.4684	0.1353	0.0390	1.0983	0
LRRK1	3.4664	0.1339	0.0386	1.0972	0
TCN2	3.4646	0.2145	0.0619	1.1603	0
RUNX2	3.4637	0.1278	0.0369	1.0926	0
SLC16A3	3.4626	0.2788	0.0805	1.2132	0
HLA-DPB1	3.4605	0.2737	0.0791	1.2089	0
CSNK1A1	3.4599	0.1108	0.0320	1.0798	0

SPON1	3.4560	0.3898	0.1128	1.3102	0
C11orf95	3.4545	0.1343	0.0389	1.0976	0
PARP8	3.4475	0.1889	0.0548	1.1399	0
F13A1	3.4460	0.3267	0.0948	1.2541	0
KRT14	3.4452	0.6404	0.1859	1.5588	0
ACVRL1	3.4408	0.1497	0.0435	1.1094	0
NES	3.4397	0.1957	0.0569	1.1453	0
HAT1	3.4390	0.1735	0.0505	1.1278	0
LTB	3.4384	0.2906	0.0845	1.2231	0
SATB2	3.4355	0.2000	0.0582	1.1487	0
AOX1	3.4321	0.2173	0.0633	1.1625	0
CRIP1	3.4303	0.3230	0.0942	1.2510	0
C9orf3	3.4294	0.1776	0.0518	1.1310	0
ARHGAP15	3.4288	0.2822	0.0823	1.2160	0
SCG2	3.4274	0.2639	0.0770	1.2007	0
RNH1	3.4252	0.1335	0.0390	1.0969	0
CXorf21	3.4245	0.0888	0.0259	1.0635	0
STEAP4	3.4232	0.1699	0.0496	1.1250	0
LDHA	3.4206	0.1965	0.0575	1.1459	0
POU2F2	3.4133	0.0985	0.0289	1.0707	0
FBXO5	3.4126	0.1823	0.0534	1.1347	0
SORBS1	3.4120	0.1646	0.0483	1.1209	0
PFKP	3.4119	0.2524	0.0740	1.1912	0
FOXD1	3.4111	0.3613	0.1059	1.2846	0
PPP2R3C	3.4101	0.1313	0.0385	1.0952	0
PGK1	3.4068	0.1973	0.0579	1.1466	0
CYB5R3	3.4032	0.1469	0.0432	1.1072	0
KLF12	3.4014	0.1231	0.0362	1.0891	0
PVRIG	3.3991	0.2403	0.0707	1.1813	0
EXOC5	3.3980	0.1169	0.0344	1.0844	0
PER1	3.3977	0.0989	0.0291	1.0709	0
PSME2	3.3947	0.1979	0.0583	1.1471	0
TOX	3.3925	0.1411	0.0416	1.1028	0
SLC6A9	3.3919	0.1724	0.0508	1.1269	0
YIPF5	3.3896	0.1988	0.0587	1.1477	0
DAAM2	3.3873	0.1420	0.0419	1.1034	0
ANPEP	3.3868	0.2844	0.0840	1.2179	0
MAP2	3.3867	0.1969	0.0582	1.1463	0
TRDMT1	3.3859	0.1041	0.0307	1.0748	0
ETS1	3.3841	0.1861	0.0550	1.1377	0
ACAT1	3.3824	0.1900	0.0562	1.1408	0

AK1	3.3823	0.1847	0.0546	1.1366	0
SCEL	3.3801	0.2624	0.0776	1.1995	0
SCML1	3.3793	0.1904	0.0564	1.1411	0
CLDND1	3.3759	0.1616	0.0479	1.1185	0
CASP5	3.3737	0.1071	0.0318	1.0771	0
IL1B	3.3717	0.4536	0.1345	1.3695	0
CCL11	3.3708	0.2706	0.0803	1.2063	0
VAMP1	3.3703	0.2043	0.0606	1.1521	0
EGR1	3.3701	0.3331	0.0989	1.2598	0
CD70	3.3693	0.2565	0.0761	1.1945	0
CMKLR1	3.3665	0.1045	0.0310	1.0751	0
LAMC1	3.3653	0.1713	0.0509	1.1260	0
TRIM36	3.3647	0.0987	0.0293	1.0708	0
MAGEH1	3.3535	0.1290	0.0385	1.0936	0
PDZK1IP1	3.3527	0.3737	0.1115	1.2957	0
C11orf73	3.3497	0.1551	0.0463	1.1135	0
MICB	3.3469	0.2566	0.0767	1.1947	0
SSR1	3.3457	0.1348	0.0403	1.0979	0
IRX5	3.3455	0.2984	0.0892	1.2298	0
DUSP7	3.3449	0.1041	0.0311	1.0748	0
KIF18A	3.3437	0.2061	0.0616	1.1536	0
P2RX7	3.3426	0.1240	0.0371	1.0898	0
PNMA2	3.3399	0.2211	0.0662	1.1656	0
FAM134B	3.3388	0.1712	0.0513	1.1260	0
TOM1	3.3386	0.1304	0.0391	1.0946	0
NACAD	3.3384	0.2131	0.0638	1.1592	0
SNX6	3.3359	0.0967	0.0290	1.0693	0
CLEC2D	3.3347	0.1323	0.0397	1.0960	0
ZFP36L1	3.3342	0.1807	0.0542	1.1334	0
ASB9	3.3310	0.1794	0.0539	1.1324	0
ATOX1	3.3308	0.1593	0.0478	1.1167	0
PLD1	3.3272	0.1851	0.0556	1.1369	0
ATF2	3.3259	0.1145	0.0344	1.0826	0
EYA1	3.3248	0.1691	0.0509	1.1244	0
LILRB5	3.3222	0.1744	0.0525	1.1285	0
PIM2	3.3218	0.2950	0.0888	1.2269	0
BCHE	3.3192	0.2519	0.0759	1.1908	0
CDCA4	3.3192	0.1418	0.0427	1.1033	0
RHOH	3.3189	0.1360	0.0410	1.0988	0
STARD8	3.3187	0.1287	0.0388	1.0933	0
CD247	3.3180	0.2971	0.0895	1.2286	0

YWHAH	3.3136	0.1414	0.0427	1.1030	0
USP25	3.3105	0.1063	0.0321	1.0765	0
HERC6	3.3104	0.2775	0.0838	1.2121	0
PID1	3.3102	0.1878	0.0567	1.1390	0
CCNA1	3.3079	0.2219	0.0671	1.1663	0
AKAP13	3.3072	0.1349	0.0408	1.0980	0
CYSLTR1	3.3070	0.1867	0.0564	1.1381	0
PNMAL1	3.3052	0.2230	0.0675	1.1672	0
KCNE4	3.3034	0.0932	0.0282	1.0668	0
KIR2DL3	3.3004	0.2093	0.0634	1.1561	0
PARVA	3.2998	0.1511	0.0458	1.1104	0
PITPNB	3.2975	0.1185	0.0359	1.0856	0
SEMA6B	3.2972	0.1149	0.0348	1.0829	0
KIAA0040	3.2936	0.1225	0.0372	1.0886	0
LPHN2	3.2918	0.2284	0.0694	1.1716	0
AGPS	3.2909	0.1726	0.0525	1.1271	0
COLGALT1	3.2840	0.1809	0.0551	1.1336	0
HSPB11	3.2829	0.2029	0.0618	1.1510	0
LSP1	3.2794	0.1173	0.0358	1.0847	0
WDR44	3.2770	0.1077	0.0329	1.0775	0
CHI3L2	3.2749	0.2523	0.0770	1.1911	0
BST2	3.2728	0.3643	0.1113	1.2873	0
LILRA3	3.2715	0.1671	0.0511	1.1228	0
LCK	3.2705	0.1802	0.0551	1.1331	0
STAMBPL1	3.2704	0.1796	0.0549	1.1326	0
NFKB2	3.2698	0.1231	0.0376	1.0890	0
FJX1	3.2671	0.2487	0.0761	1.1881	0
CH25H	3.2661	0.2858	0.0875	1.2191	0
XRCC4	3.2593	0.1052	0.0323	1.0756	0
GNG11	3.2592	0.2635	0.0809	1.2004	0
TFE3	3.2512	0.1069	0.0329	1.0769	0
PLEKHG3	3.2497	0.2115	0.0651	1.1579	0
SH3TC1	3.2496	0.2031	0.0625	1.1512	0
P2RY14	3.2483	0.1436	0.0442	1.1047	0
TMSB10	3.2469	0.1158	0.0357	1.0835	0
IQCG	3.2462	0.1725	0.0531	1.1270	0
MAP3K7	3.2441	0.1026	0.0316	1.0737	0
RABEPK	3.2433	0.1215	0.0375	1.0878	0
FAM171A1	3.2418	0.2649	0.0817	1.2016	0
CD3G	3.2417	0.2009	0.0620	1.1494	0
SERPINE1	3.2398	0.3505	0.1082	1.2750	0

APOL3	3.2370	0.2448	0.0756	1.1850	0
NUMB	3.2352	0.1213	0.0375	1.0877	0
RARRES2	3.2337	0.3521	0.1089	1.2765	0
TRIM3	3.2334	0.0966	0.0299	1.0693	0
TNNT1	3.2330	0.1846	0.0571	1.1365	0
MME	3.2325	0.3499	0.1083	1.2745	0
CSF3	3.2300	0.1290	0.0399	1.0935	0
IGFBP5	3.2297	0.4261	0.1319	1.3436	0
AEN	3.2270	0.1502	0.0466	1.1097	0
PPIC	3.2268	0.2113	0.0655	1.1577	0
VNN2	3.2243	0.2019	0.0626	1.1502	0
NCL	3.2197	0.1166	0.0362	1.0842	0
GNB5	3.2181	0.1273	0.0395	1.0922	0
ATP1B3	3.2180	0.1619	0.0503	1.1188	0
FAT4	3.2165	0.1297	0.0403	1.0941	0
GABBR1	3.2118	0.1954	0.0609	1.1451	0
MGLL	3.2113	0.1834	0.0571	1.1355	0
CDK17	3.2098	0.0861	0.0268	1.0615	0
PTTG1	3.2090	0.2233	0.0696	1.1674	0
BICD1	3.2080	0.0996	0.0311	1.0715	0
HCLS1	3.2075	0.3409	0.1063	1.2665	0
SCD5	3.1997	0.1209	0.0378	1.0874	0
ADORA1	3.1981	0.1372	0.0429	1.0998	0
CSF3R	3.1980	0.2265	0.0708	1.1700	0
AKT3	3.1970	0.1217	0.0381	1.0880	0
ADORA2B	3.1952	0.3037	0.0951	1.2343	0
SLC7A6	3.1948	0.1313	0.0411	1.0953	0
HSPA4L	3.1948	0.2392	0.0749	1.1803	0
PCMT1	3.1943	0.1198	0.0375	1.0866	0
FMO2	3.1932	0.1505	0.0471	1.1099	0
DHRS9	3.1860	0.3408	0.1070	1.2665	0
DNAJC24	3.1854	0.1217	0.0382	1.0880	0
FGF7	3.1830	0.1048	0.0329	1.0754	0

APPENDIX B: PAM GENE LIST

List of Significant Genes				
Offset Quantile	50		Offset Value	0.283592351
	both		RNG Seed	420473
Prior Distribution (Sample Prior)				
		Class	1	2
		Prob.	0.541984733	0.458015267
	id	name	1 score	2 score
	UPK2	UPK2	-0.1166	0.138
	SCNN1B	SCNN1B	-0.0955	0.113
	PPARG	PPARG	-0.0815	0.0965
	TOX3	TOX3	-0.0652	0.0771
	GATA3	GATA3	-0.0629	0.0745
	HMGCS2	HMGCS2	-0.0611	0.0723
	RAB15	RAB15	-0.0583	0.069
	AHNAK2	AHNAK2	0.0569	-0.0674
	ADIRF	ADIRF	-0.0558	0.066
	SEMA5A	SEMA5A	-0.0491	0.0581
	CHST15	CHST15	0.0476	-0.0563
	TRAK1	TRAK1	-0.0453	0.0536
	SCNN1G	SCNN1G	-0.0433	0.0512
	MT1X	MT1X	0.0411	-0.0486

	TMPRSS2	TMPRSS2	-0.041	0.0485
	VGLL1	VGLL1	-0.036	0.0426
	TBX2	TBX2	-0.0326	0.0386
	UPK1A	UPK1A	-0.03	0.0355
	GAREM	GAREM	-0.0296	0.035
	BHMT	BHMT	-0.0234	0.0277
	SPINK1	SPINK1	-0.0209	0.0248
	GPD1L	GPD1L	-0.0196	0.0232
	RNF128	RNF128	-0.0196	0.0232
	CYP2J2	CYP2J2	-0.0194	0.023
	EMP3	EMP3	0.0194	-0.0229
	GDPD3	GDPD3	-0.0188	0.0222
	FBP1	FBP1	-0.0184	0.0218
	MSN	MSN	0.0174	-0.0206
	MT2A	MT2A	0.0153	-0.0181
	CDK6	CDK6	0.0149	-0.0176
	ALOX5AP	ALOX5AP	0.0125	-0.0148
	PRRX1	PRRX1	0.0107	-0.0127
	SLC27A2	SLC27A2	-0.0097	0.0115
	TMEM97	TMEM97	-0.0077	0.0091
	CD14	CD14	0.007	-0.0082
	PLEKHG6	PLEKHG6	-0.006	0.0071
	CYP4B1	CYP4B1	-0.005	0.0059

	GLIPR1	GLIPR1	0.0047	-0.0055
	PDGFC	PDGFC	0.0046	-0.0055
	PRKCDBP	PRKCDBP	0.0045	-0.0053
	FAP	FAP	0.0035	-0.0042
	CAPN5	CAPN5	-0.0035	0.0041
	PALLD	PALLD	0.0025	-0.003
	TUBB6	TUBB6	0.0024	-0.0028
	SLC9A2	SLC9A2	-0.0022	0.0026
	PPFIBP2	PPFIBP2	-0.0013	0.0015
	FAM174B	FAM174B	-0.001	0.0012

APPENDIX C: GENE SET ENRICHMENT ANALYSIS

	Enriched in Basal (nom pvalue<1%)				
Rank	MSigDB	SIZE	ES	NES	NOM p-val
1	CHARAFE_BREAST_CANCER_LUMINAL_V S_MESENCHYMAL_DN	364	0.69	2.25	0
2	HOSHIDA_LIVER_CANCER_SUBCLASS_S 1	224	0.64	2.18	0
3	AZARE_NEOPLASTIC_TRANSFORMATION _BY_STAT3_DN	114	0.64	2.16	0
4	PANGAS_TUMOR_SUPPRESSION_BY_SM AD1_AND_SMAD5_UP	88	0.64	2.11	0
5	VECCHI_GASTRIC_CANCER_ADVANCED_ VS_EARLY_UP	128	0.74	2.11	0
6	CUI_TCF21_TARGETS_UP	33	0.71	2.1	0
7	SCHUETZ_BREAST_CANCER_DUCTAL_IN VASIVE_UP	327	0.78	2.1	0
8	CHARAFE_BREAST_CANCER_LUMINAL_V S_BASAL_DN	374	0.64	2.09	0
9	LIM_MAMMARY_STEM_CELL_UP	356	0.65	2.09	0.002
10	TURASHVILI_BREAST_LOBULAR_CARCIN OMA_VS_DUCTAL_NORMAL_UP	54	0.8	2.06	0
11	LAIHO_COLORECTAL_CANCER_SERRAT ED_UP	103	0.6	2.06	0
12	IGLESIAS_E2F_TARGETS_UP	140	0.59	2.06	0
13	POOLA_INVASIVE_BREAST_CANCER_UP	258	0.69	2.06	0
14	WAMUNYOKOLI_OVARIAN_CANCER_LMP	153	0.58	2.04	0

	_DN				
15	RODWELL_AGING_KIDNEY_UP	352	0.62	2.04	0.002
16	SERVITJA_ISLET_HNF1A_TARGETS_UP	136	0.62	2.04	0
17	TURASHVILI_BREAST_LOBULAR_CARCIN OMA_VS_LOBULAR_NORMAL_DN	57	0.74	2.03	0
18	HINATA_NFKB_TARGETS_FIBROBLAST_U P	79	0.59	2.03	0
19	KHETCHOUMIAN_TRIM24_TARGETS_UP	43	0.7	2.03	0.002
20	PLASARI_TGFB1_TARGETS_10HR_UP	158	0.59	2.03	0
21	LINDGREN_BLADDER_CANCER_CLUSTER R_2B	318	0.72	2.02	0
22	CHIARADONNA_NEOPLASTIC_TRANSFO RMATION_CDC25_UP	98	0.57	2.01	0
23	ROZANOV_MMP14_TARGETS_UP	199	0.56	2.01	0
24	LINDSTEDT_DENDRITIC_CELL_MATURATI ON_A	59	0.73	2.01	0
25	BOQUEST_STEM_CELL_UP	244	0.64	2.01	0
26	PETROVA_ENDOTHELIUM_LYMPHATIC_V S_BLOOD_DN	151	0.61	2.01	0
27	SMID_BREAST_CANCER_LUMINAL_B_DN	500	0.58	2.01	0
28	THUM_SYSTOLIC_HEART_FAILURE_UP	328	0.53	2	0
29	LINDVALL_IMMORTALIZED_BY_TERT_DN	62	0.67	2	0.002
30	VERHAAK_GLIOMASTOMA_NEURAL	195	0.59	2	0.002
31	LINDGREN_BLADDER_CANCER_CLUSTER R_2A_DN	115	0.65	2	0
32	RODWELL_AGING_KIDNEY_NO_BLOOD_ UP	161	0.6	2	0

33	SENESE_HDAC1_AND_HDAC2_TARGETS _UP	181	0.54	1.99	0
34	KIM_GLIS2_TARGETS_UP	77	0.72	1.99	0.002
35	BURTON_ADIPOGENESIS_7	47	0.62	1.98	0
36	OKAMOTO_LIVER_CANCER_MULTICENT RIC_OCCURRENCE_UP	23	0.69	1.98	0
37	AZARE_STAT3_TARGETS	23	0.72	1.98	0
38	LIEN_BREAST_CARCINOMA_METAPLASTI C_VS_DUCTAL_UP	66	0.67	1.98	0.002
39	CROMER_TUMORIGENESIS_UP	58	0.77	1.98	0
40	CHICAS_RB1_TARGETS_CONFLUENT	436	0.52	1.98	0
41	MARKEY_RB1_ACUTE_LOF_UP	174	0.61	1.98	0.002
42	MCMURRAY_TP53_HRAS_COOPERATION _RESPONSE_UP	23	0.7	1.98	0
43	MCLACHLAN_DENTAL_CARIES_DN	219	0.68	1.97	0.002
44	MCLACHLAN_DENTAL_CARIES_UP	228	0.72	1.97	0.002
45	PID_INTEGRIN1_PATHWAY	62	0.72	1.97	0
46	BRUECKNER_TARGETS_OF_MIRLET7A3_ DN	61	0.66	1.97	0
47	SASSON_RESPONSE_TO_FORSKOLIN_D N	86	0.55	1.97	0.002
48	JISON_SICKLE_CELL_DISEASE_UP	169	0.54	1.97	0
49	TAKEDA_TARGETS_OF_NUP98_HOXA9_F USION_8D_DN	149	0.63	1.96	0
50	DASU_IL6_SIGNALING_UP	57	0.62	1.96	0.002
51	LINDGREN_BLADDER_CANCER_HIGH_RE CURRENCE	44	0.74	1.96	0

52	ICHIBA_GRAFT_VERSUS_HOST_DISEASE _D7_UP	86	0.74	1.96	0.004
53	POTTI_TOPOTECAN_SENSITIVITY	120	0.56	1.96	0
54	MIYAGAWA_TARGETS_OF_EWSR1_ETS_ FUSIONS_DN	159	0.59	1.95	0
55	JECHLINGER_EPITHELIAL_TO_MESENC YMAL_TRANSITION_UP	65	0.7	1.95	0.004
56	LIM_MAMMARY_LUMINAL_MATURE_DN	82	0.63	1.95	0.006
57	RAMALHO_STEMNESS_DN	57	0.66	1.95	0
58	ZWANG_CLASS_2_TRANSIENTLY_INDUC ED_BY_EGF	35	0.63	1.95	0.004
59	NIELSEN_MALIGNAT_FIBROUS_HISTIOCY TOMA_UP	18	0.83	1.95	0.002
60	KONDO_EZH2_TARGETS	172	0.48	1.95	0
61	PID_UPA_UPAR_PATHWAY	38	0.66	1.94	0.002
62	REN_ALVEOLAR_RHABDOMYOSARCOMA _DN	391	0.56	1.94	0.008
63	YAMASHITA_METHYLATED_IN_PROSTAT E_CANCER	41	0.65	1.94	0
64	LABBE_TARGETS_OF_TGFB1_AND_WNT3 A_UP	89	0.54	1.94	0
65	HAN_JNK_SINGALING_UP	28	0.69	1.94	0.002
66	CHARAFE_BREAST_CANCER_BASAL_VS _MESENCHYMAL_DN	38	0.72	1.93	0
67	NADLER_OBESITY_UP	58	0.66	1.93	0.004
68	WANG_SMARCE1_TARGETS_UP	193	0.56	1.93	0.004
69	GRAESSMANN_RESPONSE_TO_MC_AND	156	0.54	1.93	0

	_SERUM_DEPRIVATION_UP				
70	DOANE_BREAST_CANCER_CLASSES_DN	29	0.72	1.93	0
71	KEEN_RESPONSE_TO_ROSIGLITAZONE_DN	92	0.6	1.93	0.002
72	APRELIKOVA_BRCA1_TARGETS	46	0.55	1.93	0.002
73	LIAN_LIPA_TARGETS_6M	55	0.69	1.93	0.002
74	ZHAN_LATE_DIFFERENTIATION_GENES_UP	32	0.59	1.92	0
75	PID_CXCR4_PATHWAY	92	0.55	1.92	0
76	KEGG_FOCAL_ADHESION	172	0.54	1.92	0.004
77	HUANG_DASATINIB_RESISTANCE_UP	70	0.71	1.92	0.002
78	SASSON_RESPONSE_TO_GONADOTROP_HINS_DN	84	0.53	1.92	0.002
79	HOFFMANN_PRE_BI_TO_LARGE_PRE_BII_LYMPHOCYTE_DN	59	0.57	1.92	0
80	PASINI_SUZ12_TARGETS_DN	255	0.54	1.92	0.004
81	CHEN_ETV5_TARGETS_SERTOLI	19	0.82	1.92	0
82	REACTOME_CELL_SURFACE_INTERACTIONS_AT_THE_VASCULAR_WALL	76	0.57	1.92	0.006
83	LENAOUR_DENDRITIC_CELL_MATURATION_DN	121	0.59	1.92	0.004
84	GROSS_ELK3_TARGETS_DN	28	0.66	1.92	0
85	VART_KSHV_INFECTION_ANGIOGENIC_MARCKERS_UP	138	0.57	1.91	0.002
86	HUANG_GATA2_TARGETS_UP	125	0.54	1.91	0.004
87	FONTAINE_FOLLICULAR_THYROID_ADENOMA_DN	60	0.51	1.91	0

88	ICHIBA_GRAFT_VERSUS_HOST_DISEASE _35D_UP	104	0.64	1.91	0.006
89	NIELSEN_GIST_AND_SYNOVIAL_SARCO MA_DN	20	0.85	1.91	0
90	WIEDERSCHAIN_TARGETS_OF_BMI1_AN D_PCGF2	49	0.65	1.9	0.006
91	SWEET_KRAS_TARGETS_UP	79	0.63	1.9	0.002
92	WAMUNYOKOLI_OVARIAN_CANCER_GRA DES_1_2_DN	54	0.59	1.9	0.004
93	GAL_LEUKEMIC_STEM_CELL_DN	220	0.5	1.9	0.002
94	SARTIPY_BLUNTED_BY_INSULIN_RESIST ANCE_UP	17	0.77	1.9	0
95	ONO_AML1_TARGETS_DN	29	0.68	1.9	0.002
96	NAKAYAMA_SOFT_TISSUE_TUMORS_PC A1_UP	68	0.76	1.9	0.006
97	PETROVA_PROX1_TARGETS_DN	60	0.68	1.9	0.002
98	BOQUEST_STEM_CELL_CULTURED_VS_ FRESH_UP	400	0.5	1.9	0
99	MAHADEVAN_GIST_MORPHOLOGICAL_S WITCH	15	0.8	1.9	0
100	EBAUER_MYOGENIC_TARGETS_OF_PAX 3_FOXO1_FUSION	41	0.62	1.9	0.006
101	KEGG_CYTOKINE_CYTOKINE_RECEPTO R_INTERACTION	185	0.57	1.9	0
102	GOTZMANN_EPITHELIAL_TO_MESENCHY MAL_TRANSITION_UP	62	0.58	1.89	0.002
103	GALINDO_IMMUNE_RESPONSE_TO_ENT	73	0.65	1.89	0.004

	EROTOXIN				
104	RIGGI_EWING_SARCOMA_PROGENITOR_DN	133	0.54	1.89	0.002
105	WOO_LIVER_CANCER_RECURRENCE_UP	97	0.56	1.89	0.004
106	LIU_PROSTATE_CANCER_DN	371	0.53	1.89	0.002
107	GERHOLD_ADIPOGENESIS_DN	60	0.57	1.89	0.002
108	PID_INTEGRIN3_PATHWAY	40	0.68	1.89	0.006
109	PICCALUGA_ANGIOIMMUNOBLASTIC_LYMPHOMA_UP	176	0.66	1.89	0.012
110	GRUETZMANN_PANCREATIC_CANCER_UP	338	0.47	1.89	0.002
111	FOSTER_TOLERANT_MACROPHAGE_DN	303	0.5	1.89	0.002
112	CHIARADONNA_NEOPLASTIC_TRANSFORMATION_KRAS_CDC25_DN	41	0.65	1.89	0.002
113	MIKKELSEN_MEF_LCP_WITH_H3K4ME3	85	0.56	1.89	0
114	ROY_WOUND_BLOOD_VESSEL_UP	46	0.71	1.89	0.008
115	GHANDHI_BYSTANDER_IRRADIATION_UP	70	0.64	1.89	0.01
116	KEGG_COMPLEMENT_AND_COAGULATION_CASCADES	52	0.63	1.88	0.002
117	DANG_REGULATED_BY_MYC_DN	227	0.49	1.88	0
118	KAN_RESPONSE_TO_ARSENIC_TRIOXIDE	116	0.55	1.88	0.002
119	REACTOME_INTEGRIN_CELL_SURFACE_INTERACTIONS	74	0.58	1.88	0.002
120	MATSUDA_NATURAL_KILLER_DIFFERENTIATION	374	0.4	1.88	0
121	PID_AMB2_NEUTROPHILS_PATHWAY	38	0.65	1.88	0.004

122	RASHI_RESPONSE_TO_IONIZING_RADIA TION_6	64	0.57	1.87	0.004
123	NIELSEN_LEIOMYOSARCOMA_CNN1_UP	18	0.8	1.87	0.004
124	HINATA_NFKB_TARGETS_KERATINOCYT E_UP	90	0.6	1.87	0.004
125	COWLING_MYCN_TARGETS	31	0.7	1.87	0.004
126	CERVERA_SDHB_TARGETS_2	91	0.5	1.87	0.002
127	IWANAGA_CARCIANOGENESIS_BY_KRAS_ PTEN_DN	235	0.43	1.87	0
128	REACTOME_EXTRACELLULAR_MATRIX_ ORGANIZATION	68	0.66	1.87	0.01
129	RUTELLA_RESPONSE_TO_HGF_VS_CSF2 RB_AND_IL4_UP	381	0.49	1.87	0.006
130	WIELAND_UP_BY_HBV_INFECTION	96	0.73	1.87	0.01
131	ROZANOV_MMP14_TARGETS_SUBSET	30	0.77	1.87	0.004
132	BROCKE_APOPTOSIS_REVERSED_BY_IL 6	139	0.54	1.87	0.006
133	WALLACE_PROSTATE_CANCER_RACE_U P	263	0.7	1.87	0.004
134	RUTELLA_RESPONSE_TO_CSF2RB_AND_ IL4_DN	297	0.51	1.86	0.012
135	KEGG_HEMATOPOIETIC_CELL_LINEAGE	68	0.68	1.86	0
136	LIAN_LIPA_TARGETS_3M	45	0.7	1.86	0.008
137	QI_PLASMACYTOMA_UP	226	0.56	1.86	0.006
138	SAMOLS_TARGETS_OF_KHSV_MIRNAS_ DN	52	0.52	1.86	0.002
139	HADDAD_T_LYMPHOCYTE_AND_NK_PRO	57	0.63	1.86	0.004

	GENITOR_DN				
140	ANASTASSIOU_CANCER_MESENCHYMAL _TRANSITION_SIGNATURE	61	0.86	1.86	0.01
141	SEITZ_NEOPLASTIC_TRANSFORMATION_ BY_8P_DELETION_UP	71	0.61	1.86	0.006
142	SMID_BREAST_CANCER_RELAPSE_IN_B ONE_DN	269	0.48	1.86	0.006
143	IZADPANAH_STEM_CELL_ADIPOSE_VS_B ONE_UP	103	0.53	1.86	0.006
144	BEGUM_TARGETS_OF_PAX3_FOXO1_FU SION_DN	45	0.63	1.86	0.004
145	FULCHER_INFLAMMATORY_RESPONSE_ LECTIN_VS_LPS_DN	354	0.51	1.86	0.008
146	FRIDMAN_SENESCENCE_UP	75	0.55	1.86	0
147	HUANG_FOXA2_TARGETS_DN	35	0.67	1.86	0.002
148	DUNNE_TARGETS_OF_AML1_MTG8_FUSI ON_DN	19	0.7	1.86	0.002
149	LIU_VAV3_PROSTATE_CARCINOGENESIS _UP	80	0.59	1.86	0.012
150	NAKAMURA_METASTASIS	32	0.57	1.86	0.002
151	BOYALT_LIVER_CANCER_SUBCLASS_G 5_DN	26	0.73	1.85	0.006
152	FLECHNER_BIOPSY_KIDNEY_TRANSPLA NT_REJECTED_VS_OK_UP	82	0.74	1.85	0.006
153	ALONSO_METASTASIS_EMT_UP	34	0.63	1.85	0.002
154	PID_IL23PATHWAY	32	0.7	1.85	0.004
155	JEON_SMAD6_TARGETS_UP	21	0.74	1.85	0.004

156	KANG_GIST_WITH_PDGFRA_UP	46	0.64	1.85	0.008
157	PID_IL6_7PATHWAY	46	0.56	1.85	0.004
158	GAZDA_DIAMOND_BLACKFAN_ANEMIA_P ROGENITOR_UP	39	0.57	1.85	0.004
159	DER_IFN_GAMMA_RESPONSE_UP	68	0.6	1.85	0.006
160	KEGG_ECM_RECEPTOR_INTERACTION	71	0.61	1.84	0.008
161	REACTOME_SMOOTH_MUSCLE_CONTRA CTION	23	0.75	1.84	0.004
162	REACTOME_G_ALPHA_I_SIGNALLING_EV ENTS	120	0.52	1.84	0.004
163	HOSHIDA_LIVER_CANCER_SURVIVAL_UP	69	0.51	1.84	0
164	FONTAINE_THYROID_TUMOR_UNCERTAI N_MALIGNANCY_DN	22	0.64	1.84	0.002
165	LI_INDUCED_T_TO_NATURAL_KILLER_UP	236	0.5	1.84	0.006
166	BOYLAN_MULTIPLE_MYELOMA_D_UP	59	0.5	1.84	0
167	GARGALOVIC_RESPONSE_TO_OXIDIZED _PHOSPHOLIPIDS_GREEN_UP	17	0.65	1.84	0.004
168	HAN_JNK_SINGALING_DN	34	0.62	1.84	0.006
169	DORSEY_GAB2_TARGETS	29	0.67	1.83	0.004
170	SMIRNOV_CIRCULATING_ENDOTHELIOC YTES_IN_CANCER_UP	153	0.54	1.83	0.004
171	RAGHAVACHARI_PLATELET_SPECIFIC_G ENES	65	0.53	1.83	0.002
172	LIN_TUMOR_ESCAPE_FROM_IMMUNE_A TTACK	15	0.66	1.83	0.002
173	REACTOME_COLLAGEN_FORMATION	46	0.69	1.83	0.02
174	PID_ILK_PATHWAY	39	0.56	1.83	0.004

175	BOYLAN_MULTIPLE_MYELOMA_C_D_DN	195	0.52	1.83	0.004
176	GAVIN_FOXP3_TARGETS_CLUSTER_P7	60	0.57	1.83	0
177	WILCOX_PRESPONSE_TO_ROGESTERO NE_DN	56	0.58	1.83	0.008
178	DEMAGALHAES_AGING_UP	45	0.61	1.83	0.01
179	BOSCO_TH1_CYTOTOXIC_MODULE	77	0.68	1.83	0.012
180	GAVIN_FOXP3_TARGETS_CLUSTER_T4	73	0.5	1.83	0.002
181	ALTEMEIER_RESPONSE_TO_LPS_WITH_ MECHANICAL_VENTILATION	100	0.66	1.83	0.006
182	VART_KSHV_INFECTION_ANGIOGENIC_M ARKERS_DN	112	0.49	1.83	0.002
183	SENESE_HDAC2_TARGETS_UP	91	0.53	1.83	0.006
184	HELLEBREKERS_SILENCED_DURING_TU MOR_ANGIOGENESIS	75	0.57	1.83	0.006
185	HERNANDEZ_MITOTIC_ARREST_BY_DOC ETAXEL_1_DN	34	0.59	1.83	0.004
186	PID_SYNDECAN_1_PATHWAY	42	0.64	1.82	0.022
187	LEE_LIVER_CANCER_DENA_UP	58	0.52	1.82	0.002
188	GU_PDEF_TARGETS_UP	68	0.62	1.82	0.008
189	BURTON_ADIPOGENESIS_9	77	0.5	1.82	0.004
190	CROONQUIST_STROMAL_STIMULATION_ UP	53	0.67	1.82	0.012
191	GHANDHI_DIRECT_IRRADIATION_UP	83	0.6	1.82	0.008
192	PETRETTO_CARDIAC_HYPERTROPHY	32	0.65	1.82	0.004
193	REACTOME_RESPONSE_TO_ELEVATED_ PLATELET_CYTOSOLIC_CA2_	69	0.55	1.82	0
194	DER_IFN_BETA_RESPONSE_UP	98	0.55	1.82	0.006

195	VERRECCHIA_RESPONSE_TO_TGFB1_C2	24	0.7	1.82	0.008
196	SMID_BREAST_CANCER_NORMAL_LIKE_UP	428	0.63	1.82	0.022
197	DER_IFN_ALPHA_RESPONSE_UP	72	0.61	1.82	0.014
198	NOUSHMEHR_GBM_SILENCED_BY_METHYLATION	32	0.58	1.82	0.002
199	TURASHVILI_BREAST_DUCTAL_CARCINOMA_VS_DUCTAL_NORMAL_UP	36	0.64	1.81	0.023
200	GRAHAM_CML QUIESCENT_VS_CML_DIVIDING_UP	23	0.69	1.81	0.012
201	NGUYEN_NOTCH1_TARGETS_UP	29	0.54	1.81	0.004
202	BERENJENO_TRANSFORMED_BY_RHOA_REVERSIBLY_DN	21	0.7	1.81	0.006
203	BHATI_G2M_ARREST_BY_2METHOXYESTRADIOL_UP	90	0.53	1.81	0.002
204	REACTOME_GPVI_MEDIATED_ACTIVATION_CASCADE	29	0.58	1.81	0.006
205	GROSS_HYPOXIA_VIA_ELK3_DN	134	0.53	1.81	0.012
206	TONKS_TARGETS_OF_RUNX1_RUNX1T1_FUSION_ERYTHROCYTE_UP	145	0.51	1.81	0.006
207	BILBAN_B_CLL_LPL_DN	37	0.59	1.81	0.008
208	ZHENG_IL22_SIGNALING_UP	36	0.61	1.81	0.008
209	KYNG_DNA_DAMAGE_DN	181	0.42	1.81	0
210	ZHENG_FOXP3_TARGETS_IN_THYMUS_UP	153	0.48	1.81	0.008
211	BROWN_MYELOID_CELL_DEVELOPMENT_UP	123	0.57	1.81	0.008

212	CLASPER_LYMPHATIC_VESSELS_DURIN G_METASTASIS_DN	33	0.73	1.81	0.014
213	GAURNIER_PSMD4_TARGETS	62	0.72	1.81	0.006
214	SASAI_RESISTANCE_TO_NEOPLASTIC_T RANSFROMATION	49	0.61	1.81	0.018
215	RICKMAN_HEAD_AND_NECK_CANCER_C	76	0.61	1.81	0.016
216	HOSHIDA_LIVER_CANCER_LATE_RECUR RENCE_UP	55	0.51	1.81	0.008
217	HERNANDEZ_ABERRANT_MITOSIS_BY_D OCETACEL_4NM_UP	21	0.64	1.81	0.01
218	SHIN_B_CELL_LYMPHOMA_CLUSTER_8	31	0.63	1.81	0.006
219	MAHADEVAN_RESPONSE_TO_MP470_UP	18	0.77	1.81	0.006
220	MASRI_RESISTANCE_TO_TAMOXIFEN_A ND_AROMATASE_INHIBITORS_DN	18	0.72	1.81	0.01
221	LU_TUMOR_ANGIOGENESIS_UP	25	0.65	1.81	0.01
222	STEGER_ADIPOGENESIS_DN	21	0.78	1.8	0.008
223	NAKAMURA_ADIPOGENESIS_EARLY_DN	37	0.64	1.8	0.014
224	WORSCHCH_TUMOR_REJECTION_UP	44	0.66	1.8	0.012
225	PID_SHP2_PATHWAY	51	0.53	1.8	0
226	PID_INTEGRIN2_PATHWAY	27	0.68	1.8	0.002
227	REACTOME_HEMOSTASIS	355	0.41	1.8	0
228	KRASNOSELSKAYA_ILF3_TARGETS_UP	37	0.7	1.8	0.006
229	ONDER_CDH1_TARGETS_2_UP	237	0.57	1.8	0.022
230	RODRIGUES_THYROID_CARCINOMA_DN	65	0.52	1.8	0.006
231	LIU_SMARCA4_TARGETS	44	0.57	1.8	0.012
232	PID_IL12_STAT4PATHWAY	29	0.74	1.8	0.012
233	KIM_WT1_TARGETS_8HR_UP	153	0.49	1.8	0.006

234	YAO_TEMPORAL_RESPONSE_TO_PROG ESTERONE_CLUSTER_16	67	0.56	1.8	0.018
235	PID_AP1_PATHWAY	63	0.53	1.8	0.016
236	BOYALT_LIVER_CANCER_SUBCLASS_G 56_DN	17	0.7	1.8	0.006
237	REACTOME_PYRIMIDINE_METABOLISM	18	0.64	1.8	0.004
238	KAAB_FAILED_HEART_VENTRICLE_DN	38	0.59	1.8	0.006
239	POTTI_CYTOXAN_SENSITIVITY	31	0.58	1.8	0.01
240	MA_MYELOID_DIFFERENTIATION_DN	36	0.55	1.8	0.002
241	OSWALD_HEMATOPOIETIC_STEM_CELL_ IN_COLLAGEN_GEL_UP	206	0.45	1.8	0.004
242	TOMLINS_PROSTATE_CANCER_DN	40	0.63	1.8	0.02
243	CHIANG_LIVER_CANCER_SUBCLASS_CT NNB1_DN	125	0.53	1.8	0.01
244	BOYLAN_MULTIPLE_MYELOMA_C_CLUSTER ER_DN	25	0.63	1.8	0.006
245	LINDSTEDT_DENDRITIC_CELL_MATURATION ON_D	66	0.59	1.8	0.014
246	MCDOWELL_ACUTE_LUNG_INJURY_UP	43	0.61	1.8	0.012
247	PID_GLYPICAN_1PATHWAY	23	0.64	1.8	0
248	FOSTER_TOLERANT_MACROPHAGE_UP	115	0.49	1.79	0.004
249	ONDER_CDH1_SIGNALING_VIA_CTNNB1	78	0.56	1.79	0.002
250	DAVICIONI_MOLECULAR_ARMES_VS_ERM S_DN	163	0.48	1.79	0.004
251	WANG_CISPLATIN_RESPONSE_AND_XPC _DN	202	0.41	1.79	0.002
252	KIM_WT1_TARGETS_UP	202	0.5	1.79	0.012

253	MAHAJAN_RESPONSE_TO_IL1A_UP	74	0.52	1.79	0.006
254	HESS_TARGETS_OF_HOXA9_AND_MEIS1_DN	66	0.61	1.79	0.02
255	REACTOME_CLASS_A1_RHODOPSIN_LIKE_RECEPTORS	164	0.5	1.79	0.004
256	SENESE_HDAC1_TARGETS_UP	353	0.46	1.79	0.004
257	PAPASPYRIDONOS_UNSTABLE_ATHEROSCLEROTIC_PLAQUE_DN	38	0.66	1.79	0.014
258	LA_MEN1_TARGETS	21	0.63	1.79	0.006
259	KAMIKUBO_MYELOID_MN1_NETWORK	16	0.66	1.79	0.006
260	VERRECCHIA_EARLY_RESPONSE_TO_TGFB1	56	0.6	1.79	0.014
261	RUTELLA_RESPONSE_TO_HGF_UP	392	0.45	1.79	0.008
262	NEMETH_INFLAMMATORY_RESPONSE_LPS_UP	80	0.57	1.79	0.008
263	BERTUCCI_MEDULLARY_VS_DUCTAL_BREAST_CANCER_DN	124	0.52	1.79	0.018
264	DUNNE_TARGETS_OF_AML1_MTG8_FUSION_ON_UP	42	0.68	1.78	0.008
265	WINTER_HYPOXIA_METAGENE	212	0.48	1.78	0.012
266	VALK_AML_CLUSTER_5	29	0.69	1.78	0.014
267	BROWNE_HCMV_INFECTION_24HR_DN	137	0.47	1.78	0.002
268	SENESE_HDAC3_TARGETS_UP	389	0.42	1.78	0.004
269	GAUSSMANN_MLL_AF4_FUSION_TARGETS_F_DN	27	0.59	1.78	0.008
270	WANG_MLL_TARGETS	197	0.44	1.78	0.004
271	SPIELMAN_LYMPHOBLAST_EUROPEAN_	20	0.71	1.78	0.004

	VS_ASIAN_2FC_DN				
272	ZHANG_PROLIFERATING_VS_QUIESCEN T	50	0.53	1.78	0.009
273	GAVIN_PDE3B_TARGETS	19	0.73	1.78	0.008
274	SWEET_LUNG_CANCER_KRAS_DN	361	0.47	1.78	0.01
275	WU_HBX_TARGETS_2_UP	22	0.58	1.78	0.008
276	NAKAMURA_METASTASIS_MODEL_DN	32	0.59	1.78	0.01
277	MANTOVANI_NFKB_TARGETS_UP	32	0.56	1.78	0.006
278	NUTT_GBM_VS_AO_GLIOMA_UP	44	0.54	1.77	0.01
279	TAKEDA_TARGETS_OF_NUP98_HOXA9_F USION_16D_UP	115	0.52	1.77	0.01
280	DIAZ_CHRONIC_MEYLOGENOUS_LEUKE MIA_DN	107	0.54	1.77	0.01
281	MARCHINI_TRABECTEDIN_RESISTANCE_ DN	46	0.56	1.77	0.01
282	ZHU_CMV_24_HR_DN	84	0.57	1.77	0.042
283	BROWNE_HCMV_INFECTION_20HR_DN	92	0.46	1.77	0.004
284	NAKAMURA_ADIPOGENESIS_LATE_DN	36	0.62	1.77	0.014
285	FAELT_B_CLL_WITH_VH_REARRANGEME NTS_UP	43	0.51	1.77	0.008
286	DELACROIX_RAR_TARGETS_DN	18	0.63	1.77	0.01
287	PID_AVB3_OPN_PATHWAY	29	0.59	1.77	0.013
288	KEGG_JAK_STAT_SIGNALING_PATHWAY	110	0.49	1.77	0.008
289	TSAI_RESPONSE_TO_IONIZING_RADIATI ON	135	0.46	1.77	0.004
290	PID_LYMPHANGIOGENESIS_PATHWAY	24	0.61	1.77	0.014
291	SENGUPTA_NASOPHARYNGEAL_CARCI	226	0.51	1.77	0.018

	OMA_UP				
292	HOELZEL_NF1_TARGETS_UP	100	0.49	1.77	0.002
293	PID_AVB3_INTEGRIN_PATHWAY	70	0.53	1.77	0.028
294	GRAESSMANN_APOPTOSIS_BY_SERUM_DEPRIVATION_UP	401	0.39	1.77	0
295	BEGUM_TARGETS_OF_PAX3_FOXO1_FUSION_UP	55	0.53	1.77	0.008
296	ZHOU_INFLAMMATORY_RESPONSE_LPS_UP	242	0.43	1.76	0.006
297	HELLER_HDAC_TARGETS_DN	260	0.43	1.76	0.002
298	GRAHAM_NORMAL QUIESCENT VS NORMAL DIVIDING_UP	58	0.57	1.76	0.012
299	ZHAN_MULTIPLE_MYELOMA_CD1_AND_CD2_DN	36	0.53	1.76	0.006
300	ZHANG_TARGETS_OF_EWSR1_FLI1_FUSION	82	0.49	1.76	0.002
301	EBAUER_TARGETS_OF_PAX3_FOXO1_FUSION_UP	178	0.43	1.76	0.002
302	JAATINEN_HEMATOPOIETIC_STEM_CELL_DN	176	0.6	1.76	0.025
303	PID_INTEGRIN_CS_PATHWAY	23	0.66	1.76	0.01
304	LEI_HOXC8_TARGETS_DN	16	0.68	1.76	0.014
305	HIRSCH_CELLULAR_TRANSFORMATION_SIGNATURE_UP	228	0.47	1.76	0.014
306	GRAHAM_CML QUIESCENT VS NORMAL DIVIDING_UP	46	0.6	1.76	0.01
307	MISHRA_CARCINOMA_ASSOCIATED_FIBRIN	20	0.72	1.76	0.012

	ROBLAST_UP				
308	WUNDER_INFLAMMATORY_RESPONSE_ AND_CHOLESTEROL_UP	45	0.66	1.76	0.018
309	PID_IL12_2PATHWAY	54	0.64	1.76	0.03
310	KATSANOUELAVL1_TARGETS_DN	106	0.45	1.76	0.004
311	HECKER_IFNB1_TARGETS	76	0.7	1.76	0.01
312	WU_HBX_TARGETS_3_UP	18	0.58	1.76	0.004
313	SCHAEFFER_PROSTATE_DEVELOPMENT _6HR_UP	127	0.44	1.76	0.007
314	DEURIG_T_CELL_PROLYMPHOCYTIC_LE UKEMIA_DN	291	0.46	1.76	0.024
315	MARKEY_RB1_CHRONIC_LOF_DN	97	0.52	1.76	0.014
316	WONG_ENDMETRIUM_CANCER_DN	60	0.64	1.76	0.024
317	AMUNDSON_POOR_SURVIVAL_AFTER_G AMMA_RADIATION_8G	90	0.48	1.76	0.01
318	KEGG_PRION_DISEASES	28	0.61	1.76	0.004
319	BURTON_ADIPOGENESIS_8	73	0.53	1.76	0.01
320	BOYLAN_MULTIPLE_MYELOMA_PCA1_UP	84	0.56	1.76	0.013
321	BOYLAN_MULTIPLE_MYELOMA_PCA3_UP	56	0.48	1.76	0.004
322	LIANG_SILENCED_BY_METHYLATION_2	49	0.67	1.75	0.01
323	DELASERNA_MYOD_TARGETS_DN	42	0.53	1.75	0.01
324	SCHAEFFER_PROSTATE_DEVELOPMENT _12HR_UP	90	0.46	1.75	0.002
325	WEINMANN_ADAPTATION_TO_HYPOXIA_ DN	38	0.58	1.75	0.008
326	AMIT_SERUM_RESPONSE_60_MCF10A	54	0.57	1.75	0.016
327	GAUSSMANN_MLL_AF4_FUSION_TARGET	136	0.47	1.75	0.006

	S_F_UP				
328	ZHOU_TNF_SIGNALING_4HR	51	0.46	1.75	0.004
329	SCHAEFFER_PROSTATE_DEVELOPMENT _48HR_DN	275	0.45	1.75	0.008
330	XU_HGF_SIGNALING_NOT_VIA_AKT1_48 HR_UP	34	0.62	1.75	0.01
331	KEGG_LEISHMANIA_INFECTION	60	0.6	1.75	0.016
332	CHEN_LVAD_SUPPORT_OF_FAILING_HE ART_UP	97	0.52	1.75	0.016
333	FULCHER_INFLAMMATORY_RESPONSE_ LECTIN_VS_LPS_UP	435	0.41	1.75	0.004
334	SNIJDERS_AMPLIFIED_IN_HEAD_AND_NE CK_TUMORS	34	0.58	1.75	0.014
335	PID_PTP1BPATHWAY	45	0.52	1.75	0.004
336	ZHANG_RESPONSE_TO_IKK_INHIBITOR_ AND_TNF_UP	177	0.54	1.75	0.018
337	WU_HBX_TARGETS_1_UP	15	0.69	1.75	0.002
338	DURAND_STROMA_MAX_UP	210	0.43	1.74	0.004
339	KUROZUMI_RESPONSE_TO_ONCOCYTIC _VIRUS	41	0.68	1.74	0.02
340	WANG_RESPONSE_TO_BEXAROTENE_D N	23	0.56	1.74	0.006
341	PARK_APL_PATHOGENESIS_DN	47	0.55	1.74	0.014
342	HALMOS_CEBPA_TARGETS_UP	49	0.55	1.74	0.014
343	CHIARADONNA_NEOPLASTIC_TRANSFO RMATION_KRAS_DN	123	0.49	1.74	0.012
344	SEKI_INFLAMMATORY_RESPONSE_LPS_ _	62	0.6	1.74	0.02

	UP				
345	TAKEDA_TARGETS_OF_NUP98_HOXA9_F USION_10D_DN	104	0.56	1.74	0.019
346	GAVIN_FOXP3_TARGETS_CLUSTER_P2	63	0.49	1.74	0
347	PAPASPYRIDONOS_UNSTABLE_ATEROS CLEROTIC_PLAQUE_UP	49	0.59	1.74	0.025
	Enriched in Luminal (nom pvalue<1%)				
Rank	MSigDB	SIZE	ES	NES	NOM p-val
1	CHARAFE_BREAST_CANCER_LUMINAL_V S_MESENCHYMAL_UP	321	-0.63	-2.1	0
2	WAMUNYOKOLI_OVARIAN_CANCER_LMP _UP	192	-0.59	-2.05	0
3	REACTOME_PEROXISOMAL_LIPID_META BOLISM	18	-0.77	-1.96	0
4	LIM_MAMMARY_STEM_CELL_DN	313	-0.52	-1.96	0
5	KEGG_LINOLEIC_ACID_METABOLISM	19	-0.71	-1.94	0
6	SHEDDEN_LUNG_CANCER_GOOD_SURVI VAL_A5	60	-0.62	-1.88	0.004
7	CHARAFE_BREAST_CANCER_LUMINAL_V S_BASAL_UP	272	-0.48	-1.88	0
8	KEGG_GLYCEROPHOSPHOLIPID_METAB OLISM	52	-0.5	-1.85	0
9	WOO_LIVER_CANCER_RECURRENCE_D	63	-0.56	-1.84	0.008

	N				
10	WALLACE_PROSTATE_CANCER_RACE_D N	66	-0.5	-1.83	0
11	SMID_BREAST_CANCER_RELAPSE_IN_B RAIN_DN	76	-0.53	-1.82	0.008
12	SCHUETZ_BREAST_CANCER_DUCTAL_IN VASIVE_DN	78	-0.49	-1.79	0.008
13	KEGG_PEROXISOME	63	-0.54	-1.79	0.004
14	DOANE_BREAST_CANCER_CLASSES_UP	69	-0.53	-1.76	0.01
15	KEGG_VALINE_LEUCINE_AND_ISOLEUCI NE_DEGRADATION	40	-0.6	-1.76	0.019
16	REACTOME_SULFUR_AMINO_ACID_MET ABOLISM	22	-0.58	-1.75	0.008
17	COLDREN_GEFITINIB_RESISTANCE_DN	148	-0.56	-1.75	0.034
18	LIEN_BREAST_CARCINOMA_METAPLASTI C_VS_DUCTAL_DN	74	-0.53	-1.74	0.012
19	REACTOME_FATTY_ACID_TRIACYLGLYC EROL_AND_KETONE_BODY_METABOLIS M	135	-0.4	-1.74	0
20	FONTAINE_FOLLICULAR_THYROID_ADEN OMA_UP	50	-0.47	-1.74	0.006
21	REACTOME_BRANCHED_CHAIN_AMINO_ ACID_CATABOLISM	16	-0.69	-1.74	0.01
22	DOANE_BREAST_CANCER_ESR1_UP	99	-0.49	-1.74	0.006

REFERENCES

1. R. Siegel, J. Ma, Z. Zou, A. Jemal, Cancer statistics, 2014, *CA Cancer J Clin* **64**, 9–29 (2014).
2. K. D. Sievert *et al.*, Economic aspects of bladder cancer: what are the benefits and costs? *World J Urol* **27**, 295–300 (2009).
3. M. May *et al.*, Gender-specific differences in cancer-specific survival after radical cystectomy for patients with urothelial carcinoma of the urinary bladder in pathologic tumor stage T4a, *Urol Oncol* **31**, 1141–1147 (2013).
4. J. C. Messer *et al.*, Female Gender Is Associated With a Worse Survival After Radical Cystectomy for Urothelial Carcinoma of the Bladder: A Competing Risk Analysis, *Urology* (2014), doi:10.1016/j.urology.2013.10.060.
5. K. Mallin, K. A. David, P. R. Carroll, M. I. Milowsky, D. M. Nanus, Transitional cell carcinoma of the bladder: racial and gender disparities in survival (1993 to 2002), stage and grade (1993 to 2007), *J. Urol.* **185**, 1631–1636 (2011).
6. G. R. Prout *et al.*, Survival experience of black patients and white patients with bladder carcinoma, *Cancer* **100**, 621–630 (2004).
7. D. S. Yee, N. M. Ishill, W. T. Lowrance, H. W. Herr, E. B. Elkin, Ethnic differences in bladder cancer survival, *Urology* **78**, 544–549 (2011).
8. E. Scosyrev, K. Noyes, C. Feng, E. Messing, Sex and racial differences in bladder cancer presentation and mortality in the US, *Cancer* **115**, 68–74 (2009).
9. Z. Kirkali *et al.*, Bladder cancer: epidemiology, staging and grading, and diagnosis, *Urology* **66**, 4–34 (2005).
10. A. Henning *et al.*, Do differences in clinical symptoms and referral patterns contribute to the gender gap in bladder cancer? *BJU international* **112**, 68–73 (2013).
11. M. Cárdenas-Turanzas *et al.*, Comparative outcomes of bladder cancer, *Obstet Gynecol* **108**, 169–175 (2006).
12. S. Letašiová *et al.*, Bladder cancer, a review of the environmental risk factors, *Environ Health* **11 Suppl 1**, S11 (2012).
13. M. P. A. Zeegers, E. Kellen, F. Buntinx, P. A. van den Brandt, The association between smoking, beverage consumption, diet and bladder cancer: a systematic

- literature review, *World J Urol* **21**, 392–401 (2004).
14. M. Burger *et al.*, Epidemiology and risk factors of urothelial bladder cancer, *Eur Urol* **63**, 234–241 (2013).
 15. R. A. CASE, M. E. HOSKER, Tumour of the urinary bladder as an occupational disease in the rubber industry in England and Wales, *Br J Prev Soc Med* **8**, 39–50 (1954).
 16. K. J. Kiriluk, S. M. Prasad, A. R. Patel, G. D. Steinberg, N. D. Smith, Bladder cancer risk from occupational and environmental exposures, *Urol Oncol* **30**, 199–211 (2012).
 17. W. P. Tseng *et al.*, Prevalence of skin cancer in an endemic area of chronic arsenicism in Taiwan, *J Natl Cancer Inst* **40**, 453–463 (1968).
 18. W. P. Tseng, Effects and dose–response relationships of skin cancer and blackfoot disease with arsenic, *Environ. Health Perspect.* **19**, 109–119 (1977).
 19. C. J. Chen, Y. C. Chuang, T. M. Lin, H. Y. Wu, Malignant neoplasms among residents of a blackfoot disease-endemic area in Taiwan: high-arsenic artesian well water and cancers, *Cancer Res.* **45**, 5895–5899 (1985).
 20. M. M. Wu, T. L. Kuo, Y. H. Hwang, C. J. Chen, Dose-response relation between arsenic concentration in well water and mortality from cancers and vascular diseases, *Am. J. Epidemiol.* **130**, 1123–1132 (1989).
 21. J. S. Tsuji, D. D. Alexander, V. Perez, P. J. Mink, Arsenic exposure and bladder cancer: Quantitative assessment of studies in human populations to detect risks at low doses, *Toxicology* **317**, 17–30 (2014).
 22. M. S. Zaghloul, Bladder cancer and schistosomiasis, *J Egypt Natl Canc Inst* **24**, 151–159 (2012).
 23. M. H. Mostafa, S. A. Sheweita, P. J. O'Connor, Relationship between schistosomiasis and bladder cancer, *Clin. Microbiol. Rev.* **12**, 97–111 (1999).
 24. D. S. Michaud, Chronic inflammation and bladder cancer, *Urol Oncol* **25**, 260–268 (2007).
 25. M. P. Rosin, W. A. Anwar, A. J. Ward, Inflammation, chromosomal instability, and cancer: the schistosomiasis model, *Cancer Res.* **54**, 1929s–1933s (1994).
 26. C. La Vecchia, E. Negri, B. D'Avanzo, R. Savoldelli, S. Franceschi, Genital and urinary tract diseases and bladder cancer, *Cancer Res.* **51**, 629–631 (1991).
 27. A. F. Kantor *et al.*, Urinary tract infection and risk of bladder cancer, *Am. J. Epidemiol.* **119**, 510–515 (1984).

28. G. Lee, Uroplakins in the lower urinary tract, *Int Neurorol J* **15**, 4–12 (2011).
29. P. Hu *et al.*, Role of membrane proteins in permeability barrier function: uroplakin ablation elevates urothelial permeability, *Am. J. Physiol. Renal Physiol.* **283**, F1200–7 (2002).
30. X.-T. Kong *et al.*, Roles of uroplakins in plaque formation, umbrella cell enlargement, and urinary tract diseases, *J. Cell Biol.* **167**, 1195–1204 (2004).
31. K. Shin *et al.*, Hedgehog/Wnt feedback supports regenerative proliferation of epithelial stem cells in bladder, *Nature* **472**, 110–114 (2011).
32. K. Shin *et al.*, Cellular origin of bladder neoplasia and tissue dynamics of its progression to invasive carcinoma, *Nat. Cell Biol.* (2014), doi:10.1038/ncb2956.
33. K. S. Chan *et al.*, Identification, molecular characterization, clinical prognosis, and therapeutic targeting of human bladder tumor-initiating cells, *Proceedings of the National Academy of Sciences* **106**, 14016–14021 (2009).
34. P. J. Goebell, M. A. Knowles, Bladder cancer or bladder cancers? Genetically distinct malignant conditions of the urothelium, *Urol Oncol* **28**, 409–428 (2010).
35. M. Brausi *et al.*, A review of current guidelines and best practice recommendations for the management of nonmuscle invasive bladder cancer by the International Bladder Cancer Group, *J. Urol.* **186**, 2158–2167 (2011).
36. A. V. van Lingen, J. A. Witjes, Current intravesical therapy for non-muscle invasive bladder cancer, *Expert Opin Biol Ther* **13**, 1371–1385 (2013).
37. C. R. Lockyer, D. A. Gillatt, BCG immunotherapy for superficial bladder cancer, *J R Soc Med* **94**, 119–123 (2001).
38. N. Sapre, N. M. Corcoran, Modulating the immune response to Bacillus Calmette-Guérin (BCG): a novel way to increase the immunotherapeutic effect of BCG for treatment of bladder cancer? *BJU international* **112**, 852–853 (2013).
39. H. von der Maase *et al.*, Long-term survival results of a randomized trial comparing gemcitabine plus cisplatin, with methotrexate, vinblastine, doxorubicin, plus cisplatin in patients with bladder cancer, *J Clin Oncol* **23**, 4602–4608 (2005).
40. H. von der Maase *et al.*, Gemcitabine and cisplatin versus methotrexate, vinblastine, doxorubicin, and cisplatin in advanced or metastatic bladder cancer: results of a large, randomized, multinational, multicenter, phase III study, *J Clin Oncol* **18**, 3068–3077 (2000).
41. X.-R. Wu, Urothelial tumorigenesis: a tale of divergent pathways, *Nat. Rev. Cancer* **5**, 713–725 (2005).

42. C. P. N. Dinney *et al.*, Focus on bladder cancer, *Cancer Cell* **6**, 111–116 (2004).
43. Cancer Genome Atlas Research Network, Comprehensive molecular characterization of urothelial bladder carcinoma, *Nature* **507**, 315–322 (2014).
44. Y. Gui *et al.*, Frequent mutations of chromatin remodeling genes in transitional cell carcinoma of the bladder, *Nat Genet* **43**, 875–878 (2011).
45. E. M. Haugsten, A. Wiedlocha, S. Olsnes, J. Wesche, Roles of fibroblast growth factor receptors in carcinogenesis, *Mol. Cancer Res.* **8**, 1439–1452 (2010).
46. B. W. G. van Rhijn, R. Montironi, E. C. Zwarthoff, A. C. Jöbsis, T. H. van der Kwast, Frequent FGFR3 mutations in urothelial papilloma, *J Pathol* **198**, 245–251 (2002).
47. E. López-Knowles *et al.*, PIK3CA mutations are an early genetic alteration associated with FGFR3 mutations in superficial papillary bladder tumors, *Cancer Res.* **66**, 7401–7404 (2006).
48. F. M. Platt *et al.*, Spectrum of phosphatidylinositol 3-kinase pathway gene alterations in bladder cancer, *Clin Cancer Res* **15**, 6008–6017 (2009).
49. M. A. Knowles, F. M. Platt, R. L. Ross, C. D. Hurst, Phosphatidylinositol 3-kinase (PI3K) pathway activation in bladder cancer, *Cancer Metastasis Rev.* **28**, 305–316 (2009).
50. J. S. Aveyard, A. Skilleter, T. Habuchi, M. A. Knowles, Somatic mutation of PTEN in bladder carcinoma, *Br. J. Cancer* **80**, 904–908 (1999).
51. W. Hanel, U. M. Moll, Links between mutant p53 and genomic instability, *J. Cell. Biochem.* **113**, 433–439 (2012).
52. D. L. Burkhardt, J. Sage, Cellular mechanisms of tumour suppression by the retinoblastoma gene, *Nat. Rev. Cancer* **8**, 671–682 (2008).
53. M. Oeggerli *et al.*, E2F3 amplification and overexpression is associated with invasive tumor growth and rapid tumor cell proliferation in urinary bladder cancer, *Oncogene* **23**, 5616–5623 (2004).
54. S. C. Smith *et al.*, A 20-gene model for molecular nodal staging of bladder cancer: development and prospective assessment, *Lancet Oncol.* **12**, 137–143 (2011).
55. J.-S. Lee *et al.*, Expression signature of E2F1 and its associated genes predict superficial to invasive progression of bladder tumors, *J Clin Oncol* **28**, 2660–2667 (2010).
56. M. Sanchez-Carbayo, N. D. Socci, J. Lozano, F. Saint, C. Cordon-Cardo, Defining molecular profiles of poor outcome in patients with invasive bladder cancer using

- oligonucleotide microarrays, *J Clin Oncol* **24**, 778–789 (2006).
57. M. Riestler *et al.*, Combination of a novel gene expression signature with a clinical nomogram improves the prediction of survival in high-risk bladder cancer, *Clin Cancer Res* **18**, 1323–1333 (2012).
 58. E. Blaveri *et al.*, Bladder cancer outcome and subtype classification by gene expression, *Clin Cancer Res* **11**, 4044–4055 (2005).
 59. O. O. Modlich *et al.*, Identifying superficial, muscle-invasive, and metastasizing transitional cell carcinoma of the bladder: use of cDNA array analysis of gene expression profiles, *Clin Cancer Res* **10**, 3410–3421 (2004).
 60. W.-J. Kim *et al.*, A four-gene signature predicts disease progression in muscle invasive bladder cancer, *Mol Med* (2011), doi:10.2119/molmed.2010.00274.
 61. D. Lindgren *et al.*, Combined gene expression and genomic profiling define two intrinsic molecular subtypes of urothelial carcinoma and gene signatures for molecular grading and outcome, *Cancer Res* **70**, 3463–3472 (2010).
 62. D. Lindgren *et al.*, Integrated genomic and gene expression profiling identifies two major genomic circuits in urothelial carcinoma, *PLoS One* **7**, e38863 (2012).
 63. G. Sjö Dahl *et al.*, A molecular taxonomy for urothelial carcinoma, *Clin Cancer Res* **18**, 3377–3386 (2012).
 64. J.-P. Volkmer *et al.*, Three differentiation states risk-stratify bladder cancer into distinct subtypes, *Proceedings of the National Academy of Sciences* **109**, 2078–2083 (2012).
 65. J. S. Damrauer *et al.*, Intrinsic subtypes of high-grade bladder cancer reflect the hallmarks of breast cancer biology, *Proceedings of the National Academy of Sciences* **111**, 3110–3115 (2014).
 66. W. Choi *et al.*, Identification of distinct basal and luminal subtypes of muscle-invasive bladder cancer with different sensitivities to frontline chemotherapy, *Cancer Cell* **25**, 152–165 (2014).
 67. D. Lindgren, A. Frigyesi, S. Gudjonsson, G. Sjö Dahl, Combined gene expression and genomic profiling define two intrinsic molecular subtypes of urothelial carcinoma and gene signatures for molecular grading and ..., *Cancer Res.* (2010).
 68. G. G. Sjö Dahl *et al.*, A systematic study of gene mutations in urothelial carcinoma; inactivating mutations in TSC2 and PIK3R1, *PLoS One* **6**, e18583–e18583 (2011).
 69. G. Iyer *et al.*, Prevalence and Co-Occurrence of Actionable Genomic Alterations

- in High-Grade Bladder Cancer, *J Clin Oncol* (2013), doi:10.1200/JCO.2012.46.5740.
70. L. L. Dyrskjøt *et al.*, Identifying distinct classes of bladder carcinoma using microarrays, *Nat Genet* **33**, 90–96 (2003).
 71. W.-J. Kim *et al.*, Predictive value of progression-related gene classifier in primary non-muscle invasive bladder cancer, *Mol Cancer* **9**, 3 (2010).
 72. A. B. Als *et al.*, Emmprin and survivin predict response and survival following cisplatin-containing chemotherapy in patients with advanced bladder cancer, *Clin Cancer Res* **13**, 4407–4414 (2007).
 73. M. Castillo-Martin, J. Domingo-Domenech, O. Karni-Schmidt, T. Matos, C. Cordon-Cardo, Molecular pathways of urothelial development and bladder tumorigenesis, *Urol Oncol* **28**, 401–408 (2010).
 74. H. Donsky, S. Coyle, E. Scosyrev, E. M. Messing, Sex differences in incidence and mortality of bladder and kidney cancers: National estimates from 49 countries, *Urol Oncol* (2013), doi:10.1016/j.urolonc.2013.04.010.
 75. E. Lim *et al.*, Aberrant luminal progenitors as the candidate target population for basal tumor development in BRCA1 mutation carriers, *Nat. Med.* **15**, 907–913 (2009).
 76. C. M. Perou *et al.*, Molecular portraits of human breast tumours, *Nature* **406**, 747–752 (2000).
 77. T. Sørlie *et al.*, Gene expression patterns of breast carcinomas distinguish tumor subclasses with clinical implications, *Proc. Natl. Acad. Sci. U.S.A.* **98**, 10869–10874 (2001).
 78. Cancer Genome Atlas Network, Comprehensive molecular portraits of human breast tumours, *Nature* **490**, 61–70 (2012).
 79. A. Prat *et al.*, Phenotypic and molecular characterization of the claudin-low intrinsic subtype of breast cancer, *Breast Cancer Res.* **12**, R68 (2010).
 80. J. S. Parker *et al.*, Supervised risk predictor of breast cancer based on intrinsic subtypes, *J Clin Oncol* **27**, 1160–1167 (2009).
 81. E. A. Rakha, J. S. Reis-Filho, I. O. Ellis, Basal-like breast cancer: a critical review, *J Clin Oncol* **26**, 2568–2581 (2008).
 82. E. A. Kurzrock, D. K. Lieu, L. A. Degraffenried, C. W. Chan, R. R. Isseroff, Label-retaining cells of the bladder: candidate urothelial stem cells, *Am. J. Physiol. Renal Physiol.* **294**, F1415–21 (2008).

83. M. D. Wilkerson, D. N. Hayes, ConsensusClusterPlus: a class discovery tool with confidence assessments and item tracking, *Bioinformatics* **26**, 1572–1573 (2010).
84. V. G. Tusher, R. Tibshirani, G. Chu, Significance analysis of microarrays applied to the ionizing radiation response, *Proc. Natl. Acad. Sci. U.S.A.* **98**, 5116–5121 (2001).
85. V. K. Mootha *et al.*, PGC-1alpha-responsive genes involved in oxidative phosphorylation are coordinately downregulated in human diabetes, *Nat Genet* **34**, 267–273 (2003).
86. A. Subramanian *et al.*, Gene set enrichment analysis: a knowledge-based approach for interpreting genome-wide expression profiles, *Proc. Natl. Acad. Sci. U.S.A.* **102**, 15545–15550 (2005).
87. R. Tibshirani, T. Hastie, B. Narasimhan, G. Chu, Diagnosis of multiple cancer types by shrunken centroids of gene expression, *Proc. Natl. Acad. Sci. U.S.A.* **99**, 6567–6572 (2002).
88. C. Fan *et al.*, Building prognostic models for breast cancer patients using clinical variables and hundreds of gene expression signatures, *BMC Med Genomics* **4**, 3 (2011).
89. V. A. Malkov *et al.*, Multiplexed measurements of gene signatures in different analytes using the Nanostring nCounter Assay System, *BMC Res Notes* **2**, 80 (2009).
90. G. K. Geiss *et al.*, Direct multiplexed measurement of gene expression with color-coded probe pairs, *Nat. Biotechnol.* **26**, 317–325 (2008).
91. Z. A. Wang *et al.*, Lineage analysis of basal epithelial cells reveals their unexpected plasticity and supports a cell-of-origin model for prostate cancer heterogeneity, *Nat. Cell Biol.* **15**, 274–283 (2013).